

Molecular mechanisms of mitochondrial DNA replication

Inaugural-Dissertation

zur

Erlangung des Doktorgrades

der Mathematisch-Naturwissenschaftlichen Fakultät

der Universität zu Köln

vorgelegt von

STANKA MATIĆ

aus Ljubovija

Berichterstatter: Prof. Dr. Nils-Göran Larsson
Prof. Dr. Aleksandra Trifunovic

Tag der mündlichen Prüfung: 16/01/2017

Molecular mechanisms of mitochondrial DNA replication

PhD Thesis

Submitted by Stanka Matic
Supervisor: Nils-Göran Larsson

Graduate School for Biological Sciences, University of Cologne



“The nitrogen in our DNA, the calcium in our teeth, the iron in our blood, the carbon in our apple pies were made in the interiors of collapsing stars. We are made of starstuff.”

Carl Sagan, Cosmos

“Scientific research is one of the most exciting and rewarding of occupations. It is like a voyage of discovery into unknown lands, seeking not for new territory but for new knowledge. It should appeal to those with a good sense of adventure.”

Frederick Sanger

Abstract

Mitochondria are cellular organelles responsible for energy conversion to form the cell's energy currency, adenosine triphosphate (ATP), through the process of oxidative phosphorylation. In addition, mitochondria play a vital role in diverse cellular processes including apoptosis, calcium homeostasis and intracellular signalling. As a consequence, mitochondrial dysfunction can lead to numerous disorders that display variability in clinical presentation and tissue specificity. Mitochondria contain their own genome, known as mitochondrial DNA (mtDNA), and have distinct enzymes involved in mtDNA expression and maintenance. Even though the core components of the machinery necessary for mtDNA replication have been identified and reconstituted *in vitro*, its underlying regulatory mechanisms are largely unknown. The displacement (D) loop, a triple stranded structure that is formed by premature replication termination generating the 7S DNA, likely plays an important role in the control of mammalian mtDNA replication in response to cellular bioenergetics demands.

The work described in this thesis aimed to study the effects of the mitochondrial replicative helicase TWINKLE and the mitochondrial nuclease MGME1 on mtDNA replication regulation. Both of these factors were previously described to impact 7S DNA levels.

The effects of TWINKLE on mtDNA levels were studied by generating *Twinkle* bacterial artificial chromosome (BAC) transgenic mice. This TWINKLE overexpressor model showed that TWINKLE upregulation leads to an increased replication and augmented mtDNA copy number.

To study the *in vivo* role of the MGME1 nuclease in mtDNA replication regulation, *Mgme1* knockout mice were generated and analyzed. Our results show that MGME1 is not essential for mouse embryonic development and survival. This MGME1 knockout model showed mtDNA depletion, and accumulation of an 11-kb linear mtDNA fragment that spans the entire major arc of the mtDNA and is present in different mouse tissues. Interestingly, a similar linear fragment was also present in

mice carrying an exonuclease deficient DNA polymerase (mtDNA mutator mice). These mice show a progeroid phenotype that is likely not driven by linear deletions as *Mgme1* knockout mice do not display a premature ageing phenotype. Finally, we dissected the role of MGME1 in mtDNA replication and transcription. The lack of abortive replication events and diminished H-strand transcription termination in *Mgme1* knockout mice suggests a possible role of MGME1 in the regulation of those processes at the end of the D-loop region.

Zusammenfassung

Mitochondrien sind essentielle Zellorganellen, die durch den Prozess der oxidativen Phosphorylierung für die Energiegewinnung der Zelle in Form von Adenosintriphosphat (ATP), zuständig sind. Zusätzlich spielen Mitochondrien eine wesentliche Rolle in verschiedenen zellulären Prozessen, einschließlich Apoptose, Kalziumhomöostase und intrazellulärer Signalwege. Daraus folgt, dass mitochondriale Dysfunktion zu einer Vielzahl von Funktionsstörungen führen kann, die eine ganze Bandbreite von klinischen Befunden und gewebsspezifischen Auswirkungen widerspiegeln. Mitochondrien besitzen ihr eigenes Genom, bekannt als mitochondriale DNA (mtDNA), und haben eigene, spezielle Enzyme, die bei der mtDNA Expression und Replikation involviert sind. Obwohl die Hauptkomponenten, die zur Replikation der mtDNA benötigt werden, bekannt sind und *in vitro* rekonstruiert wurden, sind die zugrunde liegenden regulatorischen Mechanismen weitestgehend unbekannt. Der *Displacement (D) Loop*, eine dreisträngige Struktur, die durch einen verfrühten Replikationsabbruch entsteht und aus der die 7S DNA hervorgeht, spielt vermutlich in Säugetieren eine wichtige Rolle bei der Kontrolle der mtDNA Replikation als Antwort auf bioenergetische Bedürfnisse.

Die hier vorliegende Arbeit befasst sich mit der Untersuchung der Effekte der mitochondrialen replikativen Helikase TWINKLE und der mitochondrialen Nuklease MGME1 auf die Regulation der Replikation von mtDNA. In der Vergangenheit wurde bereits für beide Faktoren gezeigt, dass sie die Quantität von 7S DNA beeinflussen.

Die Auswirkungen von TWINKLE auf die mtDNA Level wurden anhand von transgenen Mäusen, die *Twinkle* in einem künstlichen Bakterienchromosom (BAC) tragen und überexprimieren, untersucht. Anhand dieses Modells konnte gezeigt werden, dass die Hochregulierung von TWINKLE zu einer vermehrten Replikation und erhöhten Kopienzahl von mtDNA führt.

Um die *in vivo* Rolle der Nuklease MGME1 während der Regulation der mtDNA Replikation zu untersuchen, wurden *Mgme1* knockout Mäuse generiert und analysiert. Unsere Ergebnisse zeigen, dass MGME1 für die Entwicklung und Vitalität von

Mausembryonen nicht essentiell ist. Die Mäuse des MGME1 Knockout Modells zeigten eine Depletion der mtDNA und eine Akkumulierung eines linearen 11-kb-Fragments von mtDNA, welches den gesamten *major arc* der mtDNA umfasst und in verschiedenen Mausgeweben präsent ist. Interessanterweise gibt es ein vergleichbares lineares Fragment in Mäusen, die eine mutierte DNA Polymerase mit defizienter Exonuklease besitzen (mtDNA Mutator Mäuse). Diese Mäuse zeigen einen vorzeitigen Alterungsphänotyp, der vermutlich nicht von linearen Deletionen verursacht wird, da dies bei *Mgme1* knockout Mäuse nicht der Fall ist. Abschließend untersuchten wir die Rolle von MGME1 sowohl bei der mitochondrialen Replikation als auch bei der Transkription. Das Ausbleiben verfrühter Replikationsabbrüche sowie verminderter Termination der H-Strang Transkription in *Mgme1* knockout Mäusen deutet auf eine mögliche Rolle von MGME1 bei der Regulation dieser wichtigen Prozesse am Ende der D-Loop Region hin.

Contents

Cover page and title	2
Erklärung.....	98
Abstract	5
Zusammenfassung.....	7
Contents	9
Table of figures.....	12
Table of abbreviations	14
1. INTRODUCTION.....	17
1.1 Mitochondrial origin	17
1.2 Mitochondrial function and form	18
1.3 Organization of mtDNA.....	20
1.4 Replication of mtDNA	22
1.4.1 The strand-displacement model.....	23
1.4.2 The strand-coupled model.....	24
1.4.3 RITOLS model.....	24
1.4.4 Mitochondrial non-coding region (D-loop region).....	25
1.4.5 Mitochondrial DNA polymerase POL γ	26
1.4.6 Mitochondrial replicative helicase - TWINKLE.....	27
1.4.7 Mitochondrial single-stranded DNA binding protein - mtSSB.....	29
1.4.8 Additional proteins involved in mitochondrial DNA replication	30
1.4.9 Mitochondrial genome maintenance exonuclease 1 – MGME1	31
1.5 Transcription of mtDNA	32
1.5.1 The basic components of the mitochondrial transcription machinery.....	32
1.5.2 Regulation of transcription termination.....	34
1.6 Mitochondrial DNA repair	35
1.7 Mitochondrial genetics and diseases	37

1.7.1 Mitochondrial disorders caused by mtDNA mutations	39
1.7.2 Mitochondrial disorders caused by nDNA mutations	39
2. AIMS	41
3. RESULTS	42
3.1 Twinkle overexpression leads to elevated mtDNA levels	42
3.2 Generation and verification of <i>Mgme1</i> knockout mice	47
3.2.1 <i>Mgme1</i> knockout mice display multiple mtDNA deletions and depletion of mtDNA in various tissues	49
3.2.2 <i>Mgme1</i> knockout mice have an increase in steady-state levels of 7S DNA but severely diminished de novo synthesis of 7S DNA	52
3.2.3 MGME1 deficiency results in accumulation of 7S DNA with extended 5 ends ...	55
3.2.4 Lack of MGME1 affects mitochondrial transcription differentially	56
3.2.6. <i>Mgme1</i> deficiency causes stalled mtDNA replication close to O _L in liver and accumulation of replication intermediates	60
3.2.7. Sequence coverage for <i>Mgme1</i> knockout mice from different tissues	63
3.2.8 Steady-state protein levels in <i>Mgme1</i> knockout mice	66
4. DISSCUSSION	68
5. METHODS	76
Generation of MGME1 knockout mice	76
Generation of BAC and BAC FLAG TWINKLE transgenic mice	76
Southern blot analysis	77
<i>De novo</i> DNA synthesis	77
Northern blot analysis	78
<i>De novo</i> Transcription Assay	78
Quantitative PCR	78
Western Blot analysis	79
Long-extension PCR	79
Phenol chloroform extraction	79
DNA extraction with Puregene® Core Kit A (Qiagen)	80
RNA isolation with ToTALLY RNA TM kit (Ambion)	80
DNA/RNA quantification with Qubit® 1.0 fluorometer (Invitrogen)	80
DNA agarose gelelectrophoresis	81
	10

Reverse transcription.....	81
Isolation of mitochondria from mouse tissue.....	81
Blue Native PAGE	82
Probe labelling with [α - ³² P] dCTP using Prime-It® II Random Primer Labeling Kit (Agilent)	82
Oligonucleotide labelling with [γ - ³² P] ATP using T4-polynucleotide kinase.....	82
ACR transcript labeling using Riboprobe System T7 Kit (Promega).....	83
Preparation of purified mitochondria from different tissue and mitochondrial DNA	83
Northern Blotting using biotinylated probes.....	84
Sequencing library preparation and pair-end DNA sequencing.....	84
Two-Dimensional (2D) Agarose Gel Electrophoresis.....	85
Cell culture and ddC treatment	85
Material.....	85
6. REFERENCES.....	88
Acknowledgments	98
Curriculum Vitae	102

Table of figures

Figure 1: Structure of mitochondria and biogenesis of the oxidative phosphorylation system.....	18
Figure 2: Schematic illustration of the structure and function the oxidative phosphorylation system.	19
Figure 3: Organization of mammalian mtDNA.....	21
Figure 4: Components of the basic mtDNA replication machinery.....	23
Figure 5: Mitochondrial D-loop region with regulatory elements.	25
Figure 6: Schematic representation of the MGME1 protein and localization of the investigated homozygous mutations causing disease..	31
Figure 7: Common clinical manifestations of mitochondrial disorders.....	38
Figure 3.1: BAC transgenic strategy.....	42
Figure 3.2: TWINKLE BAC screening and protein levels	43
Figure 3.3: mtDNA levels in TWINKLE overexpressor mice.....	44
Figure 3.4: Transcript levels and levels of respiratory chain complex subunits in TWINKLE overexpressor mice.....	45
Figure 3.5: Western blot analysis in TFAM knockout and overexpressor mice.	46
Figure 3.6: Mgme1 knockout mice.	47
Figure 3.7: MGME1 protein levels in Mgme1 knockout mice..	48
Figure 3.8: mtDNA levels in Mgme1 homozygous and tissue-specific knockout mice..	50
Figure 3.9: mtDNA levels in Mgme1 homozygous knockout mice in different tissues...	51
Figure 3.10: 7S DNA synthesis and steady-state level Mgme1 knockout mice.....	53
Figure 3.11: mtDNA and 7S DNA quantification in Mgme1 knockout mice.	54
Figure 3.12: Mapping 7S DNA ends in Mgme1 knockout mice..	55
Figure 3.13: Steady-state transcript levels in Mgme1 knockout mice.....	57
Figure 3.14: De novo and relative transcript levels in Mgme1 knockout mice.....	59
Figure 3.16: Replication in heart of Mgme1 knockout mice.....	61
Figure 3.17: Replication in liver of Mgme1 knockout mice.....	62
Figure 3.18: Heart mtDNA pair-end sequencing from PolyA ^{mut} and Mgme1 knockout mice.....	64

Figure 3.19: Brain and liver mtDNA pair-end sequencing from Mgme1 knockout mice.
..... 65

Figure 3.20: Protein levels in Mgme1 knockout mice. 67

Figure 4.1: Origin of the linear deletion. 70

Figure 4.2: The termination complex at the end of D-loop region. 74

Table of abbreviations

Abbreviation	Meaning
AMP	adenosine monophosphate
ATP	adenosine triphosphate
ACR	anti-control region
adPEO	autosomal dominant progressive external ophthalmoplegia
BAC	bacterial artificial chromosome
BER	base excision repair
BioID	biotin identification
BirA	bifunctional ligase/repressor A
BN-PAGE	blue native polyacrylamide gel electrophoresis
bp	base-pair
CoA	acetyl -coenzyme A
CoQ	Coenzyme Q
ChIP	chromatin immunoprecipitation
CSB	conserved sequence block
CytB	cytochrome <i>b</i>
D-Loop	displacement-loop
ddC	2'-3'-dideoxycytidine
DNA	deoxyribonucleic acid
DNA2	DNA replication ATP-dependent helicase/nuclease 2
dsDNA	double-stranded DNA
E. 8.5	embryonic day 8.5
ExoG	endo/exonuclease (5'-3'), endonuclease G-like
ETAS	Extended termination-associated sequence
EM	electron microscopy
EMSA	electrophoretic mobility shift assay
H2O2	hydrogen peroxide
hTFAM	human mitochondrial transcription factor A
HSP	heavy-strand promoter
HMG	high mobility group

IM	inner membrane
IMS	intermembrane space
kb	kilobase
KO	knockout
KSS	Kearns-Sayre syndrome
LHON	Leber's hereditary optic neuropathy
LM-PCR	ligation-mediated polymerase chain reaction
LSP	light-strand promoter
LP-BER	long-patch base excision repair
LRPPRC	leucine-rich PPR motif-containing protein
MGME1	mitochondrial genome maintenance exonuclease 1
MMR	mismatch repair
mRNA	messenger RNA
MUTYH	mutY DNA glycosylase
MEFs	mouse embryonic fibroblasts
mt	mitochondrial
MTS	mitochondrial targeting sequence
mtSSB	mitochondrial single-stranded DNA-binding protein
MTERF1	mitochondrial transcription termination factor 1
NCR	non-coding region
NEIL	neil DNA glycosylase
nt	nucleotide
Ni-NTA	nickel-nitrilotriacetic acid
O _H	origin of heavy-strand replication
O _L	origin of light-strand replication
O ₂ ^{-•}	superoxide anion
OH•	hydroxyl radical
OXPPOS	oxidative phosphorylation
PBS	phosphate buffered saline
PCR	polymerase chain reaction
POL _γ	DNA polymerase gamma
POLRMT	mitochondrial RNA polymerase

PD-(D/E)XK	the PD-(D/E)XK nuclease superfamily
RNA	ribonucleic acid
ROS	reactive oxygen species
RNS	reactive nitrogen species
RITOLS	ribonucleotide incorporation throughout the lagging strand
RNase H1	ribonuclease H1
rRNA	ribosomal RNA
SDM	strand-displacement model
SDS-PAGE	sodium dodecyl sulfate polyacrylamide gel electrophoresis
ssDNA	single-stranded DNA
STED	stimulated emission depletion microscopy
si-RNA	small interfering RNA
TAS	termination-associated sequence
TFB1M	rRNA dimethyladenosine transferase (previously transcription factor B1, mitochondrial)
TFB2M	transcription factor B2, mitochondrial
TTF-1	transcription termination factor
TOP1mt	mitochondrial topoisomerase 1
TCA	tricarboxylic acid cycle
tRNA	transfer RNA
WT	wild type

1. INTRODUCTION

1.1 Mitochondrial origin

Mitochondria are eukaryotic organelles that originated in an endosymbiotic event about 2 billion years ago¹. According to the most prevalent hypothesis, this event involved a facultative anaerobic α -protobacterium and a hydrogen-dependent archaeal host able to respire in the presence of oxygen². In this symbiotic relationship the endosymbiont provided the host cell with ATP in exchange for carbohydrates³.

Additional evidence consequence of the endosymbiotic origin of mitochondria is the presence of mitochondrial genome (mtDNA). During the course of evolution some of the ancient genes from the endosymbiont were transferred to the nuclear genome (nDNA), others were lost, while yet others were replaced. Interestingly many genes involved in mtDNA replication and transcription are similar to bacteriophage enzymes and have probably been acquired by specific horizontal gene transfer events⁴.

Another interesting question in mitochondrial evolution is why mitochondria have retained their genome. One theory suggests that there is a need for a minimal mitochondrial genome to encode highly hydrophobic proteins that are difficult to import into the organelle. When encoded by mtDNA, such hydrophobic proteins can be synthesized *in situ* and any import difficulties are avoided. In support of this theory, the mitochondrial highly conserved *Cox1* and *Cytb* genes encode some of the most hydrophobic proteins present in mitochondria⁵. A second theory for the retention of mtDNA is based on the variations in codon usage between the nucleus and the mitochondria, which may have prevented any further gene transfer from the mitochondrion to the nucleus⁶. A third theory is the co-location for redox regulation theory, according to which the organelle has retained the genome in order to directly regulate the expression of key components of the respiratory electron transport chain depending on the intramitochondrial redox balance^{7,8}. In support of this latter theory, hydrogenosomes (degenerate mitochondria without ETC) have not retained their genome.

1.2 Mitochondrial function and form

Mitochondria are enclosed by double membrane that separate two aqueous compartments: the mitochondrial matrix and the intermembrane space⁹ (Figure 1). The outer membrane is permeable to all molecules of 5000 daltons or less. The inner mitochondrial membrane contains an extremely high protein content and is folded into invaginations, creating characteristic cristae¹⁰. The five complexes of the mitochondrial oxidative phosphorylation system (OXPHOS) are located in the inner membrane.

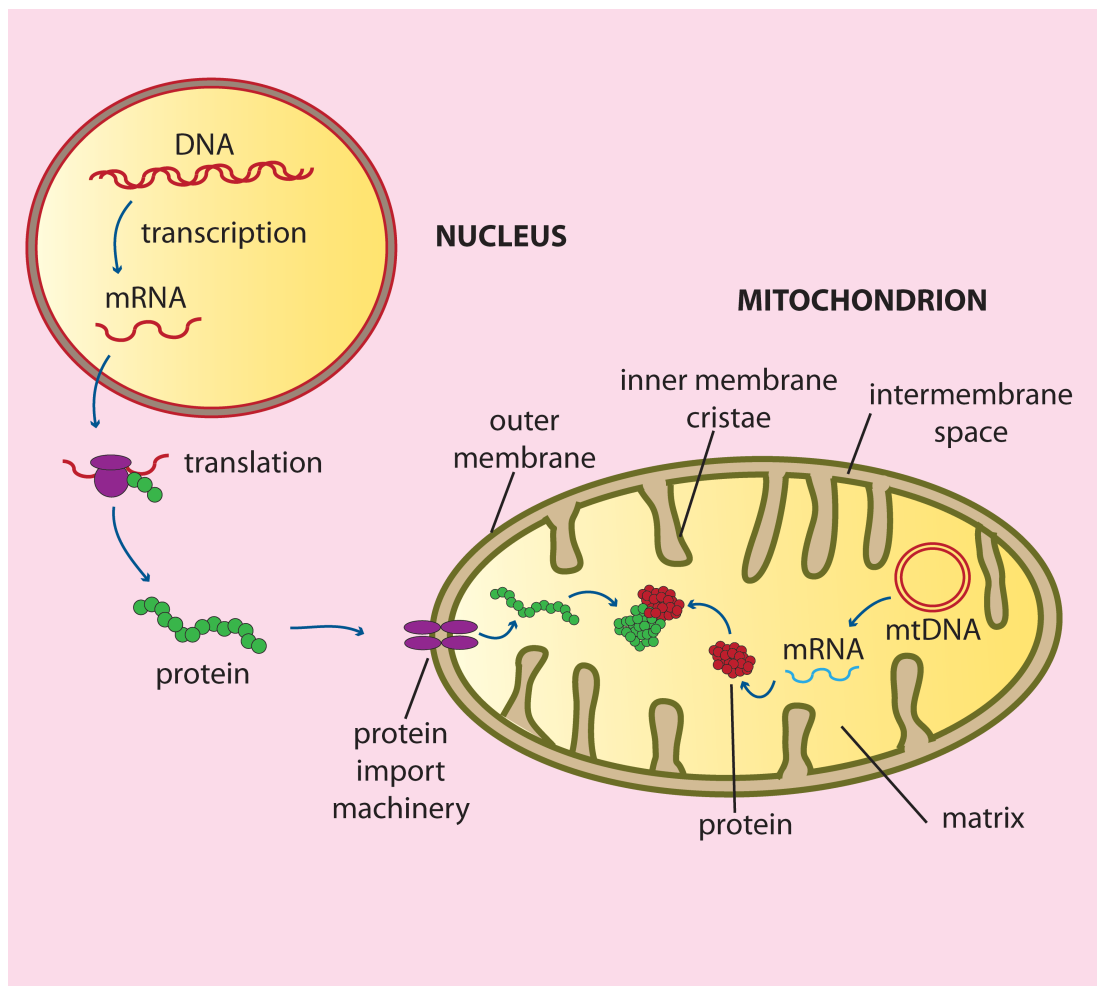


Figure 1: Structure of mitochondria and biogenesis of the oxidative phosphorylation system (OXPHOS). Mitochondrial compartments: IM (inner membrane), OM (outer membrane), IMS (intermembrane space) and matrix. The majority of the OXPHOS subunits and other proteins involved in mitochondrial metabolism or mtDNA maintenance are nuclear encoded, translated on the cytosolic ribosomes and imported into mitochondria through specialized import machineries.

The matrix contains a mixture of enzymes that metabolize pyruvate and fatty acids, and catalyze the citric acid cycle. Moreover, the matrix contains copies of mitochondrial DNA, proteins required for mtDNA replication and expression, and mitochondria ribosomes¹¹.

Mitochondria form a dynamic intracellular network and have an essential role in living systems by performing energy conversion to produce adenosine triphosphate (ATP) through the process of oxidative phosphorylation¹². The OXPHOS system is composed of five complexes (I-V) and consists of approximately 90 different subunits. Mitochondria can use both pyruvate and fatty acids as a fuel. Oxidation of carbohydrates in the citric acid cycle and lipids via β -oxidation generates the electron carriers NADH and FADH_2 which donate electrons to the ETC¹³. The ETC consists of four protein complexes, Complex I (NADH: ubiquinone oxidoreductase), complex II (succinate: ubiquinone reductase), complex III (ubiquinol-cytochrome c reductase), complex IV (cytochrome c oxidase). All of the complexes are under dual genetic control (mtDNA and nDNA) except complex II that is exclusively nuclear encoded¹⁴ (Figure 2).

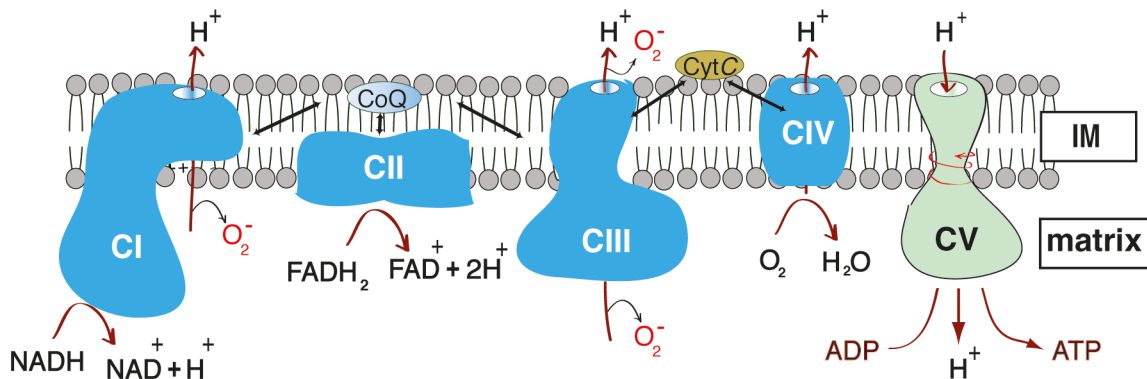


Figure 2: Schematic illustration of the structure and function the oxidative phosphorylation system. The OXPHOS system consists of five different enzyme complexes (Complexes I-V), and mobile carriers, coenzyme Q (CoQ) and cytochrome C. NADH and succinate are oxidized by complex I and II, the electrons are transferred to coenzyme Q, complex III, cytochrome C, complex IV and finally to molecular oxygen O_2 which is reduced to water (H_2O). Protons are pumped out from mitochondrial matrix by complexes I, III and IV forming a proton gradient across the inner membrane. The protons return to the matrix through ATP synthase and the energy of the proton gradient is used to drive ATP synthesis.

The electrons received by complex I and II are passed further through the ETC in a controlled series of redox reactions resulting in reduction of oxygen to water¹⁵. The electron transfer via ETC is coupled to the transfer of the protons from the matrix side, transferring them to the intermembrane space side thus creating an electrochemical proton gradient across the inner membrane. This electrochemical

gradient is fully utilized by the fifth component of the OXPHOS system, the ATP synthase or complex V, which by rotary catalysis combine ADP and phosphate into ATP, the main energy currency of the cell^{16,17}.

Besides cell energy conversion, mitochondria are also crucial for other biologically important functions including the regulation of cellular metabolism, fatty acid β -oxidation, the citric acid cycle, formation of reactive oxygen species (ROS), apoptosis, assembly of iron-sulphur clusters, and intracellular signalling¹⁸. As a consequence of their critical roles, mitochondrial dysfunction is implicated in many rare human genetic disorders and diseases such as Parkinson's and Alzheimer's disease, diabetes, as well as the ageing process¹⁸.

1.3 Organization of mtDNA

As a result of their endosymbiotic origin, mitochondria have retained their genome, and eukaryotic cells contain $\sim 10^3$ to $\sim 10^5$ copies of mtDNA. Mammalian mtDNA is a circular, double-stranded molecule of ~ 16.5 kb. The mtDNA contains 37 genes and encodes 2 ribosomal RNAs (rRNAs), 22 transfer RNAs (tRNAs), and 11 messenger RNAs (mRNAs) (Figure 3). The individual strands of the mtDNA molecules are referred to as the heavy (H) strand and the light (L) strand due to their different densities in alkaline cesium chloride gradients. Its only longer non-coding region is the so-called control region (non-coding region or displacement loop (D-loop) region), which harbors regulatory elements for transcription and replication (the promoters for the transcription of the L and H strands (LSP and HSP) and the origin of replication of the H-strand (O_H) (Figure 3). However, all of the proteins required for mtDNA maintenance and expression are encoded by the nuclear genome and have to be imported into mitochondria to fulfill their function²⁰.

The mtDNA is maintained in compact protein-coated structures known as nucleoids, with a mean diameter of ~ 100 nm²¹. In addition to its role in transcription, TFAM (mitochondrial transcription factor A) also plays a key role in mtDNA packaging into nucleoids²². Electron microscopy (EM) of biochemically *in vitro* reconstituted nucleoids combined with stimulated emission depletion (STED) microscopy of fixed cells showed that TFAM packages single mtDNA molecules in nucleoids that have a

slightly ellipsoid shape²³. TFAM is present at around 1000 copies per mtDNA molecule and has structural properties consistent with an important role in DNA compaction²⁴. Among the other suggested nucleoid associated proteins, some assist in processes such as DNA replication and transcription²⁵. Many different proteins involved in mitochondrial biogenesis and metabolism are suggested to be recruited to the nucleoids. This may allow mtDNA packaging, nucleoid division, and inheritance to be coupled to these processes²⁶.

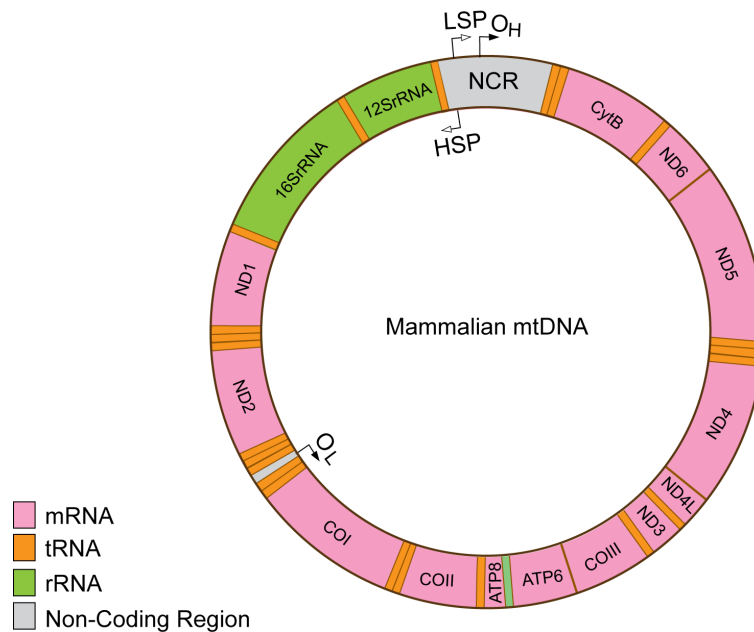


Figure 3: Organization of mtDNA. Non-coding regions harbor regulatory elements for transcription and replication. Transcription promoters: light-strand promoter (LSP) and heavy-strand promoter (HSP). Origins of replication: O_H , origin of H-strand DNA replication and O_L , origin of L-strand DNA replication. The tRNA genes encoded on each of the two strands are labeled with orange. mRNA and rRNA abbreviations: COI, cytochrome c oxidase subunit I; COII, cytochrome c oxidase subunit II; COIII, cytochrome c oxidase subunit III; Cytb, cytochrome b; ND1, NADH dehydrogenase subunit 1; ND2, NADH dehydrogenase subunit 2; ND4, NADH dehydrogenase subunit 4; ND5, NADH dehydrogenase subunit 5, ATP6, ATP Synthase 6, ATP8, ATP Synthase 8, ND6, NADH dehydrogenase subunit 6; 16S rRNA gene, 12S rRNA gene.

1.4 Replication of mtDNA

Replication of mtDNA is independent of the cell cycle and nDNA replication, and mtDNA can be replicated several times or not at all during mitosis. Replication of mtDNA occurs also in post-mitotic cells, as mitochondrial turnover continues in order to support their post-mitotic metabolic requirements. Complex machineries that are required for faithful mtDNA replication are present in the mitochondria and their basic components have been reconstituted *in vitro*²⁷. Cooperation of the mitochondrial heterotrimeric DNA polymerase (POL γ), the hexameric helicase TWINKLE, the tetrameric mitochondrial single-stranded binding protein (mtSSB) and the mitochondrial RNA polymerase (POLRMT) was shown to be necessary and sufficient for mtDNA replication in a recombinant *in vitro* reconstituted system^{27,28} (Figure 4).

Numerous other factors may also play important roles in mtDNA replication. Mitochondrial isoforms of the nucleases RNaseH1, FEN1 and DNA2 are implicated in replication primer removal and/or processing of the DNA flap that is formed when the replication apparatus has circled the entire mtDNA molecule. After processing of the DNA flap is complete, the mitochondrial DNA ligase (DNA ligase III) ligates the 5' and 3' nascent DNA ends to form a completed circle²¹.

The exact mechanism of mtDNA replication is still a matter of controversy and three different models have been suggested to date: a) the strand displacement model²⁹, b) strand-coupled model³⁰, c) mtDNA replication via ribonucleotide incorporation throughout the lagging strand (RITOLS) model^{31,32}.

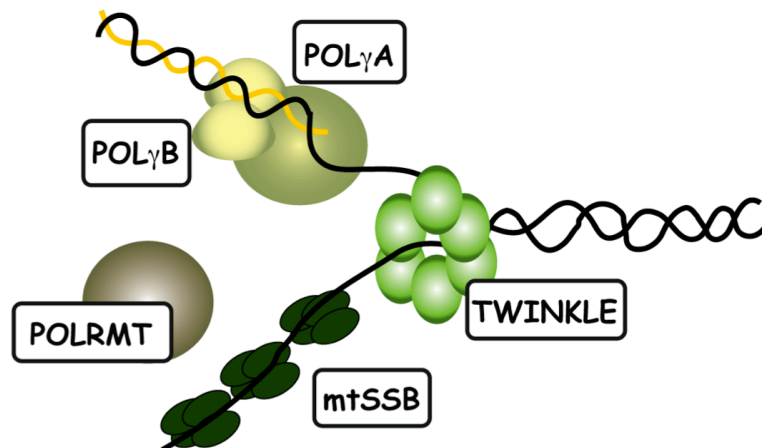


Figure 4: Components of the basic mtDNA replication machinery.

1.4.1 The strand-displacement model

Electron microscopy and atomic force microscopy analyses of replication intermediates greatly contributed to the generally accepted strand-displacement model (SDM) for mtDNA replication. This model proposes a unidirectional, asymmetrical synthesis of the leading H-strand until the region containing the origin of replication of the lagging L-strand is unwound initiating L-strand replication. Furthermore, in support of the SDM, CHIP analysis of mtSSB distribution *in vivo* has elucidated the additional role of mitochondrial single-stranded protein (mtSSB) in covering the displaced parental H-strand and blocking random primer synthesis on the displaced strand. It was shown that this wrapping with mtSSB restricted POLRMT activity and initiation of light-strand mtDNA synthesis. The finding that it is possible to initiate replication from O_L *in vitro*³³⁻³⁵ and that it is impossible to mutate some nucleotides in O_L *in vivo* lends support to the SDM as this is the only model in which O_L has a proposed function as a origin of the L-strand replication³⁴.

The origin for the L-strand replication is located in a non-coding region of ~30 nt and is flanked by five tRNA genes³⁶. O_L is activated when the growing daughter H-strand synthesis reaches about two-thirds of its total length, displacing the parental H-strand as a single strand. After strand displacement, O_L adopts a stem-loop structure

and RNA priming starts at the T-rich region. Recent work suggests that L-strand mitochondrial DNA replication is primed by mitochondrial RNA polymerase (POLRMT)³⁷. The biochemical analysis presented by Wanrooij and colleagues³⁸ demonstrated that POLRMT has two distinct modes of action. The enzyme efficiently transcribes long regions of dsDNA, but becomes much less processive on ssDNA, producing only short RNA molecules of 25-75 nt. The short RNA primers can be used by the mitochondrial DNA polymerase POLG to initiate DNA synthesis *in vitro* and this reaction is stimulated by the mitochondrial ssDNA binding protein (mtSSB). It was further demonstrated that, when combined, POLRMT, DNA polymerase POL γ , TWINKLE and mtSSB are capable of simultaneous leading and lagging-strand DNA synthesis *in vitro*. Following initiation at O_L, the lagging strand synthesis proceeds over the whole length of the mtDNA molecule³⁶.

1.4.2 The strand-coupled model

In addition to the SDM of replication, Holt and coworkers proposed an alternative mode of mammalian mtDNA replication, the so-called strand coupled model³⁹. This model for mtDNA replication proposes simultaneous leading and lagging strand mtDNA synthesis and it is based on observation of replication intermediates by two-dimensional agarose gel electrophoresis (2D-AGE)³⁹. According to the strand-displacement model, mtDNA replication starts bidirectionally from multiple origins across a region including the CytB and ND5 and ND6 genes. When the replication process reaches O_H, the replication fork is arrested and replication is restricted to one direction only⁴⁰.

1.4.3 RITOLS model

An additional model of replication called RITOLS mode (ribonucleotide incorporation throughout the lagging strand) was proposed³². This model differs from the strand displacement model by suggesting that the lagging strand is first synthesized as an RNA molecule that is later replaced by DNA. The authors speculate that the RNA may help to protect and stabilize the displaced ssDNA, or alternatively act to block transcription machineries that could interfere with the replication process³¹.

1.4.4 Mitochondrial non-coding region (D-loop region)

The mitochondrial D-loop or non-coding region (NCR) ranges between 880 and 1400 bp in length, and in its 5' domain it contains the main regulatory elements of the mitochondrial genome: the two promoters (HSP and LSP) and the origin of replication of the H strand.

Short conserved sequence blocks called CSB1, CSB2 and CSB3⁴¹ are present at the NCR 5' end. Those conserved sequences blocks are possibly involved in the RNA:DNA transitions and formation of the RNA primers for H-strand replication. Mitochondrial replication is coupled with transcription in mitochondria because transcription from LSP terminates prematurely at the conserved sequence block 2 (CSB2)^{42,43}. This termination event generates an RNA replication primer of ~100 nt (Figure 5).

A remarkable feature of mtDNA replication is the premature termination of the replication of the newly synthesized H-strands at the end of the mtDNA control region that results in the formation of a ~650 bp long structure known as 7S DNA or D-loop⁴⁴ (Figure 5). Nearly 95% of the H-strand initiation events are terminated in this manner.²⁹ The D-loop structure is triple stranded since the newly replicated DNA molecule remains bound and displaces the non-replicated strand⁴⁵. The half-life of the D-loop in cell culture is around 70 min, which shows that it is rapidly turned over²⁹.

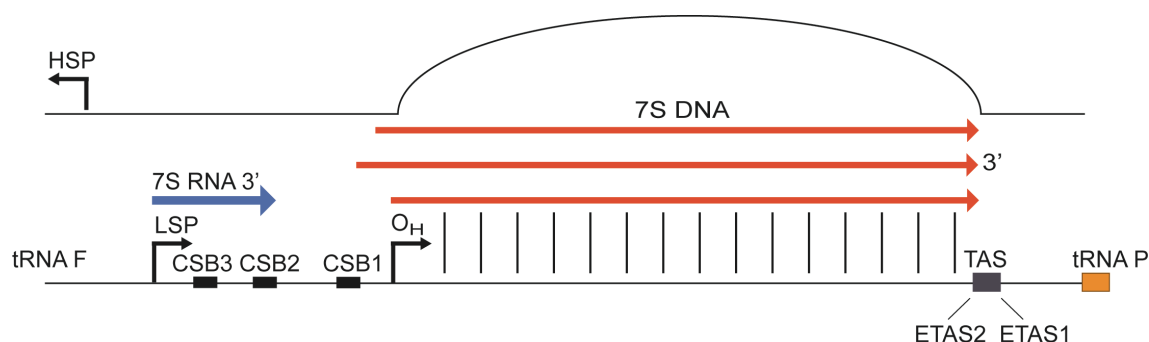


Figure 5: Mitochondrial D-loop region with regulatory elements.

Important roles for the 7S DNA have been proposed in mtDNA replication regulation, maintenance of DNA topology, recombination, dNTP metabolism and nucleoid

segregation, but its exact function and the mechanisms underlying its formation are still not understood⁴⁶.

In support for a regulatory role for the D-loop, the termination associated sequences (TAS sequences) composed of ~15-bp long repetitive conserved sequences are present at the end of the D-loop region⁴⁵ (Figure 5). Furthermore two new conserved blocks of about 60 bp were mapped at the 3' end of D-loop region called ETAS1 and ETAS2 (extended TAS sequences). Mapping such a region of conserved sequences suggested their possible role in multiple terminations signals functioning between mitochondrial transcription and replication. Potentially, protein factor(s) that are binding to the conserved TAS sequences are leading to premature DNA synthesis and 7S DNA formation. *In vitro*, *in organello*, and *in vivo* footprinting approaches in different mammalian species identified protein-binding sites at the 3' region of the control region of mitochondrial DNA. Proteins with contrahelicase activity have been described in prokaryotic and eukaryotic systems^{47,48}. In sea urchin, the mitochondrial D-loop binding protein (mtDBP) has been shown to bind to the 3' end of the D-loop region, to display contra-helicase activity, and to negatively regulate DNA synthesis⁴⁹. In *Escherichia coli*, the replication termination factor TUS arrests the replication fork via protein-protein interaction with the replicative helicase⁵⁰. Moreover a 48 kDa protein of unknown function has been reported to bind to ETAS sequences and promote 7S DNA formation in bovine mitochondria⁴⁷. However no TAS-binding protein in mammals has yet been identified.

1.4.5 Mitochondrial DNA polymerase POL γ

There are 16 specialized polymerases present in mammalian cells required for nuclear and mitochondrial genome maintenance. POL γ is a highly efficient and processive polymerase located in mitochondria, and is responsible for mtDNA replication and repair. Disruption of the POL γ in mice causes an early developmental arrest between E7.5 and E8.5 associated with severe mtDNA depletion, confirming its essential role in mtDNA maintenance⁵¹. POL γ is a member of a family A class of DNA polymerases which also includes the *E. coli* DNA polymerase I and the T7 DNA polymerase⁵². The mammalian mtDNA polymerase holoenzyme is a heterotrimer with one catalytic POL γ A subunit and two accessory POL γ B subunits.

The POL γ A subunit is a 140 kDa peptide with a 3'-5' exonuclease domain that is connected with the 5'-3' polymerase domain via a linker region. In humans, the linker region is a 482 amino acids long region and mutations in this region have been linked to several mitochondrial disorders. The exonuclease domain has proofreading activity during replication and it can remove inaccurately incorporated nucleotides⁵³. Recently it has been reported that the exonuclease activity of POL γ is required for successful DNA ligation in the final step of mtDNA replication at O_H⁵⁴. Moreover the coordination between POL γ and newly described mitochondrial nuclease MGME1 has been shown to be sufficient for flap removal and ligation to complete mtDNA replication⁵⁵. Mice that have an exonuclease-deficient version of POL γ have increased levels of point mutations, linear mtDNA fragments, and develop symptoms of premature ageing⁵⁶.

The accessory subunit POL γ B has a molecular mass of 55 kDa. POL γ B was demonstrated to stimulate the catalytic activity and processivity of POL γ A, by enhancing DNA binding and increasing the polymerase rate⁵⁷. POL γ B has sequence and structural similarities with the anticodon-binding pocket of the prokaryotic aminoacyl-tRNA synthetases, a group of enzymes that catalyze the attachment of each amino acid to its corresponding tRNA. The accessory subunit of DNA polymerase is present in *Homo sapiens*, *Mus musculus*, and *Drosophila melanogaster*, but is absent from *Saccharomyces cerevisiae*⁵⁸. The protein has dsDNA binding activity and is required to ensure that the polymerase stays bound to the template behind the moving TWINKLE helicase⁵⁹.

In conclusion, the role of POL γ is vital for mitochondrial function, and defects in this enzyme are the most common cause of mtDNA stability disorders causing conditions such as progressive external ophthalmoplegia (PEO), Alpers syndrome, adult onset ataxia, and infertility.

1.4.6 Mitochondrial replicative helicase - TWINKLE

Helicases are universally present enzymes in prokaryotes, eukaryotes and viruses with key functions in DNA and RNA metabolic processes, including replication, recombination, DNA repair, transcription and translation⁶⁰. During DNA replication, helicases play an essential role in unwinding the double-stranded template in front of

the DNA polymerase and the resulting ssDNA strands are used as a templates for the synthesis of the complementary DNA strands²³. The mitochondrial replicative helicase TWINKLE unwinds double-stranded DNA in a 5' -> 3' direction using NTP hydrolysis as an energy source. This protein is homologous to the bacteriophage T7 gene 4 primase/helicase (T7gp4 protein), especially in its helicase domain. Interestingly, the TWINKLE protein has not retained the primase role in mitochondrial replication, hence POLRMT is responsible for priming DNA synthesis at both strands^{61,37}.

The *Twinkle* gene was originally discovered just over a decade ago, in a screen for mutations linked to autosomal dominant PEO (adPEO)⁶¹. Patients with this human disorder present exercise intolerance, muscle weakness, peripheral neuropathy, deafness, ataxia, hypogonadism, and cataracts⁶². adPEO patients accumulate various mtDNA deletions across different postmitotic tissues⁶². The TWINKLE protein is comprised of a carboxy-terminal helicase domain, a middle linker domain, important for subunit interaction and multimerisation, and an amino terminal domain of unknown function.⁶¹

Over 30 different TWINKLE mutations are known to cause accumulation of deletions or depletion of mtDNA, thereby inducing mitochondrial energy defects which result in neuro-muscular symptoms^{63,64}.

The consequences of various TWINKLE mutations have been studied *in vitro* by using recombinant proteins and expressing mutant protein versions in human and insect cell lines^{65,66}. In particular, the effects of adPEO-causing mutations in the linker region have been studied as those show abolished protein hexamerisation and DNA helicase activity, which causes replication stalling. Overexpression of the mutated *Twinkle* in human cells showed mtDNA depletion and accumulation of replication intermediates and also induced changes in nucleoid structure^{64,66,67}.

Additionally, the consequences of dominant *Twinkle-PEO* mutations have been investigated *in vivo* using a transgenic mouse strategy. To this end, a so called Deletor mouse, which contains a transgene carrying a 13 amino acid-long duplication in the TWINKLE linker region, was generated⁶⁸. In this model, older mice expressing the PEO linked mutations accumulate mtDNA deletions in muscle and brain, and show a cellular phenotype similar to PEO patients with present aberrant mitochondrial structures. These mice also show mtDNA depletion in brain, but not in muscle and heart⁶⁸.

Severe phenotypes in patients with PEO mutations correlate with the amount of residual helicase activity in Twinkle mutants, suggesting that proper helicase activity is required for TWINKLE to function⁶⁴. Additionally to dominant PEO mutations, the recessive mutation Y508C has been described in the helicase domain of TWINKLE. This recessive mutation is known to cause IOSCA a form of infantile-onset spinocerebellar ataxia⁶⁹. From the analysis of patient cells and a homozygous IOSCA knockin mouse model, it has been shown that IOSCA is associated with tissue-specific mtDNA depletion in the liver and cerebellum, and decreased concentrations of all dNTPs. Furthermore, IOSCA mice eventually developed mitochondrial epileptic encephalopathy, mimicking the IOSCA phenotype seen in human patients⁷⁰.

Several mutant forms of TWINKLE have been expressed in *Drosophila melanogaster*, where they caused severe depletion of mtDNA and lethality⁶⁵. Mitochondrial impairment caused by these mutations promotes apoptosis⁶⁵. This observation is in line with the finding that *in vitro* depletion of TWINKLE in Schneider cells is decreasing mtDNA copy number⁷¹.

Finally, the *in vivo* function of TWINKLE has been investigated using a mouse model⁷². We created and analyzed conditional *Twinkle* knockout (KO) mice and proved that TWINKLE is the only mitochondrial replicative helicase since it is essential for the mouse embryonic development⁷². Tissue-specific TWINKLE KO in the heart and skeletal muscle of mice resulted in severe and rapid mtDNA depletion and consequently decreased mitochondrial encoded transcripts and protein steady-state levels. Southern blot analysis showed that TWINKLE is required for the unwinding of the entire mtDNA molecule as well as for the abortive replication at the D-loop region⁷².

1.4.7 Mitochondrial single-stranded DNA binding protein - mtSSB

A single-stranded DNA binding protein, mtSSB is present in mitochondria to maintain integrity of long single-stranded DNA regions during replication. mtSSB is a tetramer that consists of four 16 kDa subunits and shares similarities with the *E. coli* SSB protein. Besides DNA stabilization, mtSSB has a stimulatory effect on the rate of DNA unwinding by TWINKLE^{27,73}, probably due to a direct protein-protein interaction⁷⁴

1.4.8 Additional proteins involved in mitochondrial DNA replication

The list of the proteins involved in mitochondrial DNA replication has been expanded during recent years. Just like any other DNA, mtDNA requires the activity of various enzymes with nuclease, ligase, and topoisomerase activities.

Topoisomerases are enzymes that adjust DNA topology for replication and transcription processes⁷⁵. Mitochondrial topoisomerase I (TOP1mt) transiently breaks one DNA strand at a time and thereby belongs to the type I topoisomerases. In TOP1mt knockout mice, an increased negative supercoiling of mtDNA indicates that mitochondria contain an efficient topoisomerase activity that relaxes positive supercoiling of DNA⁷⁶. Apart from TOP1mt, two additional topoisomerases (Top2 α and Top2 β) were shown to localize to mitochondria in mouse and human models. Top2 α and Top2 β are type IIA topoisomerases - in mitochondria they are potentially critical for supercoil relaxation, enabling transcription and replication⁷⁷, and may also have roles in decatenating locked mtDNA circles formed during replication⁷⁶.

Ribonuclease H1 (RNase H1) is localized in both the nucleus and mitochondria. Analysis of mtDNA from knockout mouse models and human patient studies strongly indicates that RNase H1 removes the RNA primers at the origins of the light and heavy strand replication. Therefore, RNase H1 is essential for proper mtDNA replication in humans, and pathogenic RNaseH1 mutations cause mtDNA replication stalling, mtDNA depletion and deletions⁷⁸.

DNA ligase III activity is present in mitochondria, and human cells with impaired DNA ligase expression have reduced mtDNA copy number and multiple single-stranded nicks⁷⁹. Additionally, deletion of ligase III in mice causes embryonic lethality at E8.5, similar to the other mouse knockouts with germline disruption of genes essential for maintenance or expression of mtDNA⁸⁰.

1.4.9 Mitochondrial genome maintenance exonuclease 1 – MGME1

Recently, two different laboratories reported an exclusively mitochondrial protein called mitochondrial genome maintenance exonuclease 1 (MGME1 a.k.a. Ddk1) to be involved in processing of mitochondrial DNA during the replication^{81,82}. MGME1 belongs to the RecB subclass of PD-(D/E)XK endonucleases (Figure 6).

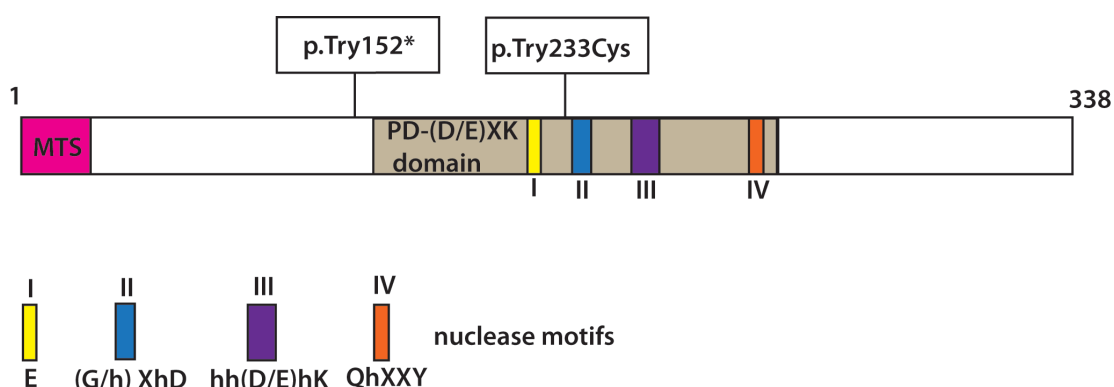


Figure 6: Schematic representation of the MGME1 protein and localization of the investigated homozygous mutations causing disease. The motifs of the PD-(D/E)XK nuclease superfamily are indicated with Roman numerals. MTS indicates mitochondrial targeting signal.

Loss of function mutations in the gene encoding MGME1 cause a severe multisystemic mitochondrial disorder⁸². The mtDNA from muscle of affected patients shows various defects, including deletions, depletions, rearrangements, and 7S DNA accumulation⁸³. *In vitro* analysis of recombinant MGME1 showed that the protein exhibits 5'-3' nuclease activity with a specificity for single-stranded DNA^{81,82}. It shows no activity on RNA, even when hybridized to DNA. *In vitro* nuclease-ligation assays have confirmed that MGME1 cleaves longer flaps efficiently but imprecisely around the flap base. The MGME1 activity requires the 3'-5' exonuclease activity of POL γ for proper flap removal and nick ligation at O_H⁵⁵. Precisely processing the long primer formed at O_H in the mitochondrial NCR may require a teamwork of different nucleases. Initiation of mtDNA synthesis includes the RNA-DNA transition immediately after CSB2, but the 5' ends of the nascent DNA are moved around 100 bp downstream of the transition site by presumably a long-flap pathway⁸⁴. In support of this, 7S DNA from MGME1 deficient patient cells contains 5' extended ends suggesting that Mgme1

activity is necessary for processing of the single-stranded flap intermediate^{83,84}. MGME1 patient cells also contain an 11 kb truncated linear mtDNA fragment, the ends of which map near O_H and O_L suggesting that MGME1 is involved in primer flap processing at O_H⁸³. Interestingly nucleases like FEN1 and DNA2 may also have roles in mtDNA base excision repair and flap processing in mitochondria^{85,86}. Therefore it has been hypothesized that additionally to its exonuclease role, which is necessary for proper replication and flap processing in mitochondria, MGME1 might have a role in mtDNA repair.

1.5 Transcription of mtDNA

RNA synthesis in mammalian mitochondria is initiated from two different promoters, both located in the D-loop; LSP and HSP. Transcription of the L-strand is initiated at the LSP, resulting in a primary transcript encoding mRNA-ND6 and eight tRNAs. Transcription of the H-strand produces a polycistronic transcript covering almost the entire H-strand^{87,88}. Almost all the mRNA and rRNA genes are flanked by one or more tRNA gene. Excision of tRNA molecules is required to produce mature mRNA and rRNA molecules from the polycistronic transcripts according to so-called tRNA punctuation model⁸⁹.

1.5.1 The basic components of the mitochondrial transcription machinery

The basal transcription initiation machinery consists of three proteins: mitochondrial RNA polymerase (POLRMT), mitochondrial transcription factor A (TFAM), and mitochondrial transcription factor B2 (TFB2M)⁹⁰⁻⁹². Recently, a transcription elongation factor (TEFM) was reported to enhance POLRMT processivity to produce large polycistronic transcripts covering almost the entire length of each strand^{93,94}.

POLRMT is a large single subunit enzyme of 140 kDa that shows a high sequence similarity with both the T3 and T7 bacteriophage polymerases. It is the only RNA polymerase operating in mammalian mitochondria. Loss of POLRMT leads to embryonic lethality at E8.5, as seen in other mouse models with germline disruption of genes essential for replication or expression of mtDNA³⁷. It has been confirmed that

POLRMT is essential for primer synthesis to initiate mtDNA replication also *in vivo*³⁷.

Although POLRMT can specifically recognize mitochondrial promoters, it cannot initiate transcription without assistance from two additional transcription factors, TFAM and TFB2M⁹⁰.

TFAM belongs to the high-mobility (HMG)-box family of proteins, and can bind, unwind and bend DNA⁹⁵. The vital importance of TFAM for mtDNA maintenance was demonstrated in studies of homozygous TFAM knockout mice, which showed embryonic lethality and severe depletion of mtDNA⁹⁶. As one of the major protein components of nucleoids, TFAM is likely to fully coat mtDNA^{21,97}. TFAM binds sequence-specifically to promoter elements immediately upstream of the HSP and LSP transcription start sites. Structural studies showed that TFAM-binding introduces sharp U-turns of mtDNA, which may facilitate promoter melting⁹⁸. The DNA bending is clearly important for transcription activation and previous studies indicate that the C-terminal tail of TFAM plays an essential role in transcription activation^{99,100}.

TFB1M and TFB2M can assist TFAM and POLRMT during the initiation of the transcription process. TFB2M is more active in stimulating specific transcription as is TFB1M *in vitro*. Both factors are closely related to the family of bacterial rRNA dimethyltransferases and our results suggest that TFB2M is a transcription factor whereas TFB1M has no role in transcription but rather functions as a 12S rRNA methyltransferase{Metodiev:2009dz}.

TFB2M is essential for complex formation during mitochondrial transcription initiation¹⁰¹, and crosslink experiments reveal a direct interaction of TFB2M with the promoter starting site, where it is involved in promoter melting to facilitate transcription initiation by POLRMT¹⁰¹. Additionally increased levels of TFB2M activates mitochondrial transcription and causes elevated steady-state levels of mitochondrial transcripts^{90,102} suggesting a direct and essential role in mitochondrial transcription.

TFB1M was shown to methylate two adenine residues in a conserved stem loop region of the 12S rRNA, which is an important post-transcriptional modification in the process of mitochondrial ribosomal biogenesis^{103,104}. Therefore, TFB1M is thought to have its main function in ribosomal maturation rather than in transcriptional initiation¹⁰⁴.

Recently, the transcription elongation factor (TEFM) was reported to enhance

POLRMT processivity by promoting the production of large polycistronic transcripts covering almost the entire length of each strand^{93,94}. Mitochondrial transcription elongation factor (TEFM) interacts with the catalytic domain of POLRMT and its depletion leads to a reduced transcription elongation and decreased promoter-distal mitochondrial transcripts. Therefore, TEFM aids the transcription of longer RNA products and the circumvention of highly structured regions. Furthermore it has been shown that interaction of the transcription elongation factor (TEFM) with the mitochondrial RNA polymerase (POLRMT) and the nascent transcript prevents the generation of replication primers, increases transcription processivity and thereby serves as a molecular switch between replication and transcription^{93,105}.

1.5.2 Regulation of transcription termination

Mechanisms regarding mtDNA transcription termination in mammalian organisms are still under debate. Previously it was reported that transcription of the heavy strand is initiated from two different sites: HSP₁ and HSP₂¹⁰⁶. Transcripts from HSP₁ were proposed to terminate immediately after the 16S site, while transcription from HSP₂ promoter continues past the termination site, along almost the entire length of the H-strand. This premature termination justified why HSP₁ transcripts resulted in a 50-times higher abundance of rRNAs than mRNAs produced downstream of the termination site¹⁰⁷. This termination event was suggested to be mediated by specific binding of mitochondrial termination factor 1 (MTERF1). However, *in vivo* studies in MTERF1 knockout mouse reported that MTERF1 blocks L-strand transcription to prevent transcription interference at the light-strand promoter, while not having an effect on H-strand transcription¹⁰⁸. Additional roles of MTERF1 have been investigated *in vitro*, where overexpression of MTERF1 causes replication pausing. These findings have been confirmed after a recent study proposed a model where the MTERF1 binding site is a pausing site for the replication machinery while POLRMT passes the rRNA region. After the halt, the transcription machinery can remove the MTERF1 block and replication can continue. Hence MTERF1 acts as contrahelicase postponing the progression of DNA replication and avoiding collisions between the replication and transcription machineries in the rDNA region¹⁰⁹. The MTERF protein family has an

important role in the regulation of mitochondrial transcription at the level of termination in different species. In addition to its transcriptional termination activity, mtDBP, the MTERF1 homologue in sea urchin, also plays a role in mtDNA replication acting as a contra-helicase, which negatively regulates mtDNA synthesis⁴⁹. The L-strand transcription is frequently terminated at the mitochondrial non-coding region, at the CSB1 and CSB2 sequences, when a G-quadruplex structure is formed between the nascent RNA and the non-template DNA strand. Interestingly, this structure covers the 3' end of the RNA primer formed by premature transcription termination at the CSB2 site, and the primer appears inaccessible to the DNA replication machinery. There are possible additional proteins involved in resolving this hybrid structure and enabling utilization of the RNA primer for initiation of mtDNA replication at OriH¹¹⁰.

H-strand transcription is initiated from only one promoter and encompasses nearly the entire mitochondrial genome with termination occurring in a region immediately upstream of the tRNA^{Phe} gene, at the termination associated sequences in the mitochondrial control region¹⁰⁸. Recent findings suggest that termination of H-strand transcription and premature mtDNA termination at core-TAS are functionally linked¹¹¹. Further studies are necessary to elucidate the exact regulatory molecular mechanisms of mitochondrial transcription and replication on both mtDNA strands.

1.6 Mitochondrial DNA repair

The mitochondrial respiratory chain is a site for ROS (reactive oxygen species) and RNS (reactive nitrogen species) production, since molecular oxygen can differently react with RC electrons¹¹². ROS are generated at several locations in the cell, but 90% is produced by the ETC in the mitochondria¹¹³. Imbalance between ROS and/or RNS production and antioxidant defense mechanisms can lead to “oxidative stress”, which is highly harmful for cell functionality. Contrary to this detrimental role of ROS, fluctuations in the steady-state levels of ROS have appeared important for cell signaling, cell cycle progression, and apoptosis¹¹⁴. ROS consist of a variety of highly reactive molecules and free radicals formed from reactions including molecular oxygen. One of the most common ROS species is the superoxide anion ($O_2^{\bullet-}$), which can produce hydrogen peroxide (H_2O_2) in a reaction catalyzed by superoxide dismutases or via spontaneous reactions. H_2O_2 can be further reduced to water or via a Fenton

reaction converted to the highly reactive hydroxyl radical (OH•). In mitochondria, the majority of O₂•⁻ production is through complex I and complex III¹¹⁵. The well-known mitochondrial free radical theory of ageing poses that ROS produced in mitochondria are a primary source of cellular free radicals contributing to the ageing process¹¹⁶. Furthermore a “vicious cycle” has been suggested whereby subsequent ROS induced mutations in mtDNA would accumulate and lead to dysfunctional OXPHOS components that would produce more ROS and mtDNA mutations, finally resulting in cell damage¹¹⁷. Therefore the main assertions for vulnerability of mtDNA and source of mtDNA mutations are: a) proximity of mtDNA to OXPHOS system and exposure to superoxide radicals b) lack of mtDNA repair mechanisms; and c) replication errors during normal DNA synthesis in mitochondria. Although mtDNA was initially thought to lack repair systems, several repair pathways have recently been reported.

The main repair pathway found in mitochondria is base excision repair (BER), which includes single-nucleotide BER (SN-BER) and long-patch BER (LP-BER)^{118,119}. Initial damage recognition and cleavage is performed by the specific glycosylases, and mitochondria contain six damage-specific glycosylases. UDG-uracil DNA-glycosylase I and OGG1-8-oxo-G DNA-glycosylase/AP lyase are expressed as both nuclear and mitochondrial isoforms. Additionally MUTYH and NTH (thymine glycol glycosylase) and two endonuclease VIII-like proteins (NEIL1 and NEIL 2) are reported to be present in mitochondria. After DNA-glycosylase cleavage, the DNA phosphate backbone is cleaved by AP endonuclease. During the single-nucleotide SN-BER, POL γ is filling single nucleotide gap prior to ligation. In the case of long patch LP-BER, during the gap filling POL γ is displacing the 5' DNA strand thus creating a 5'-flap structure. FEN1, DNA2 and EXOG enzymes were implied to play a role in 5'-flap removal prior to ligation⁸⁴. Long patch repair is mainly responsible for repairing common lesions caused by oxidative damage to sugar-phosphate backbone¹²⁰.

Nucleotide excision repair (NER) has not been reported to operate in mitochondria, even though many chemical carcinogens enter in mitochondria and interact with mtDNA, possibly causing large lesions⁵³.

Another repair mechanism required for removal of base mismatches and small insertions called mismatch repair (MMR) has been reported to operate in *S. cerevisiae* and *S. pombe*¹²¹. Regarding the MMR in higher eukaryotes, a low level MMR repair

activity was identified in rat liver mitochondrial lysate¹²² but the main MMR enzymes active in nucleus have not been identified. Many recent studies that involve knockout mouse models of repair enzymes (MUTYH, OGG1, NEIL1) develop tumors¹²³, metabolic syndrome¹²⁴ and obesity¹²⁵. Additionally disruption of OGG1/MYH genes in mice did not result in a higher mtDNA mutation rate¹²⁶. In the future, a mitochondrial specific knockout of these repair enzymes can contribute to the investigation of their specific role only in mitochondria. Finally many of the proteins playing a role in mtDNA repair are also implicated in mtDNA replication showing tight coordination of those pathways in keeping the integrity of mtDNA.

1.7 Mitochondrial genetics and diseases

Mitochondrial diseases are the most common causes of inherited metabolic disease in humans with a frequency of about 1 in 5000¹²⁷. Human mitochondrial disorders encompass a genetically heterogeneous group of different diseases, caused by mutations in mitochondrial and/or nuclear DNA and display both clinical heterogeneity and tissue specificity¹²⁸, with the brain and muscle being the most commonly affected tissues¹²⁹. The inheritance pattern of mtDNA-related diseases can vary from case to case. Some patients appear to be sporadic cases, while others are clearly inherited. Clinical heterogeneity can be explained by the specific features of mtDNA genetics; since mtDNA is maternally inherited, mutations in mtDNA are not transmitted according to Mendelian principles. In normal cells, most mtDNA copies are assumed to be identical, a condition known as homoplasmy. Pathogenic mutations of mtDNA are usually present only in a subset of all mtDNA molecules. This mixture of mutated and wild-type mtDNA molecules is called heteroplasmy¹³⁰.

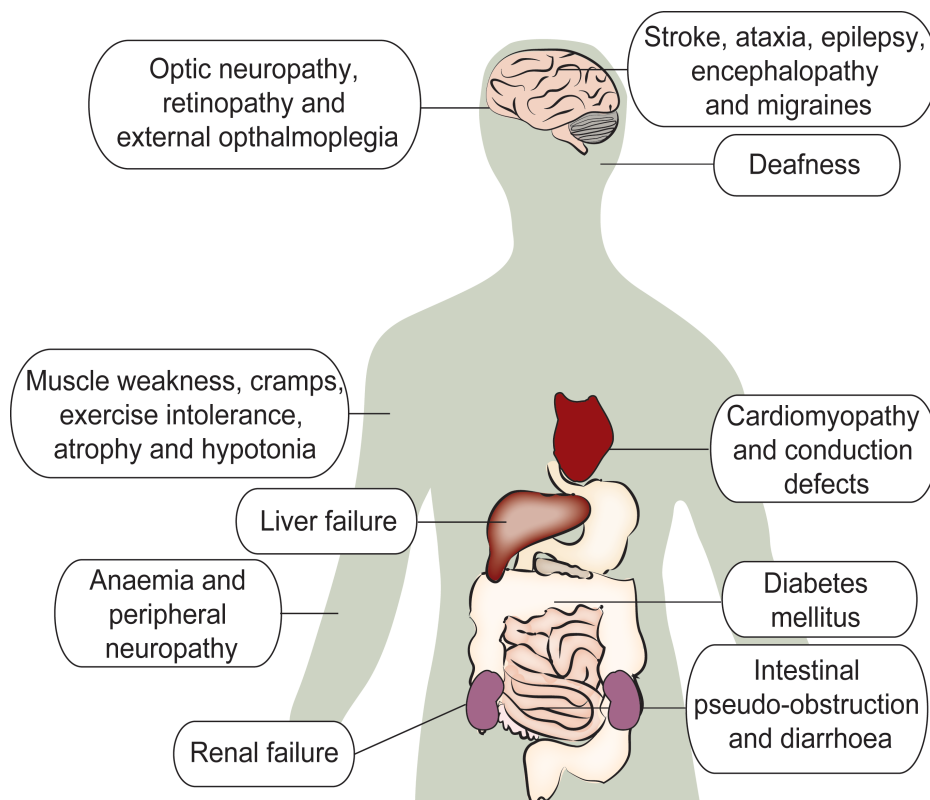


Figure 7: Common clinical manifestations of mitochondrial disorders

Very often the proportion of mutant and normal mtDNA in a tissue determines the clinical outcome of the mutation. This means that a disease or biochemical defect will be caused only when a pathogenic mtDNA mutation is above a certain threshold level¹³¹. This threshold level in turn depends on the mutation type and tissue energy demand. Furthermore, mtDNA populations undergo a bottleneck effect which means that only a small proportion of the total number of mitochondrial genomes are passed on from mother to offspring¹³². Therefore through this bottleneck effect, pathogenic mutations can segregate to very different heteroplasmy levels in the offspring. Consequently, a mother carrying a pathogenic mutation can give birth to both severely sick and healthy children¹³⁰.

1.7.1 Mitochondrial disorders caused by mtDNA mutations

There are two major types of mtDNA defects that may occur: large rearrangements (including deletions and duplications) and point mutations. The defects can be present in the germline and be transmitted maternally, or appear randomly in somatic cells¹³³.

Point mutations are the most predominant cause of disease in humans and there are several mitochondrial disorders known to be induced by them. Mitochondrial encephalomyopathy, lactic acidosis and stroke-like episodes (MELAS) syndrome is a multisystem disorder with impaired motor ability, vision and deficient cognitive activity¹³³. MELAS is caused by a few point mutations, the most prevalent of which is an A>G transition at m.3243 in tRNA^{Leu(UUR)}, but also in the ND5 gene. Another neuromuscular disorder known as myoclonus epilepsy with ragged red fibers (MERRF) syndrome is a consequence of point mutation m8344 A>G in tRNA^{Lys}. The clinical severity of MERRF correlates with heteroplasmy levels, and the biochemical manifestations of MELAS and MERRF are seen as a defect in complex I and/or IV. One of the most common mtDNA-mutation disorders is Leber's hereditary optic neuropathy (LHON), characterized by subacute bilateral visual failure in young adults¹³⁴. Usually patients carry homoplasmic point mutations m.3460 G>A, m.11778 G>A, m14484 T>C in genes coding for complex I subunits of the RC.

Another type of mitochondrial DNA mutations are mtDNA rearrangements that are sporadic. Single large-scale deletions have been associated with progressive external ophthalmoplegia (PEO), Kearns-Sayre syndrome (KSS) and Pearson's syndrome¹⁸.

1.7.2 Mitochondrial disorders caused by nDNA mutations

Several diseases have been shown to be due to mutations in nuclear genes encoding mitochondrial proteins. During the last decade, researchers have defined a list of genes linked to human mtDNA maintenance disorders mostly affecting mtDNA replication. Numerous pathogenic mutations leading to mtDNA instability are reported in the genes encoding basic replication components such as POLGA, POLGB, TWINKLE¹³⁵, and replication/repair related factors including DNA2, RNaseH1, and the recently reported MGME1 nuclease^{82,136,137}. Mutations in these genes are causing

mtDNA depletion, accumulation of replication intermediates and stalled replication. Typical clinical features include PEO, characterized by muscle weakness affecting most severely the external eye muscle, exercise intolerance and loss of strength. Known syndromes include Alpers syndrome, hepatocerebral syndromes, myopathies¹³⁸.

Mitochondrial DNA depletion syndrome (MDS) causes mtDNA depletion in the affected tissue and many mutations in many genes have been reported to be associated with MDS: *TK2*, *TYMP*, *DGUOK*, *RRM2B*, *SUCLA2*, *SUCLG1*, *SLC25A4*, *OPA1*, *POLG*, *POLG2*, *PEO1*¹³⁹. Besides these well characterized genes, mutations in the *MPV17* gene encoding the mitochondrial inner membrane protein responsible for nucleotide transport or the *ANT2* protein involved in the import of ATP into mitochondria, have been associated with MDS syndrome^{140,141}.

Furthermore mutations affecting respiratory chain protein assembly or stability encompass a large group of mitochondrial diseases. Complex I and IV deficiencies are well-recognized biochemical defects in mitochondrial disorders. Several nuclear mutations were identified in structural or assembly subunits of complex I resulting in Leigh syndrome and diverse cardiomyopathies and encephalopathies. Similarly, cytochrome oxidase deficiency mutations result in fatal, infantile diseases such as Leigh syndrome, MELAS, congenital abnormalities and motor neuron disease-like presentation⁶².

2. AIMS

Replication of mtDNA and mtDNA copy number control are essential steps in mitochondrial gene expression and may play a role in the regulatory processes coordinating nuclear and mitochondrial gene expression in response to the physiological demands of the cell. Despite the fact that the basic mitochondrial replication machinery components are known, regulatory mechanisms controlling mitochondrial replication and maintenance are still largely unknown. The goal of my PhD project is to gain further insights into mtDNA replication and its regulatory mechanisms by generating and analyzing mouse models with altered mtDNA replication.

The specific aims of my PhD project are:

1. Characterization of the *in vivo* effects of TWINKLE overexpression using a transgenic mouse model.
2. Unraveling the *in vivo* role of the MGME1 protein in mtDNA maintenance by generating and analyzing the *Mgme1* knockout mouse model.

3. RESULTS

3.1 Twinkle overexpression leads to elevated mtDNA levels

The role of TWINKLE as the mitochondrial replicative helicase has been demonstrated *in vitro*, where a combination of recombinant POL γ , mtSSB and TWINKLE efficiently generated a DNA product of around 16kb²⁷. Our group investigated the *in vivo* role of TWINKLE in mitochondrial replication and D-loop synthesis by analyzing *Twinkle* knockout mouse⁷².

To gain further insights into TWINKLE's *in vivo* function and mtDNA copy number control, we investigated the effects of TWINKLE overexpression by generating *Twinkle* bacterial artificial chromosome (BAC)-transgenic mice. The advantage of the BAC-transgene method is the utilization of the large chromosome segments that contain the chosen gene, its endogenous promoter and relevant regulatory sequences. Therefore transgene expression is regulated in a close-to-physiological manner in the mouse typically showing moderately increased total expression of the studied gene.

The transgenic animals were generated through pronuclear injections of BAC clones containing the mouse *Twinkle* gene, modified for the genotyping purposes by introduction of the *XhoI* silent mutation into exon 1 using BAC recombination technology¹⁴² (Figure 3.1).

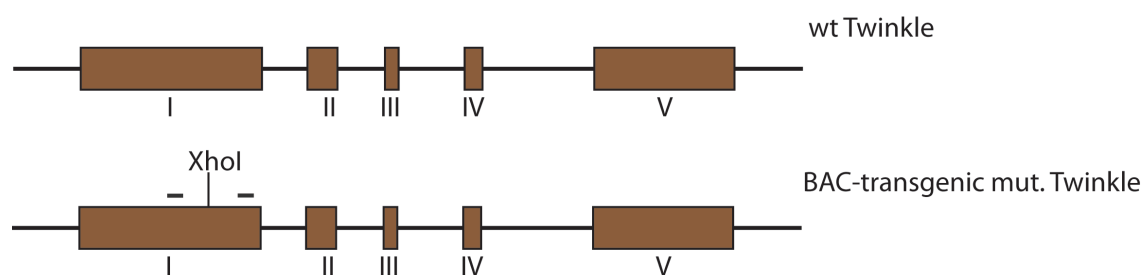


Figure 3.1: BAC transgenic strategy. Wild-type (wt) *Twinkle* gene and *Twinkle* BAC transgenic locus with silent mutation introduced in exon I. Black dashes indicate positions of the primers in exon I used for genotyping.

The presence of BAC transgenic DNA was assayed by PCR combined with restriction enzyme digestion, and electrophoretic analysis of PCR products. Figure 3.2 A illustrates PCR performed on a TWINKLE BAC transgenic construct and wild-type DNA followed by PCR performed on subsequently acquired transgenic (+/T) and wild type (+/+) DNA. Several different transgenic mouse lines were generated and one line showing stable and moderate TWINKLE overexpression in all analyzed tissues was selected for further analysis. Upon analyzing mitochondria isolated from liver and heart tissues of wild-type and Twinkle BAC transgenic mice by SDS-PAGE and western blot, we detected two to three times higher TWINKLE protein levels in TWINKLE overexpressing BAC transgenic mice (Figure 3.2 B). Furthermore, mitochondrial transcription factor A (TFAM) levels were clearly elevated in mitochondria isolated from hearts of the transgenic mice (Figure 3.2 B).

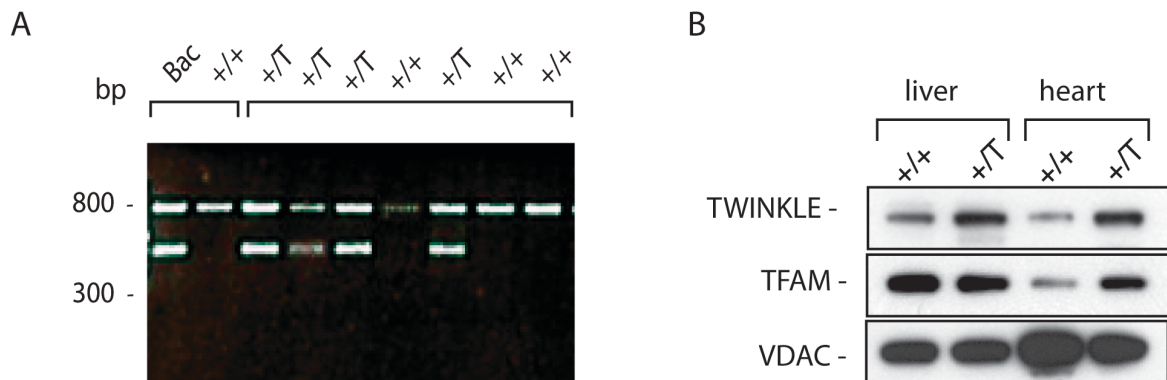


Figure 3.2: TWINKLE BAC screening and protein levels. (A) Electrophoretic analysis of PCR products of control BAC construct and wild-type DNA(+/+) followed by PCR products of DNA isolated and digested from transgenic (+/T) and wild type (+/+) mice. (B) Western blot analysis of TWINKLE and TFAM levels in heart and liver mitochondrial extracts of TWINKLE overexpressing (+/T) and wild type (+/+) mice. VDAC was used as loading control.

It has been suggested that TFAM protein levels mostly follow mtDNA levels¹⁴³, therefore the observed increase of TFAM protein levels in our model suggested an upregulation of mtDNA levels, which we confirmed using Southern blot analyses. Upon quantification, the increase of mtDNA levels was 20–50% (Figure 3.3).

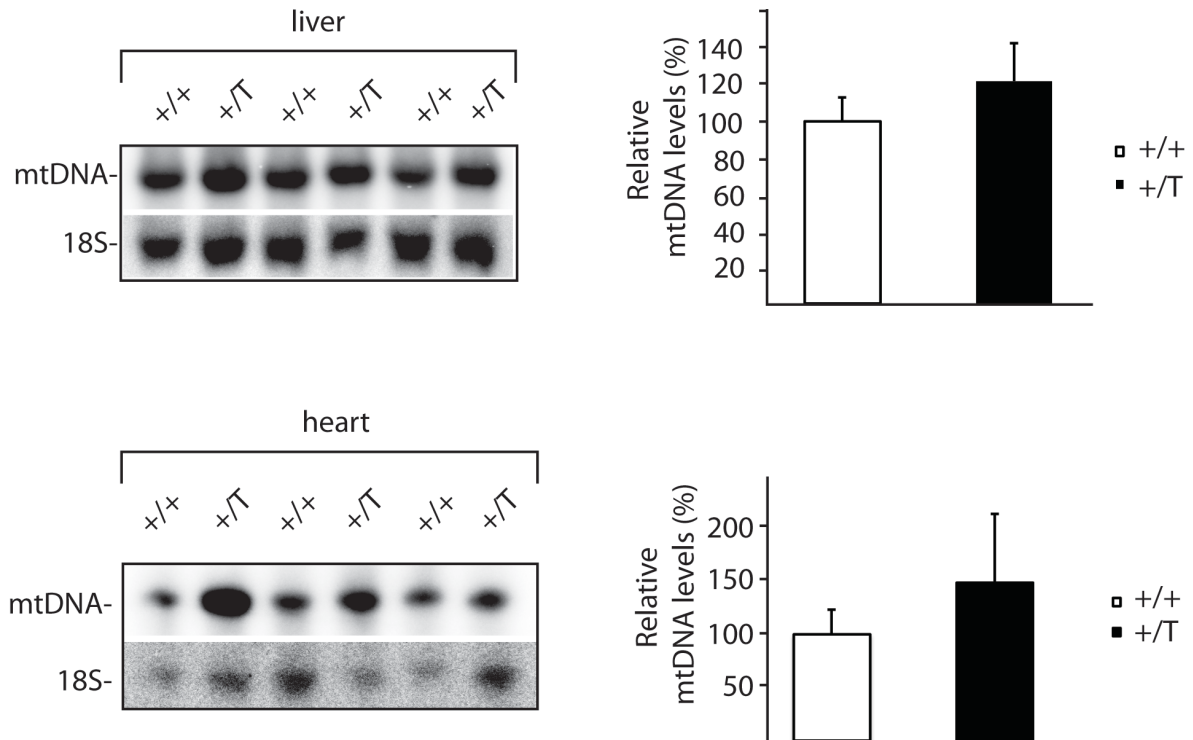


Figure 3.3: mtDNA levels in TWINKLE overexpressor mice. Southern blot analysis and quantification of mtDNA levels in total DNA extracts from liver and heart from wild-type (+/+) and transgenic (+/T) mice. The nuclear 18S rRNA gene was used as a loading control. Error bars represent SEM

Interestingly it has previously been reported that the effect on mtDNA copy number and *Twinkle* mRNA levels is more profound in transgenic mice expressing *Twinkle* under the control of strong β -actin promoter, where mice have three to four transgenic copies¹⁴⁴.

As the Southern blot investigation of TWINKLE-overexpressor animals revealed increased mtDNA levels in total DNA extracts from liver and heart, we next tested the levels of mitochondrial mtDNA transcripts. A Northern blot analysis of mRNAs, tRNAs and rRNAs in heart, kidney and liver tissue of TWINKLE BAC transgenic mice displayed no change in transcript levels compared to wild type animals (Figure 3.4A).

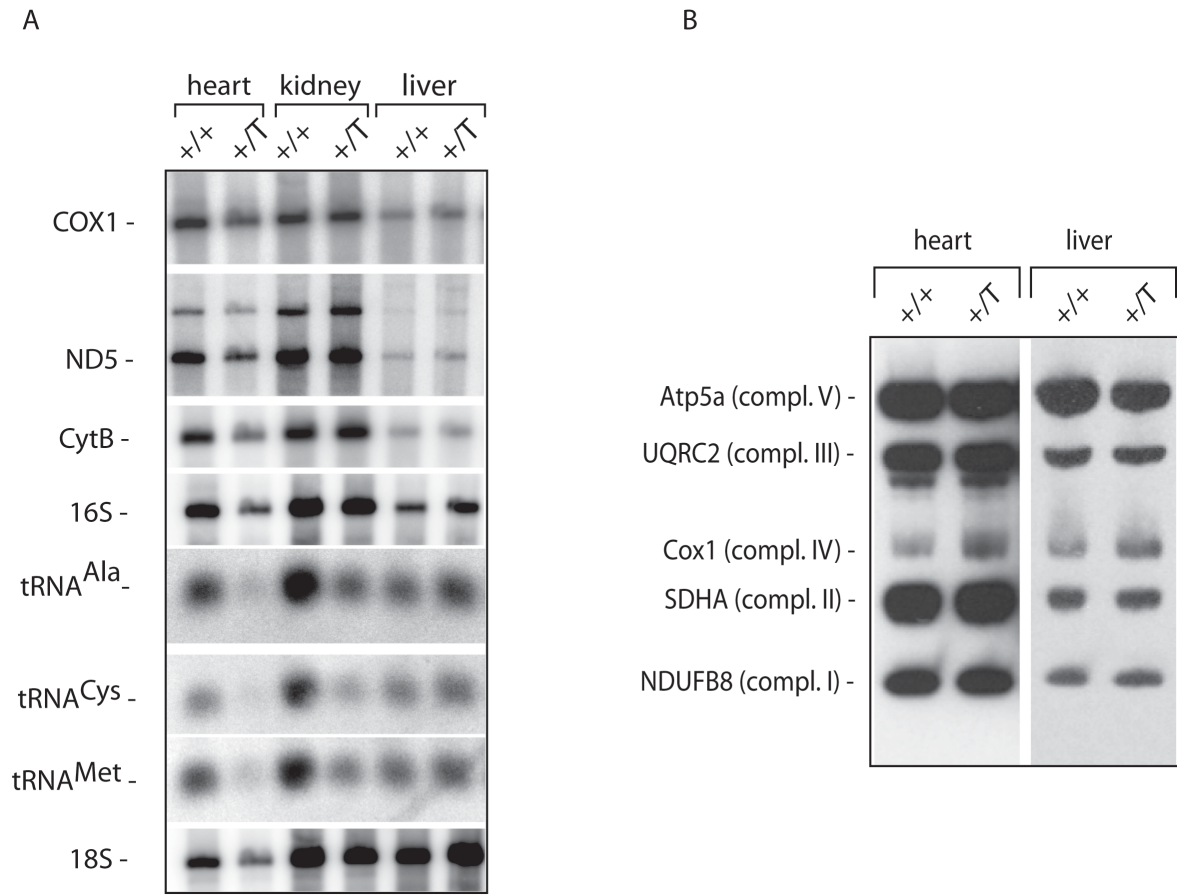


Figure 3.4: Transcript levels and levels of respiratory chain complex subunits in TWINKLE overexpressor mice. (A) Northern blot analysis of mRNAs, tRNAs and rRNAs isolated from the heart, kidney and liver tissue of TWINKLE BAC transgenic 25 weeks old mice control (+/+) and BAC transgenic (+/T) mice. The nuclear 18S rRNA was used as a loading control. (B) Western blot analysis of steady state levels of respiratory chain complex subunits in TWINKLE BAC transgenic mice.

Furthermore, we determined the steady state levels of protein subunits of mitochondrial oxidative phosphorylation system (OXPHOS) enzyme complexes and detected no change in their levels (Figure 3.4B). The SDHA protein subunit of the respiratory complex II was used as a loading control, as all components of this complex are encoded exclusively by nuclear DNA¹²⁸

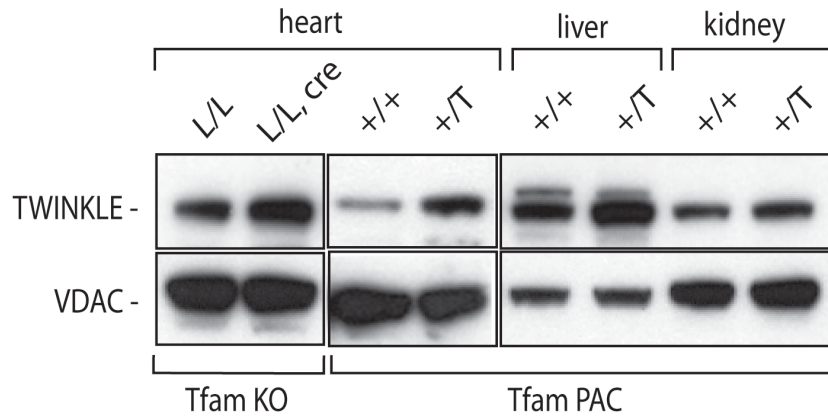
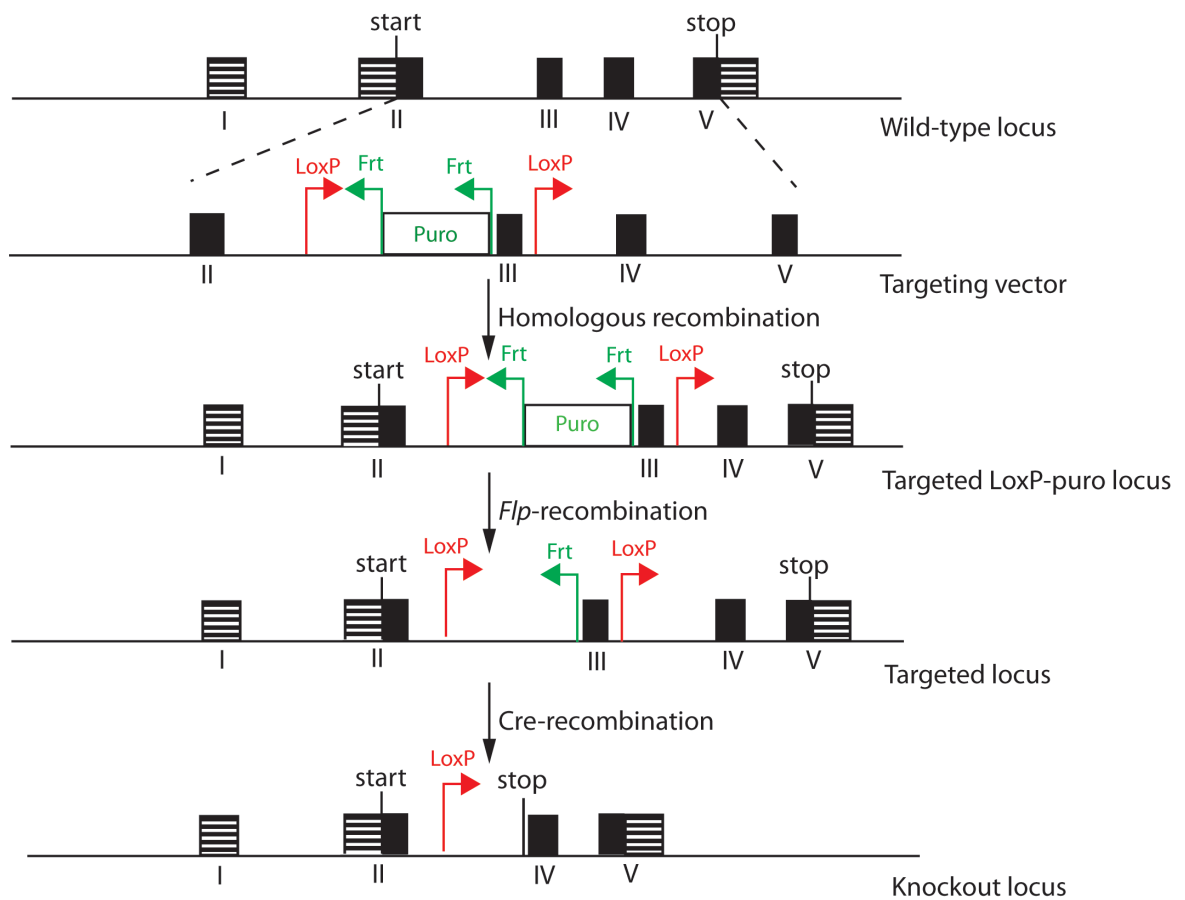


Figure 3.5: Western blot analysis in TFAM knockout and overexpressor mice. Western blot analysis of the steady-state levels of TWINKLE protein from isolated heart, liver and kidney mitochondria from TFAM knockout mice (L/L, cre) and their controls (L/L) and from human TFAM overexpressor animals (Tfam PAC). Transgenic animals (+/T); Controls (+/+). VDAC levels were used as a loading control.

Moreover, we also assessed TWINKLE protein levels in two other mouse models displaying altered mtDNA levels. Conditional tissue specific knockout of TFAM in mice causes decreased mtDNA levels⁹⁶, as seen in the TWINKLE knockout mice. In contrast, TFAM-overexpressor mice have higher levels of mtDNA, which was also observed in the TWINKLE-overexpressor mice¹⁴³. Transgenic mice in which human TFAM was globally overexpressed by utilizing P1 artificial chromosome (PAC) showed increased steady-state levels of TWINKLE in all analyzed tissues (Figure 3.5). These mice had overall overexpression of TFAM protein that resulted in 40-70% increase of mtDNA copy number. Hence upregulation of TWINKLE protein levels in TFAM PAC transgenic mice suggests that enhanced mtDNA replication results in mtDNA copy number upregulation¹⁴³. However, heart and skeletal muscle-specific TFAM knockout mice also showed elevated TWINKLE levels (Figure 3.5). This effect could be explained by the fact that replication is activated as a compensatory response because of strong mtDNA depletion in those mice.

3.2 Generation and verification of *Mgme1* knockout mice

A



B

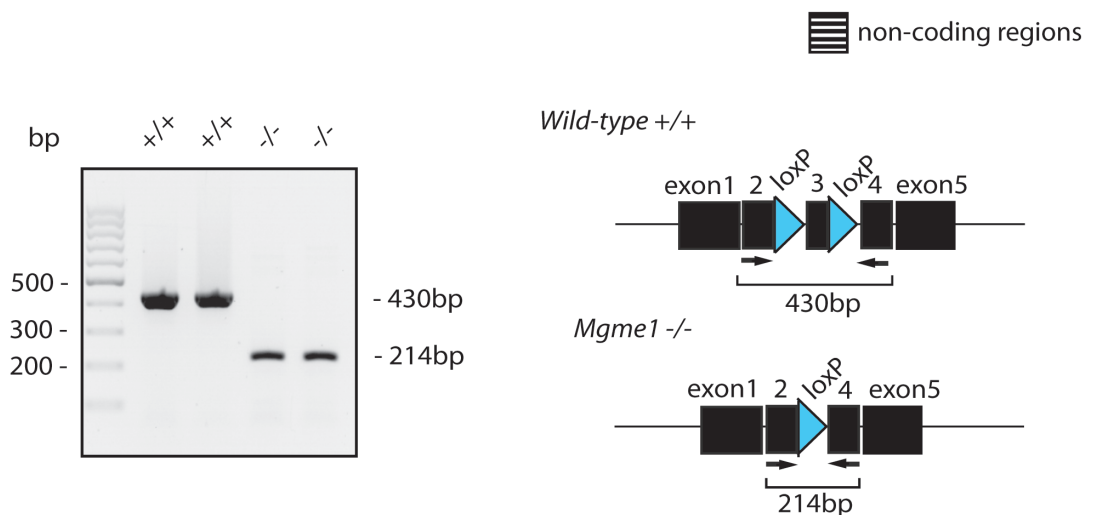


Figure 3.6: *Mgme1* knockout mice. (A) Targeting strategy for disruption of the *Mgme1* gene. (B) RT-PCR analysis result of *Mgme1* transcripts from wild-type (+/+) and *Mgme1* knockout mice (-/-) with primers in exons 2 and 4 (indicated on the scheme), left panel represents schematic representation of wild-type and knockout *Mgme1* allele.

The gene encoding MGME1 was disrupted in the mouse by utilizing homologous recombination and the cre-loxP system⁷². *Mgme1* exon 3 was flanked by loxP sequences and a puromycin cassette (flanked by F3 sites) was introduced as the selection marker (Figure 3.6 A). The puromycin selection cassette was removed by mating *Mgme1*^{+/*loxP-pur*} mice with transgenic mice ubiquitously expressing the *Flp*-recombinase, thus generating mice heterozygous for a loxP-flanked *Mgme1* allele. Heterozygous *Mgme1* knockout mice were obtained (*Mgme1*^{+/-} mice) after mating *Mgme1*^{+/*loxP*} mice to mice ubiquitously expressing *cre*-recombinase (beta-actin-cre mice). Intercrossing heterozygous *Mgme1*^{+/-} animals gave viable homozygous knockout pups. *Mgme1* homozygous knockout mice appear healthy at least until 12 months of age, thereby indicating that *Mgme1* is not essential for mouse embryonic development. Tissue-specific (heart and skeletal muscle) *Mgme1* knockout mice (*Mgme1*^{*loxP/loxP*, +/*Ckmm-cre*}) were generated by mating of *Mgme1*^{+/*loxP*} mice with mice expressing *cre*-recombinase under the control of the creatine kinase promoter (*Ckmm-cre*). The tissue-specific *Mgme1* knockout mice appear healthy up to 12 months of age and display no obvious phenotypic abnormalities by this age.

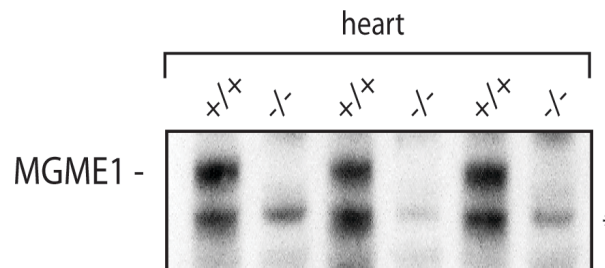


Figure 3.7: MGME1 protein levels in *Mgme1* knockout mice. Western blot analysis of MGME1 levels in heart mitochondrial extracts of MGME1 knockout (-/-) and wild type (+/+) mice. * non specific bend.

In order to verify the gene deletion we analyzed *Mgme1* knockout animals using RT-PCR (Figure 3.6B). When PCR was performed on cDNA isolated from *Mgme1*^{+/+} and *Mgme1*^{+/-} tissue using specific primers in exons 2 and 4, amplification in knockout animals resulted in a shorter band (214 bp) indicating absence of exon 3 (Figure 3.6B). Western blot analysis to assess the steady-state levels of MGME1 protein showed the absence of the MGME1 protein in knockout hearts (Figure 3.7).

3.2.1 *Mgme1* knockout mice display multiple mtDNA deletions and depletion of mtDNA in various tissues

Patients carrying homozygous nonsense and missense mutations in the *Mgme1* gene showed presence of mtDNA deletions in muscle, blood and urine samples⁸². Therefore, we directly investigated for the presence of circular mtDNA molecules with large deletions by performing long-extension PCR on heart-isolated total DNA from *Mgme1* knockout mice. Primers were designed to amplify mtDNA molecules with deletions in the major arc of the mtDNA which is the region between two origins of replication and most commonly affected by deletions (Figure 3.8A left panel). Indeed, our results confirmed that MGME1 knockout mice harbor multiple mtDNA deletions (Figure 3.8A). Moreover, Southern blot analysis of mtDNA levels of control (*Mgme1* L/L) and tissue-specific knockout mice (*Mgme1* L/L *cre*) as well as control (*Mgme1*^{+/+}) and homozygous knockout mice (*Mgme1*^{-/-}) revealed mtDNA depletion and confirmed the presence of mtDNA deletions in knockout heart tissue (Figure 3.8B).

Using *Sac I* restriction enzyme digestions we confirmed that the deletions correspond to an 11 kb truncated linear mtDNA fragment between the two origins of replication OriH and OriL⁸³. Using as a probe a radiolabelled whole mtDNA molecule, we were able to see two fragments after *Sac I* digestion of ~7,1kb and ~3,8kb (Figure 3.8 B left panel). This confirmed that we have a similar sized linear fragment in *Mgme1* homozygous knockout mice as in patient fibroblasts. We used DNA from the mtDNA mutator mouse (proof-reading-deficient version of PolyA, PolyA^{mut}) as a control, because mutator mice have an increased amount of a similar linear mtDNA deletion⁵⁶.

Furthermore, total DNA isolated from brain, skeletal muscle, kidney and liver of control (*Mgme1*^{+/+}) and homozygous knockout mice (*Mgme1*^{-/-}) was analyzed by Southern blot analysis. The mtDNA levels and deletions were found to be comparable with those of heart tissue mutants showing a widespread tissue distribution of this class of shorter mtDNA molecules (Figure 3.9).

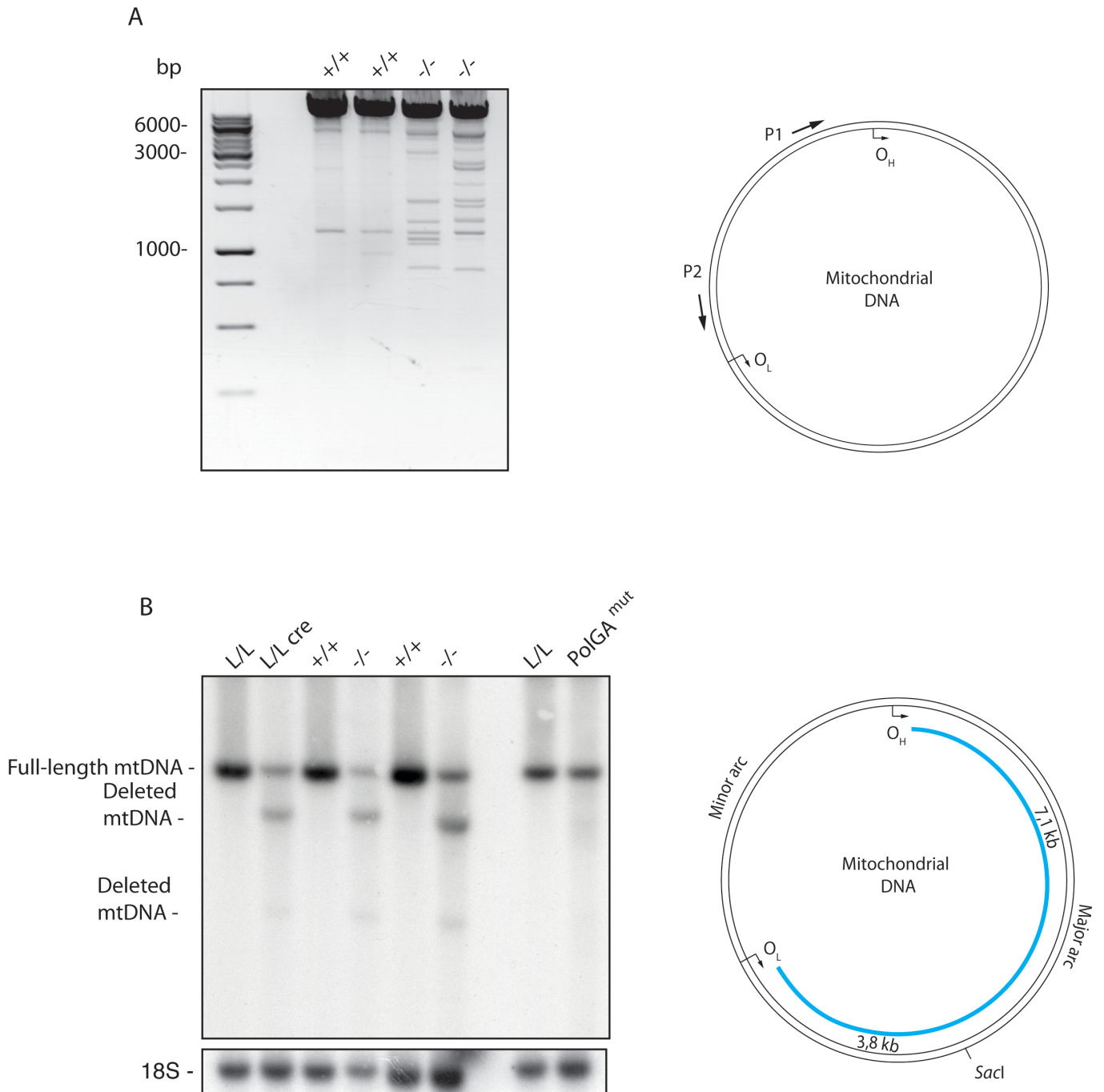
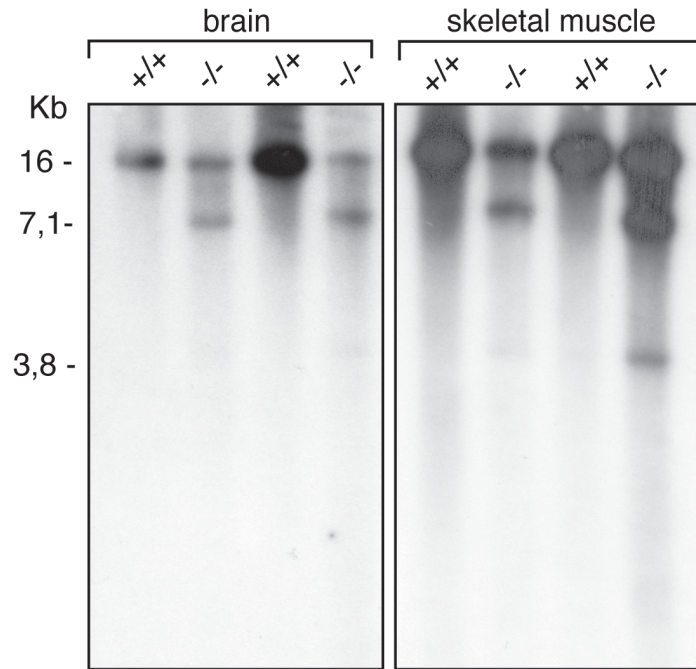


Figure 3.8: mtDNA levels in *Mgme1* homozygous and tissue-specific knockout mice. (A) Long-extension PCR of heart-isolated total DNA from 8 weeks old controls (+/+) and *Mgme1* knockout mice (-/-) using primers amplifying major arc (indicated on scheme in left panel). (B) Southern blot analysis of *SacI*-digested heart mtDNA from control (*Mgme1* L/L) and tissue-specific knockout mice (*Mgme1* L/L cre), lanes 1 and 2; wild-type (+/+) and *Mgme1* knockout mice (-/-) lanes 3-6, at 8 weeks of age, and control and mtDNA-mutator mice (lane 7 and 8).

A



B

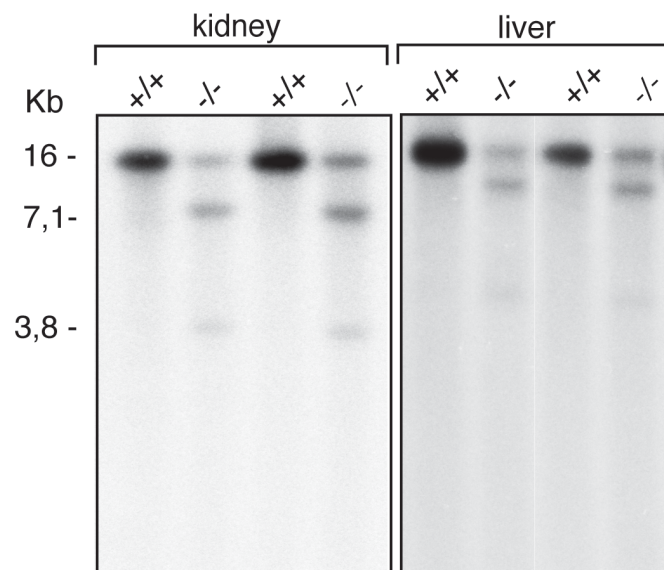


Figure 3.9: mtDNA levels in *Mgme1* homozygous knockout mice in different tissues. Southern blot analysis of *SacI*-digested DNA from brain, skeletal muscle, kidney and liver mtDNA from control wild-type (+/+) and *Mgme1* knockout mice (-/-).

3.2.2 *Mgme1* knockout mice have an increase in steady-state levels of 7S DNA but severely diminished *de novo* synthesis of 7S DNA

It has been shown that fibroblasts from patients harboring mutations in the *Mgme1* gene, or cells where MGME1 is down-regulated by small interference siRNA, have two to eight-fold elevated levels of 7S DNA. As discussed above in the introduction section 7S DNA represents pre-terminated nascent H-strand (~600nt) that remains annealed to the template strand in the mitochondrial control D-loop region (Figure 5). Its function still remains unknown.

Studies also reported that the degradation of 7S DNA is impaired in MGME1 deficient cells, rather than its synthesis⁸³. We therefore performed *in organello* replication experiments on mitochondria isolated from the heart of *Mgme1*^{+/+} and *Mgme1*^{-/-} animals to check the *de novo* 7S DNA synthesis. Freshly isolated active mitochondria from heart tissue were incubated for 2 hours with radioactive [α^{32} P] dATP to allow the incorporation of the radioactive nucleotide into the newly synthesized DNA. We also performed a subsequent 1 hour chase to follow the stability of *de novo* synthesized mtDNA and 7S DNA. Surprisingly, we could not identify any *de novo* synthesis of 7S DNA in heart mitochondria from *Mgme1* knockout mice (Figure 3.10A) under this experimental condition. As a control we used tissue-specific (heart and skeletal muscle) *Twinkle* knockout mice (*Twinkle* L/L, *cre*) since these mitochondrial helicase-deficient mice have a strong depletion of mtDNA evident from a young age due to lack of mtDNA replication⁷². Supporting the lack of essential replicative helicase and strong mtDNA depletion in *Twinkle* knockout mice, we could not detect any *de novo* synthesis of mtDNA and 7S DNA in those mice. Although *de novo* 7S DNA synthesis was completely absent, we observed substantial levels of *de novo* mtDNA synthesis in control *Mgme1*^{+/+} and knockout *Mgme1*^{-/-} animals. Additionally after a 1h chase, it was noticeable that 7S DNA has a much shorter half-life than mtDNA, supporting previous data showing that the D-loop has higher turnover than the whole-length mtDNA¹⁴⁵.

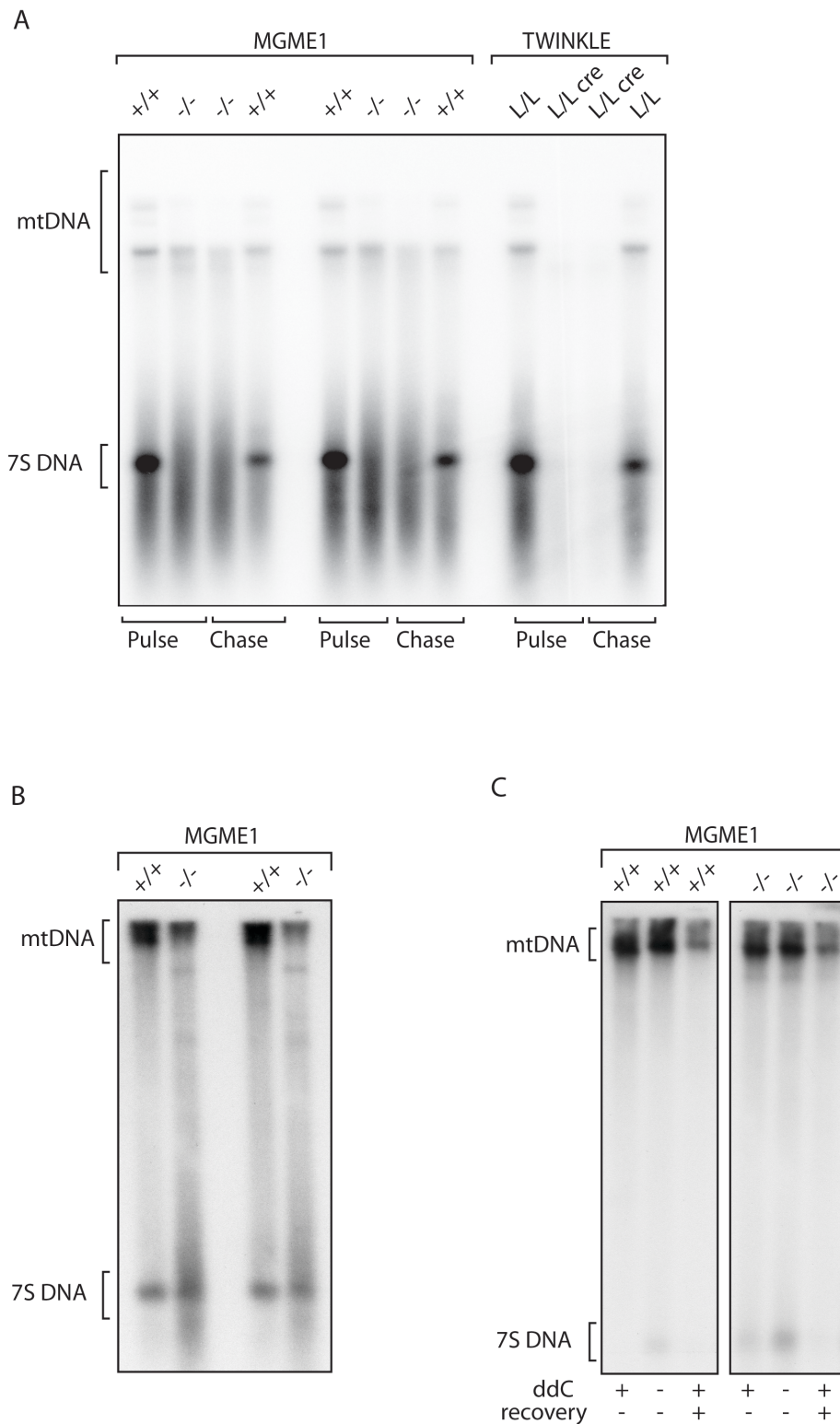


Figure 3.10: 7S DNA synthesis and steady-state level Mgme1 knockout mice. (A) *In organello* replication in heart mitochondria isolated from 8-week-old control (+/+) and *Mgme1* knockout (-/-) mice. De novo synthesized DNA was labeled using α -³²P-dATP and separated by agarose gel electrophoresis. The chase experiment was performed for 1 hour and all samples were heated to 93°C to release the 7S DNA strand (B) Southern blot analysis of 7S DNA levels in heart from control wild type (+/+) and *Mgme1* knockout mice (-/-). The Nuclear 18S level was used as a loading control (C) Southern blot analysis of mtDNA and 7S DNA from ddC treated (+) or untreated (-) fibroblasts. Lane 1 untreated cells, lane 2 ddC treated cells for 3 days; lane 3 recovered cells for 2 days.

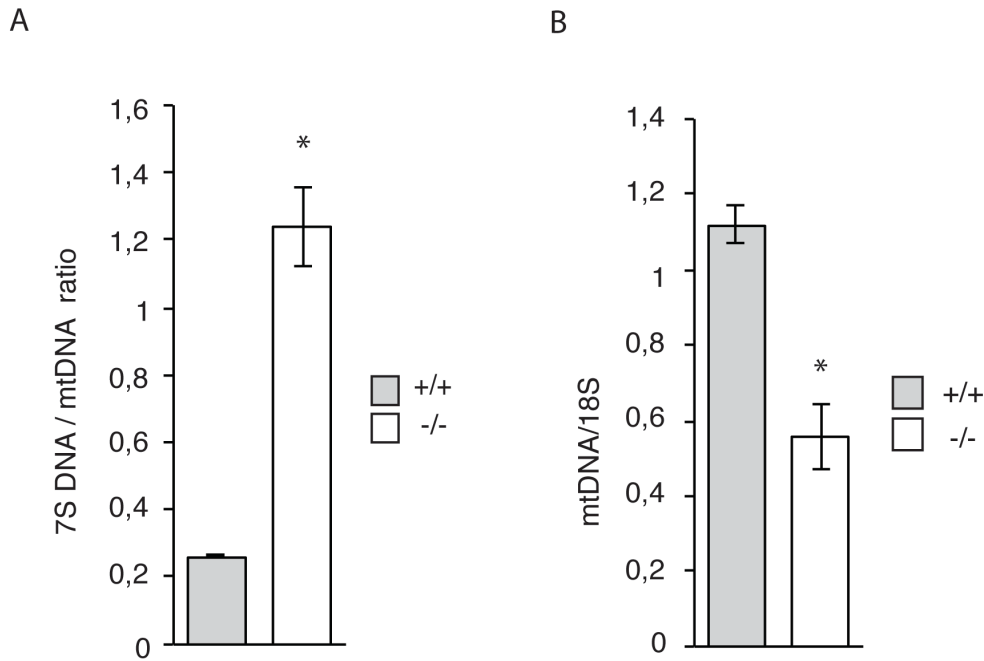


Figure 3.11: mtDNA and 7S DNA quantification in *Mgme1* knockout mice (A) Quantification of 7S DNA to mtDNA ratio by previous Southern blot (Fig.3.10B) from mouse heart. The 7S DNA signal was normalized to the mtDNA signal; $n = 2$. Error bars indicate \pm SEM (B) Quantification of mtDNA levels from Southern blot (Fig. 3.8B) from control (*Mgme1* L/L) and tissue-specific knockout mice (*Mgme1* L/L cre), lanes 1 and 2; wild-type (+/+) and *Mgme1* knockout mice (-/-) lanes 3-6, $n = 3$, Signals were normalized to the nuclear 18S signal. Error bars indicate \pm SEM

Furthermore we performed Southern blot analysis to determine the steady-state levels of 7S DNA in *Mgme1* homozygous knockout mice (*Mgme1*^{-/-}) in comparison to their wild-type counterparts (*Mgme1*^{+/+}). Interestingly, we saw a moderate increase in the ratio of 7S DNA to mtDNA in homozygous *Mgme1* knockout mice, when we take in account around 50% of mtDNA depletion in these mice (Figure 3.8B, Figure 3.11 A and B), which is not in full agreement with what was previously reported in patient fibroblasts⁸². To investigate this particular discrepancy between *de novo* synthesis and steady-state levels of 7S DNA, we followed the stability mtDNA and 7S DNA after inhibiting the *de novo* replication by use of the non-hydrolysable nucleotide analog ddC in *Mgme1* knockout mouse embryonic fibroblast cultures (MEFs) (Figure 3.10.C).

After treatment with the nucleotide analog 2',3'-dideoxycytidine (ddC), under the conditions where new DNA molecules can not be synthesized, wild-type fibroblasts showed complete lack of 7S DNA, while in *Mgme1* knockout fibroblasts a certain level of 7S DNA was maintained due to their increased stability (Figure 3.10C). mtDNA

depletion caused by ddC is the result of inhibition of mtDNA polymerase as well as termination of nascent strand elongation¹⁴⁶. Additionally when we allowed recovery of *Mgme1* knockout and control MEFs by removing ddC we could not observe de novo 7S DNA synthesis, consistent with previous results showing that during cellular recovery of mtDNA most of the replication events are productive^{111,147} (Figure 3.10C).

3.2.3 MGME1 deficiency results in accumulation of 7S DNA with extended 5 ends

To investigate the influence of MGME1 deficiency on 5' and 3' ends of 7S DNA we employed the LM-PCR, polyadenylation and primer extension on mtDNA isolated from our knock-out mouse model (Figure 3.12).

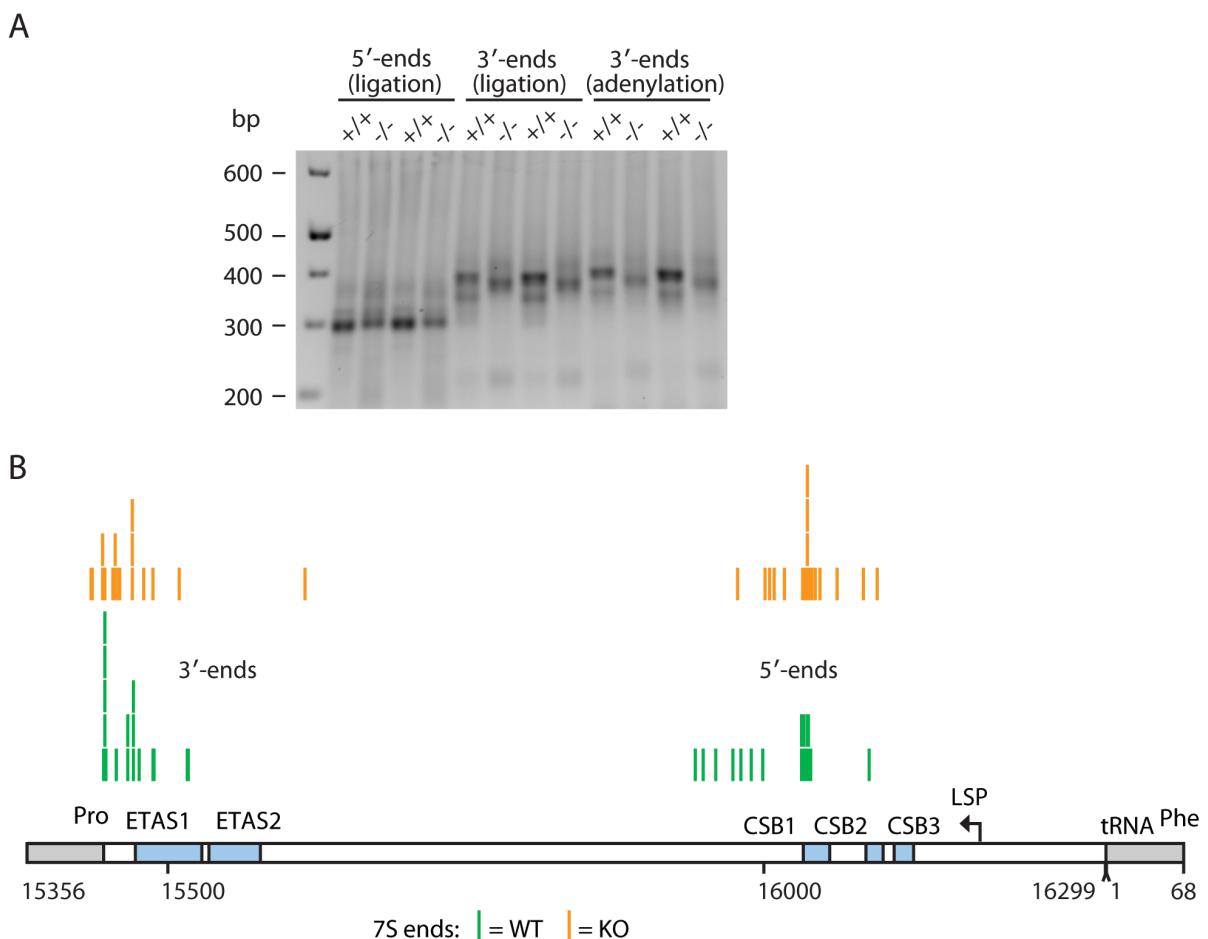


Figure 3.12: Mapping 7S DNA ends in *Mgme1* knockout mice. (A) Agarose gel electrophoresis of LM-PCR and adenylation in heart from control wild type (+/+) and *Mgme1* knockout mice (-/-). (B) Locations of the ends, determined by sequencing individual cloned PCR products in mouse heart mtDNA isolated from control (+/+) and *Mgme1* knockout (-/-).

Sequencing of those products revealed that most molecules have a 5' end located just before or within the CSB1 sequence, while in *Mgme1* knockout mice 5' DNA species protrude more towards the CSB2 region (Figure 3.12B). These data are comparable to the data from human patients⁸³ and support the function of MGME1 in 5' end mtDNA processing. Additionally, 3' end of 7S DNA of *Mgme1* knockout samples are mostly mapped upstream of tRNA^{Pro}, similar to wild-type controls.

3.2.4 Lack of MGME1 affects mitochondrial transcription differentially

To investigate transcription in *Mgme1* knockout mice, we analyzed mitochondrial rRNA, tRNA, and mRNA steady-state levels. In the heart, we observed a decreased abundance of mitochondrial transcripts generated from the HSP promoter and an increase of promoter proximal transcripts from LSP in *Mgme1* knockout mice (-/-) in comparison to control wild-type (+/+) mice. Interestingly LSP promoter distal transcripts did not change significantly in *Mgme1* knockout mice (Figure 3.13 A). In order to further elucidate MGME1's function, we performed Northern blot analysis to determine levels of 7S RNA in *Mgme1* knockout mice (Figure 3.13 B). We could observe a significant decrease in 7S RNA in *Mgme1* knockout animals, possibly suggesting that the 7S DNA *de novo* synthesis and transcription initiation at LSP are connected processes. To investigate further MGME1's role in the mitochondrial control region replication regulation we have taken in account that premature H-strand replication termination and transcription termination coming from the HSP promoter are functionally linked¹¹¹. Therefore we performed a Northern blot analysis using strand specific ribo probe specifically labeling anti-sense ACR transcript and we detected large amounts of this transcript in our *Mgme1* knockout mice (Figure 3.13 C). Previously reported 5' ends of the ACR transcript were mapped to immediately upstream of tRNAP, while 3' ends are mapped immediately upstream of tRNAF¹⁴⁸. In this experiment, the ACR transcript's size in *Mgme1* knockout mice has been estimated at <1 kb on the basis of ND1 (956 bp) and COX1 (1542 bp) transcript sizes in the same experiment.

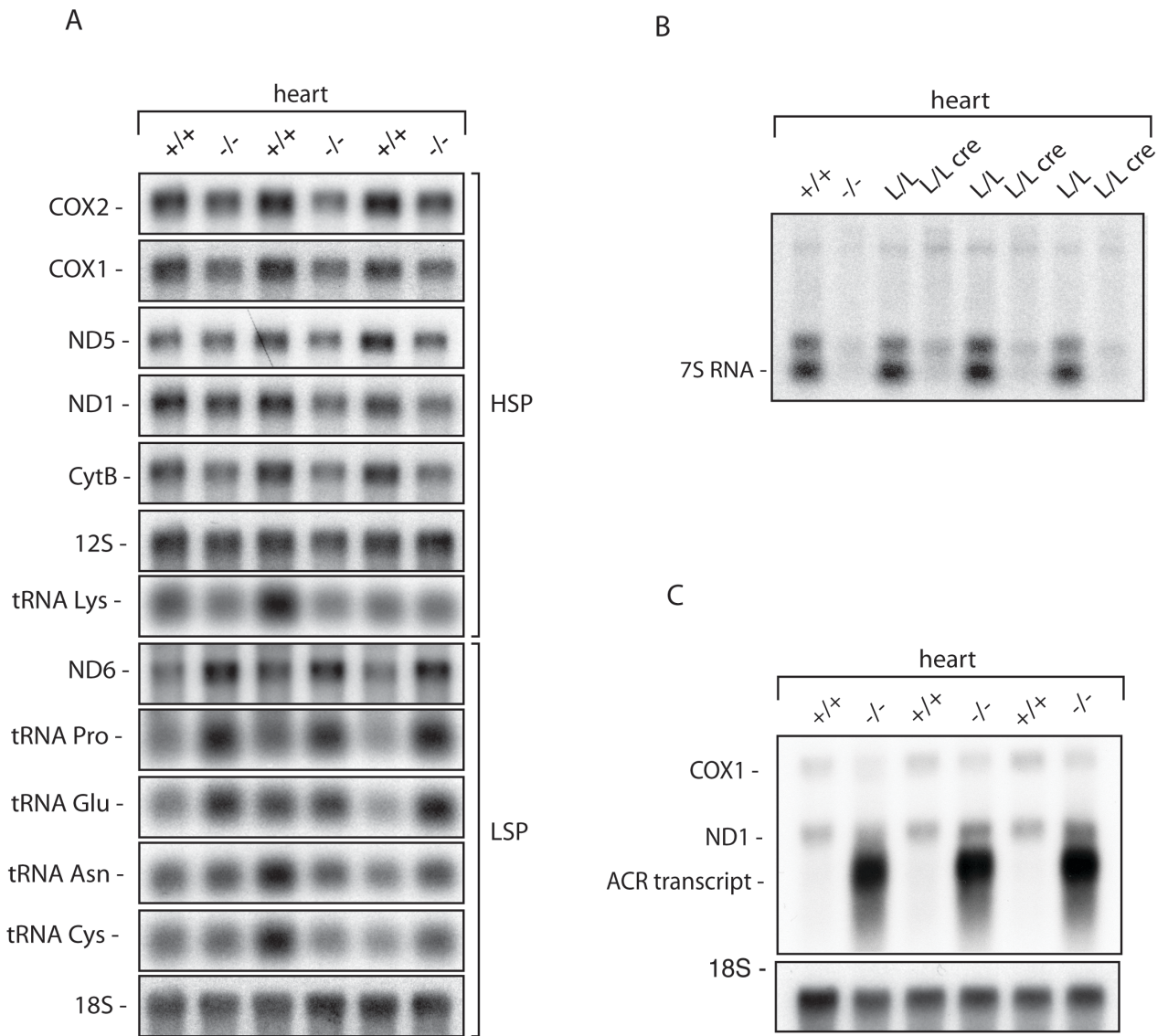


Figure 3.13: Steady-state transcript levels in *Mgme1* knockout mice. (A) Steady-state levels of mitochondrial mRNAs, rRNAs, and tRNAs; loading control is nuclear 18S rRNA (B) Northern blot analysis of 7S RNA levels in heart from control (*Mgme1* L/L) and tissue-specific knockout mice (*Mgme1* L/L cre) and *Mgme1* knockout mice (-/-) and corresponding control (+/+) (C) The ACR transcript mapped by Northern blot analysis, using D-loop probe complementary to the mtDNA light strand. ND1 and COX1 transcripts were added for ACR size assessment and 18S nuclear rRNA was used as a loading control.

To assess *de novo* mitochondrial transcription, we performed *in organello* transcripts labeling in isolated mitochondria from control and *Mgme1* knockout hearts. The levels of the newly synthesized transcripts from *Mgme1* knockout hearts were unchanged in *Mgme1* (-/-) mice when compared with wild-type (+/+) controls (Figure 3.14A). Nevertheless, if we consider that *Mgme1* knockout mice display mtDNA copy number decrease, *de novo* transcription is upregulated in those mice. Mitochondria isolated from TWINKLE tissue-specific knockout mice (Twinkle *L.L, cre*) served as a control in this experiment because those mice were previously reported to exhibit severe reduction of all of mitochondrial transcripts⁷².

Additionally, we examined the steady state levels of transcripts encoding various proteins involved in mtDNA expression, maintenance and repair by using the quantitative RT-PCR method. The levels of the transcript that encodes the mitochondrial transcription factor A (TFAM) were elevated (Figure 3.14C). Similarly, the levels of transcripts encoding the mitochondrial DNA polymerase (POLG) were increased in *Mgme1* knockout animals (Figure 3.14D). This upregulation of TFAM and POLG transcripts might be a compensatory response to mtDNA depletion in the *Mgme1* knockout mice. Indeed, as a possible consequence of such an mtDNA depletion, the levels of the mtDNA-encoded COX1 transcript were decreased in the heart tissue of the *Mgme1* homozygous knockout mice (Figure 3.14D). Transcript levels of TWINKLE replicative helicase and levels of transcription co-activator PGC1- α did not significantly change (Figure 3.14C and D).

We also checked for transcript levels of diverse nucleases (FEN1, DNA2) reported to function in mitochondrial flap processing during mtDNA repair, including the endonuclease G-like (EXOG) in *Mgme1* knockout animals, but did not detect any significant changes (Figure 3.14B). MGME1 transcripts were not detectable in *Mgme1* knockout mice, when we used a TaqMan detection probe covering part of exon 3 of *Mgme1*, which is the deleted exon in our knockout model.

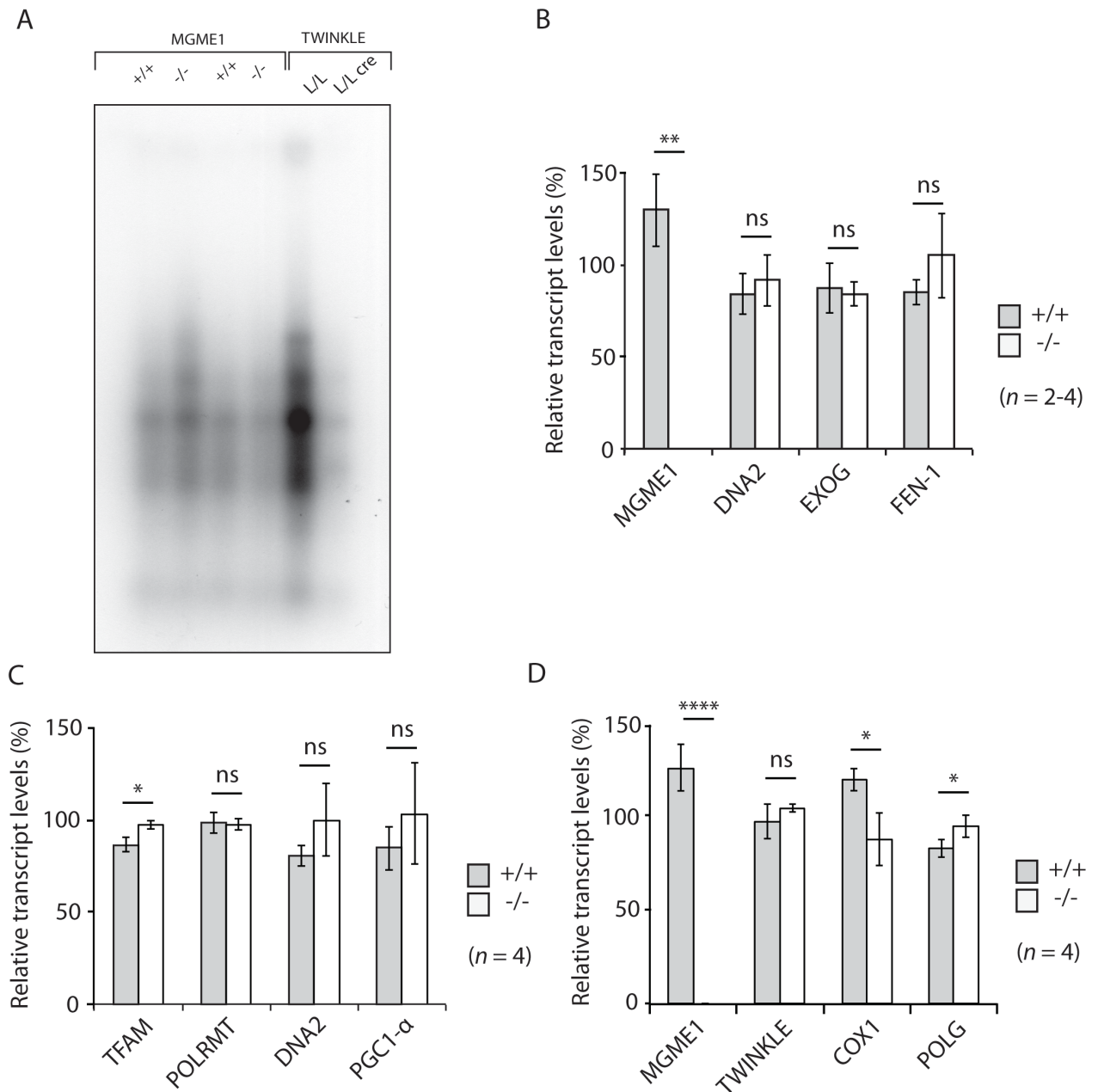


Figure 3.14: De novo and relative transcript levels in *Mgme1* knockout mice. (A) *In organello* transcription in heart mitochondria isolated from 8-week-old control (+/+) and *Mgme1* knockout (-/-) mice. De novo synthesized transcripts were labeled using α - 32 P-UTP and separated by agarose gel electrophoresis (B) Mitochondrial transcript steady-state levels assessed by qRT-PCR in hearts from 8-week old *Mgme1*+/+ (gray bars) and *Mgme1* knockout (-/-) (white bars) mice. Error bars represent SD. * p value < 0.05. ** p value < 0.01. *** p value < 0.001

3.2.6. *Mgme1* deficiency causes stalled mtDNA replication close to O_L in liver and accumulation of replication intermediates

To further investigate the effect of MGME1 deficiency on mtDNA replication, we used two-dimensional agarose gel electrophoresis (2D-AGE) to analyze putative mitochondrial replication stalling and replication intermediates in *Mgme1* knockout mice. Higher amounts of stalled mtDNA replication intermediates were found in patients with MGME1 nonsense mutations, as well as for patients carrying mutations in *Twinkle* and *PolgA* genes^{66,82}. *Mgme1* knockout hearts showed a general and unspecific accumulation of replication intermediates along the arc, suggesting that replication is stalling throughout the restriction fragment (Figure 3.16). Interestingly upon knockdown of MGME1 in cell culture⁸² a very similar, nonspecific stalling effect, with an apparent accumulation of replication intermediates was reported⁸².

Strikingly, liver tissue displays a different stalling pattern including a very obvious spot in the knockout sample for the O_L-containing fragment (Figure 3.17B) which suggests that there is a prominent stalling site somewhere in the vicinity of O_L in the *Mgme1* knockout mice (Figure 3.17B).

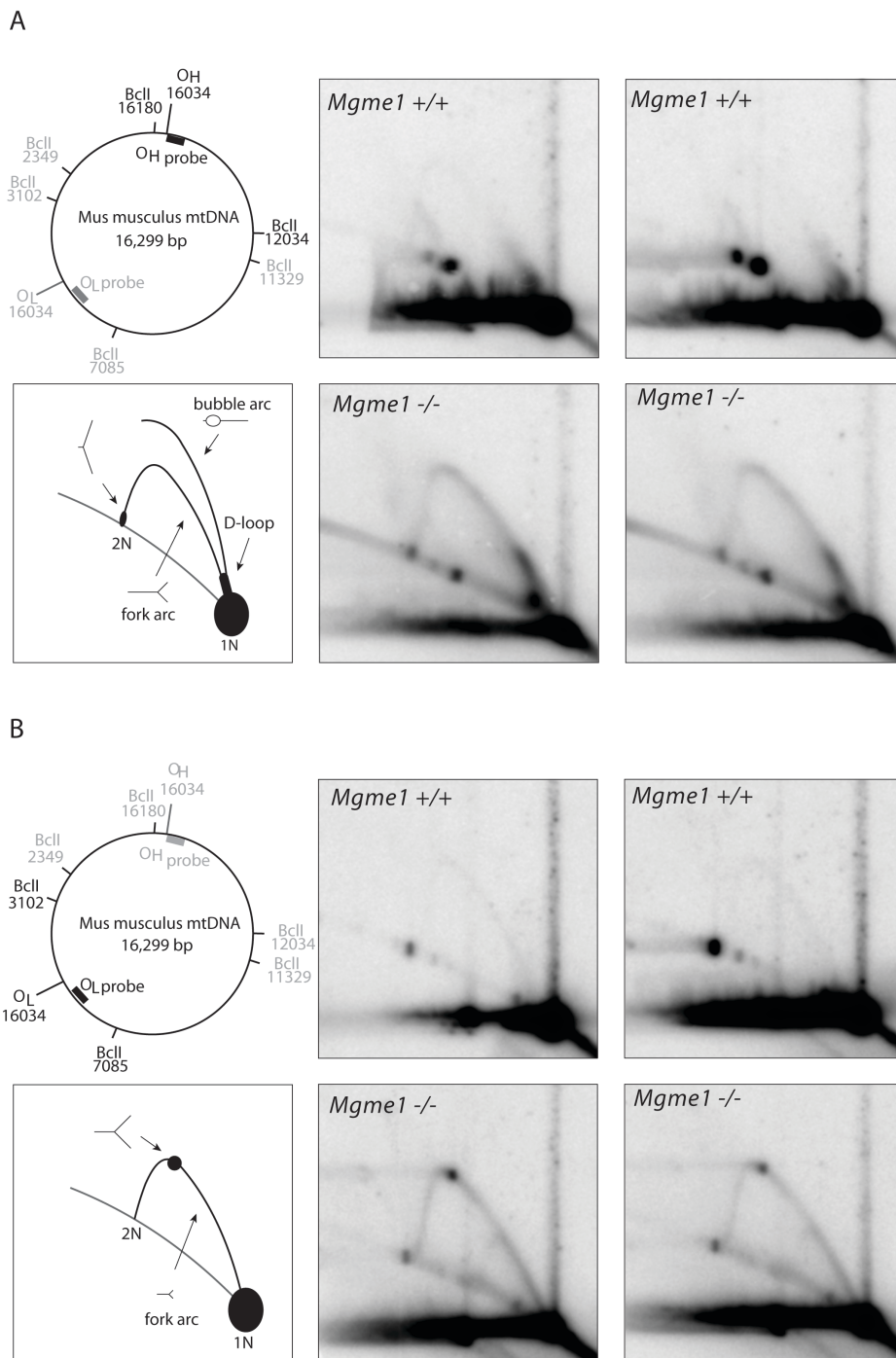
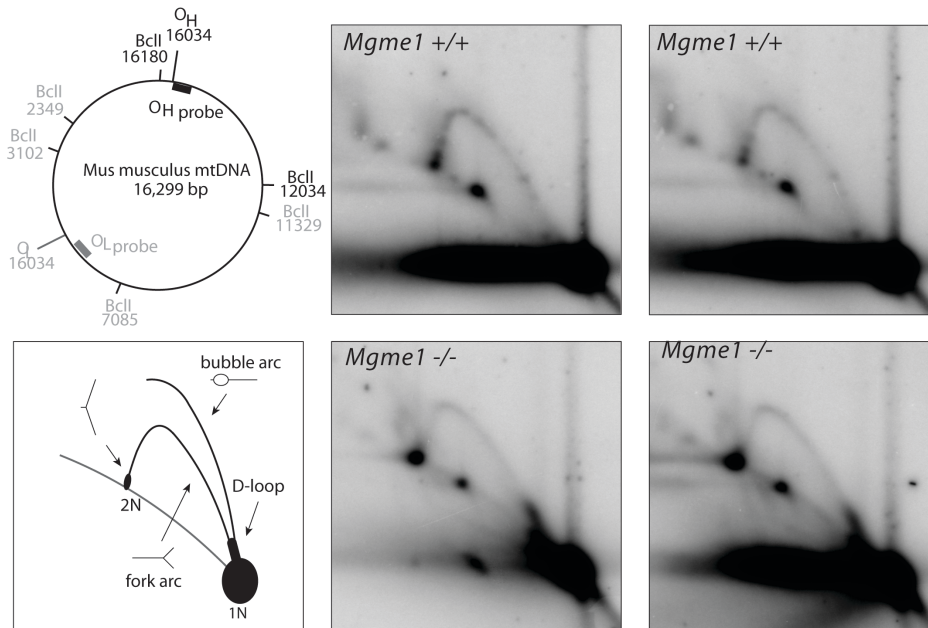


Figure 3.16: Replication in heart of *Mgme1* knockout mice. *mtDNA* replication in the heart of *Mgme1* wild-type (+/+) and *Mgme1* knockout mice (-/-) analyzed by two-dimensional neutral-agarose gel electrophoresis followed by Southern blot. Restriction enzymes and probes used (A)- O_H probe, (B)- O_L probe) are indicated to the left. The black bars indicates the non-coding regions, and O_H marks the origin of H-strand replication and O_L denotes the origin of L-strand replication. The interpretation based on previous work is provided at the bottom left corner⁶⁶.

A



B

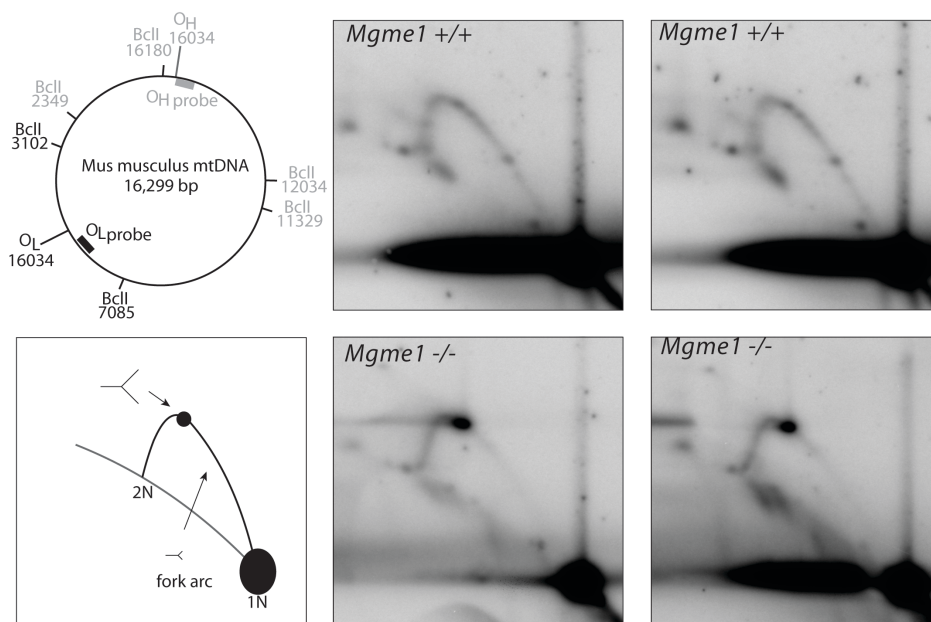


Figure 3.17: Replication in liver of *Mgme1* knockout mice. *mtDNA* replication in the liver of *Mgme1* wild-type (+/+) and *Mgme1* knockout mice (-/-) analyzed by two-dimensional neutral-agarose gel electrophoresis followed by Southern blot. Restriction enzymes and probes used (A)- OH probe, (B)- OL probe) are indicated to the left. The black bars indicates the non-coding regions, and OH marks the origin of H-strand replication and OL denotes the origin of L-strand replication. The interpretation based on previous work is provided at the bottom left corner⁶⁶

3.2.7. Sequence coverage for *Mgme1* knockout mice from different tissues

To investigate further tissue-specificity observed by 2D gels we performed pair-end sequencing to access the deletion pattern across different tissues. As a control we used mtDNA-mutator mice known to have similar 11 kb deletion⁵⁶, as do MGME1 deficient patients fibroblasts⁸³ and *Mgme1* knockout mice. The wild-types for *Poly* and *Mgme1* counterparts showed a similar sequencing coverage between all samples in brain, heart, and liver tissue (Figure 3.18 A, B) Figure 3.19 A, B black lines). For POL γ exo-nuclease deficient mice (mutator), mtDNA sequence coverage reveals control region multimers, earlier reported in heart and brain in these mice¹⁴⁹ (Figure 3.18A). The presence of a linear deletion is covered by a large control region sequencing peak (Figure 3.18A).

The coverage profiles of *Mgme1* knockout samples from brain and heart displayed similar patterns, including a pronounced peak of 7S DNA sequence and loss of sequence coverage in the direction of replication (Figure 3.18 B and Figure 3.19 A). In contrast, *Mgme1* knockout samples from the liver displayed a significant decrease in sequence coverage in the region that corresponds to the minor arc between the two origins of replication, and also showed normal levels of a 7S DNA-like sequence (Figure 3.19 B).

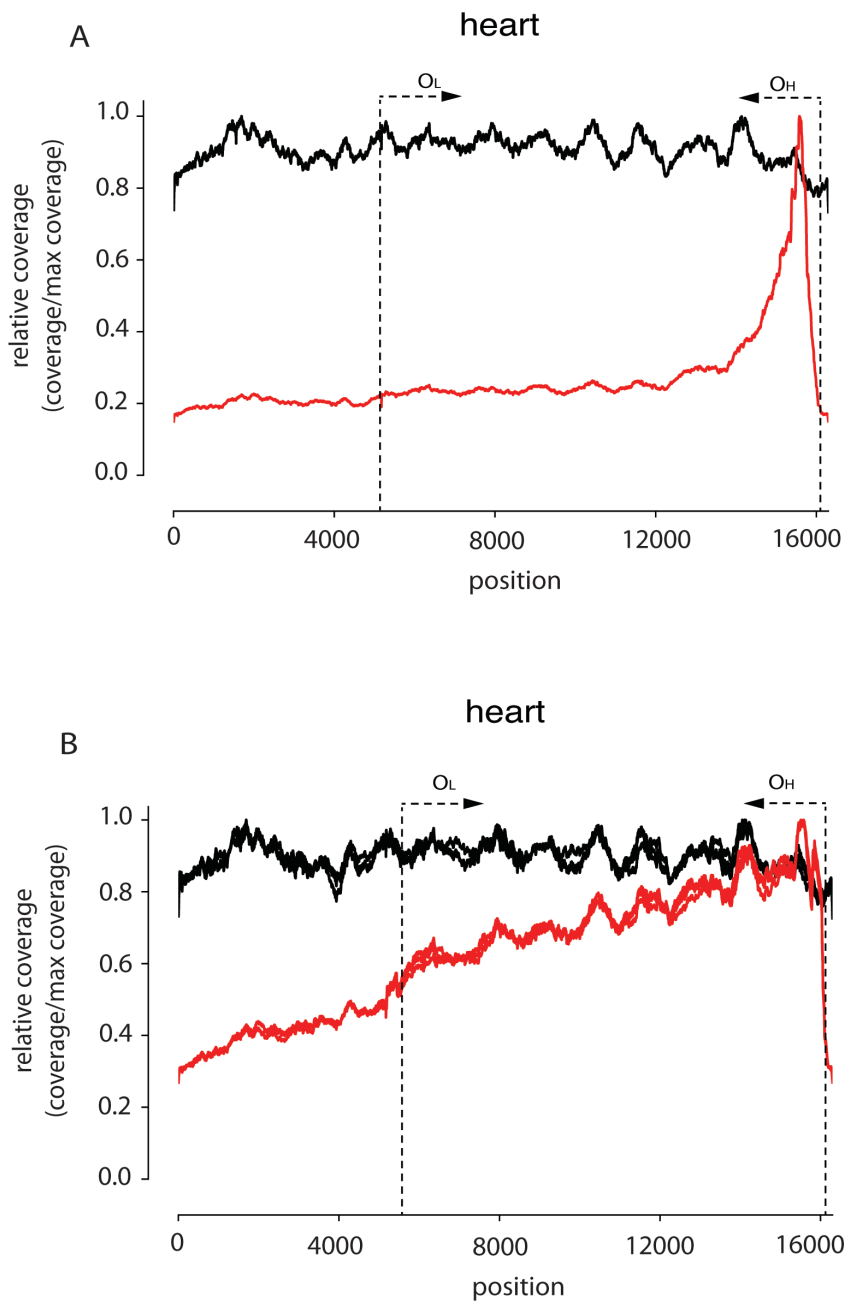


Figure 3.18: Heart mtDNA pair-end sequencing from $\text{Pol}\gamma\text{A}^{\text{mut}}$ and Mgme1 knockout mice. Sequence coverage for the mouse mtDNA samples from heart (A) heart mtDNA from $\text{Pol}\gamma\text{A}^{\text{mut}}$ (B) heart mtDNA from Mgme1 knockout mice (-/-). Mitochondrial genome position (x-axis) versus sequence coverage divided by maximum coverage for each sample. The red lines correspond to mtDNA of $\text{Pol}\gamma\text{A}^{\text{mut}}$ mice or Mgme1 knockout mice (-/-), while black lines represent $\text{Pol}\gamma\text{A}^{\text{mut}}$ control and Mgme1 wild-type (+/+). Lines numbers correspond to samples number. The approximate locations of the origins of light-strand (O_L) and heavy-strand (O_H) replication are indicated by dotted lines with arrows.

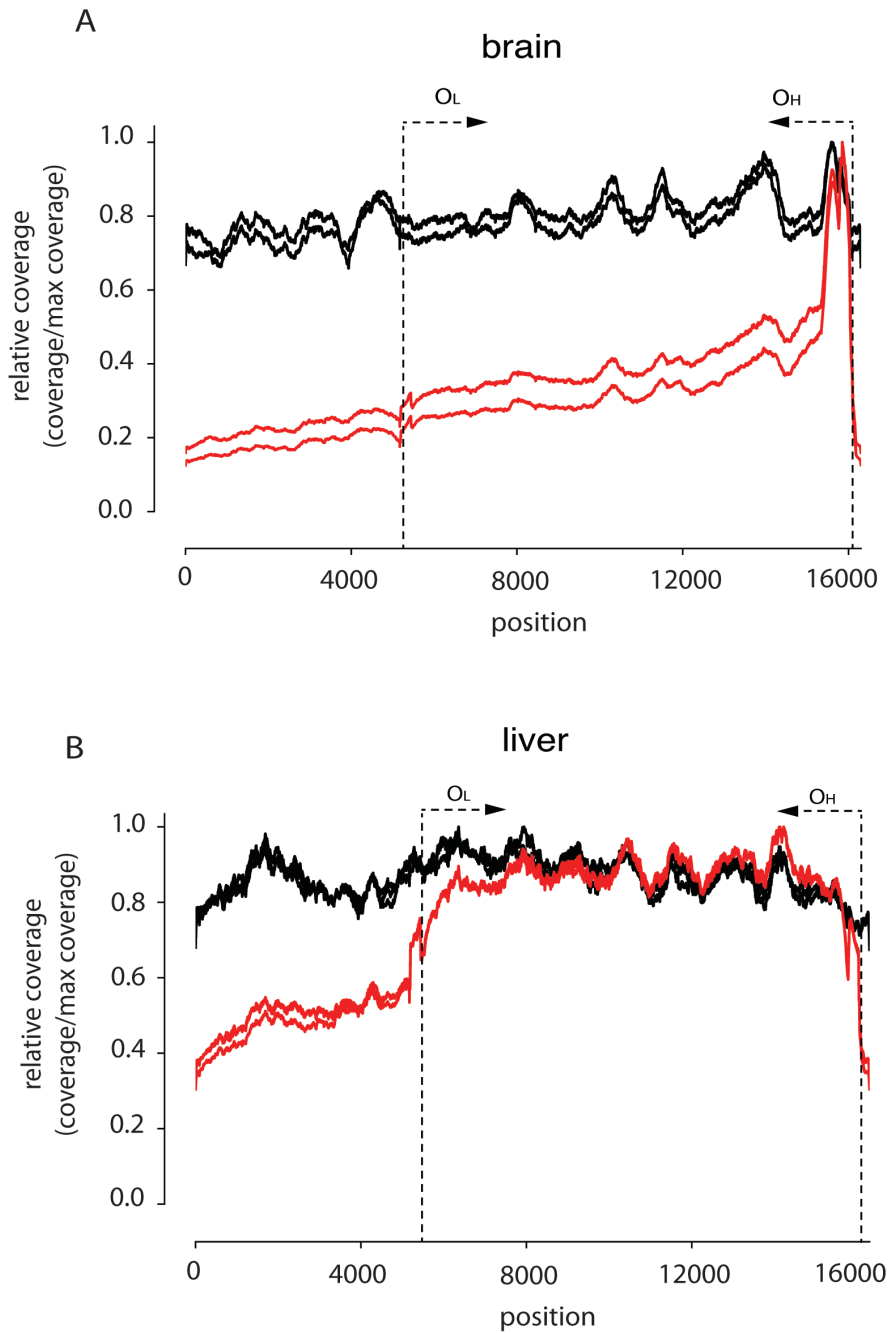


Figure 3.19: Brain and liver mtDNA pair-end sequencing from *Mgme1* knockout mice. Sequence coverage for the mouse mtDNA samples (A) brain mtDNA from *Mgme1* knockout mice (-/-) (B) liver mtDNA from *Mgme1* knockout mice (-/-). Mitochondrial genome position (x-axis) versus sequence coverage divided by maximum coverage for each sample. The red lines correspond to *Mgme1* knockout mice (-/-), while black lines represent *Mgme1* wild-type (+/+). Lines numbers correspond to samples number. The approximate locations of the origins of light-strand (OL) and heavy-strand (OH) replication are indicated by dotted lines with arrows.

3.2.8 Steady-state protein levels in *Mgme1* knockout mice

To further check the consequence of mtDNA depletion in *Mgme1* mutant animals, we assessed the steady-state protein levels of respiratory chain subunits and various mitochondrial proteins (Figure 3.20). The steady-state protein levels of replicative helicase TWINKLE and transcription and mtDNA packaging factor TFAM were not significantly changed in MGME1 deficient mice. Additionally, protein levels of mitochondrial RNA polymerase POLRMT as well as levels of LRPPRC that binds and stabilizes mtDNA-encoded transcripts, were not affected by the absence of MGME1 in the heart (Figure 3.20A). MTERF1 protein levels did not change in *Mgme1* knockout mice even though recent studies have revealed a new MTERF1 role in mitochondrial replication, as a replication contrahelicase slowing DNA replication fork and preventing replication transcription machineries collisions¹⁰⁹.

We also investigate the supramolecular organization of the respiratory chain by the BN-PAGE technique. Respiratory chain supercomplexes were resolved by BN-PAGE and visualized by in-gel enzyme activity assays for complex I and IV. No changes in the levels of respiratory complexes in *Mgme1* knockout mice were detected (Figure 3.20 B).

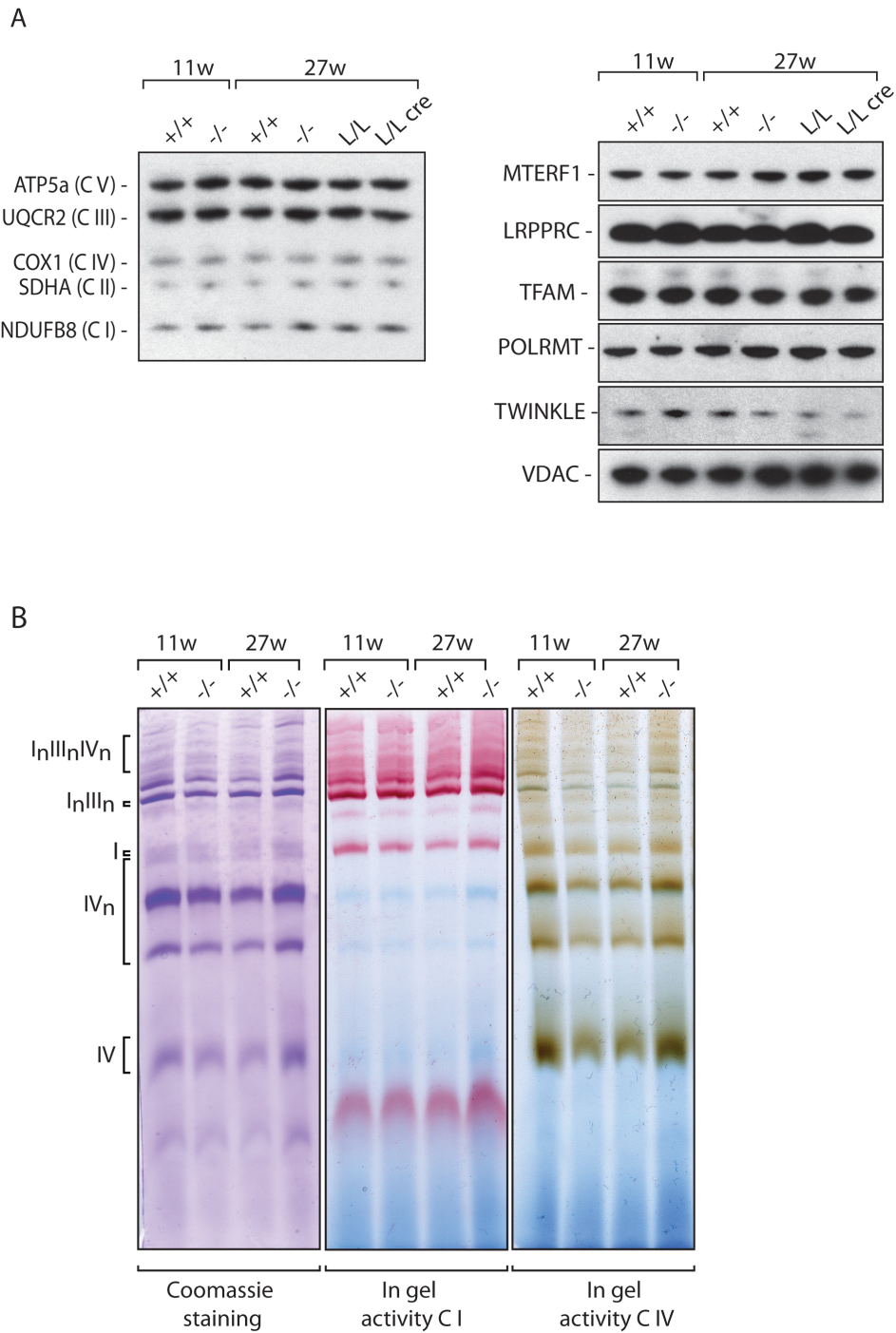


Figure 3.20: Protein levels in *Mgme1* knockout mice. (A) Western blot analysis of steady state levels of respiratory chain complex subunits and diverse mitochondrial protein in heart mitochondrial extracts from 11 and 27-week-old control (+/+) and *Mgme1* knockout mice (-/-) mice. (B) In-gel enzyme activities of complexes I and IV in *Mgme1* knockout and wild-type mouse. Coomassie staining of the BN gel was shown as a loading control.

4. DISSCUSSION

Mitochondrial DNA replication is an essential process that must be performed with high fidelity and may be controlled at multiple levels. The enzyme responsible for mtDNA replication, DNA polymerase, acts in coordination with a number of additional factors some of which can behave as putative regulators of mtDNA synthesis. In this study we have investigated the *in vivo* role of two replicative factors (TWINKLE helicase and MGME1 nuclease) and their putative function in regulation of mtDNA copy number control.

More than 95% of replication initiation events are prematurely terminated at TAS sequences, resulting in a newly synthesized, around 650bp long 7S DNA sequence (prematurely terminated nascent H-strand) called D-loop²⁹. The mechanism of D-loop formation and its role are currently unknown. One suggested role for this premature termination event is that it can act as a regulatory switch to block or release full-length mtDNA replication, thereby regulating mtDNA copy number. In support of this regulatory role of D-loop, comprehensive analysis of control region sequences from different mammalian orders mapped a conserved palindromic block of 15 nt-long sequences - CSB1 at the 5' end, and core TAS sequences at the 3' end of the D-loop region¹¹¹. It remains possible that the fate of the replication at the end of the control region is dependent on the interaction between basal replication components and unidentified protein(s). Such protein(s) employing contra-helicase or some other activity may be crucial for the disengagement of the replication machinery at the end of the D-loop region to generate abortive replication. There are many examples of similar proteins in prokaryotes and eukaryotes. In *E. coli*, the replication termination factor TUS arrests the replication fork via protein-protein interaction with the replicative helicase⁵⁰. In eukaryotes, nuclear transcription termination factor TTF-I was shown to display *in vitro* contra-helicase activity¹⁵⁰. Furthermore, decrease in 7S DNA was observed in recovery time in cell culture after mtDNA was depleted using chemical treatment, clearly indicating that the system can sense when there is a need for productive full-length DNA synthesis¹¹¹. Using ChIP-sequencing it was shown that the replication enzymes POL γ and TWINKLE are highly enriched in the D-loop region but at the 3' end of the D-loop region POL γ is enriched in the absence of TWINKLE

suggesting that the helicase is somehow displaced or unloaded¹¹¹. This unloading could be a consequence of contrahelicase or some other activity displayed by protein factor binding at this region thereby regulating replication. Similar contrahelicase activity has been recently reported for MTERF1 to prevent head-on collisions between replication and transcription machineries in the rDNA region in mtDNA¹⁰⁹.

In order to get further insights in mtDNA copy number control, we assessed the effect of TWINKLE overexpression on the mtDNA copy number and mitochondrial function by generating and studying *Twinkle* BAC transgenic mice. The BAC transgenic strategy employed assured moderate increase in TWINKLE levels (~2-3x) that led to mildly elevated mtDNA copy number (~20–50%) in the transgenic mice. However, this mtDNA copy number increase did not have any downstream consequences on the steady state levels of mitochondrial encoded transcripts and proteins. A more drastic effect of *Twinkle* overexpression on mtDNA levels (~3x) has been described previously by β -actin promoter driven overexpression¹⁴⁴. Using an *in vivo* BrdU labeling strategy and the same previously mentioned mouse model, the authors showed that TWINKLE specifically regulates *de novo* mtDNA synthesis¹⁵¹. Remarkably, when we have analyzed another mouse model displaying mtDNA copy number increase, the TFAM overexpressor mice¹⁴⁸, we also found elevated TWINKLE steady-state levels in all analyzed tissues, which is consistent with the general idea that mtDNA copy number upregulation is the result of increased mtDNA replication. Furthermore, *Twinkle* knockout mice analyzed in our laboratory displayed severe mtDNA depletion⁷². This interdependence between TWINKLE and mtDNA levels points towards an active role of TWINKLE in mtDNA copy number regulation.

Next, we studied the role of MGME1 in mtDNA replication. *Mgme1* gene is new on the list of genes linked to human mitochondrial DNA maintenance disorders⁸². Previous studies have extensively characterized MGME1 *in vitro* nuclease activity⁸¹⁻⁸³. Moreover, analysis of *Mgme1* patient fibroblasts isolated from *Mgme1* loss of function patients demonstrated its involvement in the mtDNA replication process⁸¹⁻⁸³.

Here we have investigated the *in vivo* function of the mtDNA nuclease MGME1 by creating and characterizing mouse knockout models (whole body and tissue specific - heart and skeletal muscle mouse knockout). MGME1 is not essential for the mouse embryonic development since *Mgme1* homozygous knockout mice are viable and appear healthy until at least year of age. Heart and skeletal muscle specific knockout animals of

MGME1 also do not develop any obvious morphological phenotype until week 70 of age. Long-extension PCR and Southern blot analysis showed the presence of multiple mtDNA deletions and mtDNA depletion in all analyzed knockout mouse tissues, which is in line with results obtained from muscle biopsies from individuals affected with MGME1 mutations. A linear, 11-kb mtDNA fragment that spans the entire major arc of the mtDNA is a hallmark of MGME1 deficiency in both patients and mice⁸³. Interestingly, a similar 11 kb linear fragment^{83,84} is found also in POL γ A exonuclease deficient (mtDNA mutator) mice⁵⁶.

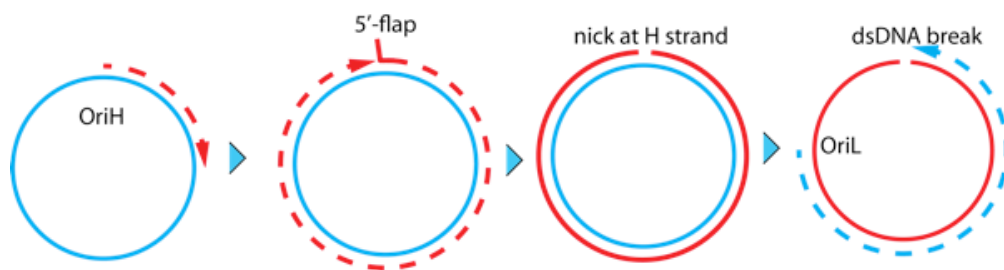


Figure 4.1: Origin of the linear deletion. Model of generation of an 11 kb linear mtDNA fragment.

It has been shown that the proofreading activity of POL γ is required for the creation of ligatable ends during mtDNA replication⁵⁴. Due to MGME1 nuclease deficiency or POL γ A exo-deficiency, an abnormal replication product arises due to the failed ligation of the nascent H-strand at O_H⁸⁴. Precisely, when POL γ reaches the 5'-end of the nascent strand, a transient 5'-flap is formed. If this flap is not processed due to an exonuclease-deficient POL γ strand displacement, or because of an MGME1 nuclease deficiency, ligation will fail, resulting in a daughter molecule with a nick on the H-strand near the OriH site. During the next round of replication, the L-strand replication will terminate when the nick on the H-strand is reached, leading to a double stranded DNA (dsDNA) break near OriH⁸⁴ (Figure 4.1). This results in a linear fragment that spans between the two origins of replication.

The data presented in this thesis demonstrate that *Mgme1* knockout hearts show a general and unspecific accumulation of replication intermediates along the replication arc, suggesting that replication is stalling along the entire restriction fragment. This result was different to what was seen in liver tissue, where a very prominent stall site was observed somewhere in the vicinity of O_L in the *Mgme1*

knockout mice. Interestingly, knockdowns of MGME1 in cell culture⁸² reveal a very nonspecific stalling effect, with an apparent accumulation of replication intermediates everywhere, similarly to *Mgme1* knockout hearts. Therefore, the *in vivo* process of replication stalling observed in our mouse model in the heart is in agreement to what has been previously reported from *in vitro* MGME1 patient fibroblasts and HeLa cells where MGME1 was depleted (siRNA). In contrast, the *in vivo* replication stalling process in the liver of *Mgme1* knockout mice is quite distinct and shows different site-specificity to that previously reported from *in vitro* MGME1 human fibroblasts and HeLa cells⁸².

Furthermore, pair-end sequencing of *Mgme1* knockout samples from the liver showed a sequence coverage curve that likely reflects the presence of linear mtDNA molecules with a large deletion. A similar sequence coverage has been previously reported from liver mtDNA mutator mice¹⁶⁴. Interestingly mtDNA mutator sequencing from heart resulted in control regions coverage increases. Similar results have been shown in a study that investigated the abundance of heteroplasmic SNVs using high-coverage next-generation sequencing in mtDNA mutator mice¹⁴⁹. They reported 2- to 4-fold increase of sequence coverage in control region in the heart and brain. These sequences are denoted as control region multimers, comprising multiple copies of sequence around the 5' end of the mtDNA control region¹⁴⁹. The coverage profiles of *Mgme1* knockout samples from brain and heart displayed a similar pattern including a pronounced peak of 7S DNA sequence and loss of sequence coverage in the direction of replication. These differences between the liver and the heart are corroborated with 2D-AGE gel data from these tissues. The elevation in sequencing reads along the major arc in the liver indicates that replication has trouble getting past O_L and predominantly just replicating the major arc, hence the specific stall in the 2D gels. The unusual slope in sequencing reads from the heart indicates replication being initiated faster than it can be completed, giving more reads closer to the origin, hence the generalized stalling in the 2D gel experiments.

There are many studies suggesting that mtDNA mutations play important role in the ageing process. Some ageing cell types accumulate point mutations and other mtDNA deletions¹²⁸. It has been reported that single large mtDNA deletions accumulated above threshold levels of >60% can cause respiratory chain dysfunction due to removal of one or more tRNA genes¹⁵². Low level of mtDNA deletions were also

detected in brain and heart of adult ageing humans¹⁵³. Furthermore, it has been also demonstrated that COX deficient muscle fibers in elderly humans have clonal accumulation of mtDNA deletions¹⁵⁴. Moreover mosaic respiratory chain deficiency has been described in many tissues in ageing humans (heart, skeletal muscle, dopaminergic neurons, colon) due to clonally expanded single large mtDNA deletions^{154,155,156, 157}. The mtDNA mutator mouse is a very important mouse model to study somatic mtDNA mutations and ageing. Those mice develop progressive premature ageing syndrome phenotypes including cardiomyopathy, reduced fertility, weight loss, kyphosis, anemia, hair loss, alopecia, hearing loss, and osteoporosis⁵⁶. Mutator mice have an increased number of point mutations due to a proofreading deficiency of the mitochondrial DNA polymerase. As described above in addition to point mutations, they also have a large linear around 11kb deletion, similar to our *Mgme1* knockout mouse model (Figure 4.1). Some reports have suggested that high levels of these linear molecules may cause the progeroid phenotype of the mtDNA mutator mouse^{158,159}. As mentioned earlier, now we know that a truncated liner fragment is a direct consequence of a failed ligation of the nascent H-strand at O_H⁸⁴. The fact that *Mgme1* knockout mice have similar linear deletion as found in mutator mice and do not display any premature ageing phenotype, suggests that progeroid phenotype is not caused by mtDNA linear deletions.

Similarly to human patient fibroblasts carrying nonsense mutations in the *Mgme1* gene, we report that loss of MGME1 in mice leads to an increase in the steady-state 7S DNA levels. Our results also confirmed the existence of extended 5' 7S DNA ends in *Mgme1* knockout mouse mitochondria. Although DNA molecules with longer 5' ends are also found in control mice, they were more abundant in *Mgme1* knockout animals. Surprisingly, especially given the increased steady state levels of 7S DNA, in isolated MGME1 knockout mitochondria the *de novo* synthesis of 7S DNA was completely abolished as judged by the *in organello* replication experiment. Under the same experimental conditions, synthesis of whole mtDNA molecule was only slightly decreased. This striking discrepancy between lack of *de novo* synthesis and increased steady-state 7S DNA levels is a likely consequence of increased stability of those molecules in absence of MGME1 nuclease activity.

The reduction of 7S synthesis in favor of full-length mtDNA replication in the *Mgme1* knockout mice suggests that MGME1 could regulate mtDNA replication and potentially may determine productivity of replication. This MGME1 action is likely

indirect as this nuclease was shown to lack direct DNA binding activity¹⁶⁰. Previous studies and analysis of displacement loop (D-loop) region sequences from different mammalian orders also have identified transcription termination events in this region¹⁶¹. Consistently, in *Mgme1* knockout model we detected a lack of HSP transcription termination and accumulation of ACR over the D-loop region. An ACR transcript has been previously described to form in response to thiamphenicol (TAP) treatment in cell culture¹⁶². In the mammalian system, the presence of an ACR transcript has been found in mice whose heart *Tfam* was disrupted, but which expressed the hTFAM protein instead. Interestingly, in those rescue mice the levels of 7S DNA were significantly reduced.

Mgme1 knockout mice display altered steady-state levels of mitochondrial transcripts. Transcripts originating from HSP promoter appear reduced while promoter proximal transcripts from LSP in *Mgme1* knockout mice appear increased and promoter distal transcripts unaltered. The possible reason for this phenomenon could be the ACR transcript's interference with the H-strand transcription promoter. As a consequence of decreased HSP transcription initiation, the transcription machinery would be available and would shift to the LSP promoter thereby resulting in an increased transcription initiation from the LSP promoter and increased levels of LSP promoter proximal transcripts.

Interestingly we observed decreased levels of 7S RNA in *Mgme1* knockout mice despite boosted L-strand promoter proximal transcription. 7S RNA was shown to serve as a primer for leading strand replication at O_H ¹⁶³. When not priming replication these transcripts can be terminated at CSB1 and polyadenylated. The exact function and termination of 7S RNA at CSB1 remains unclear.

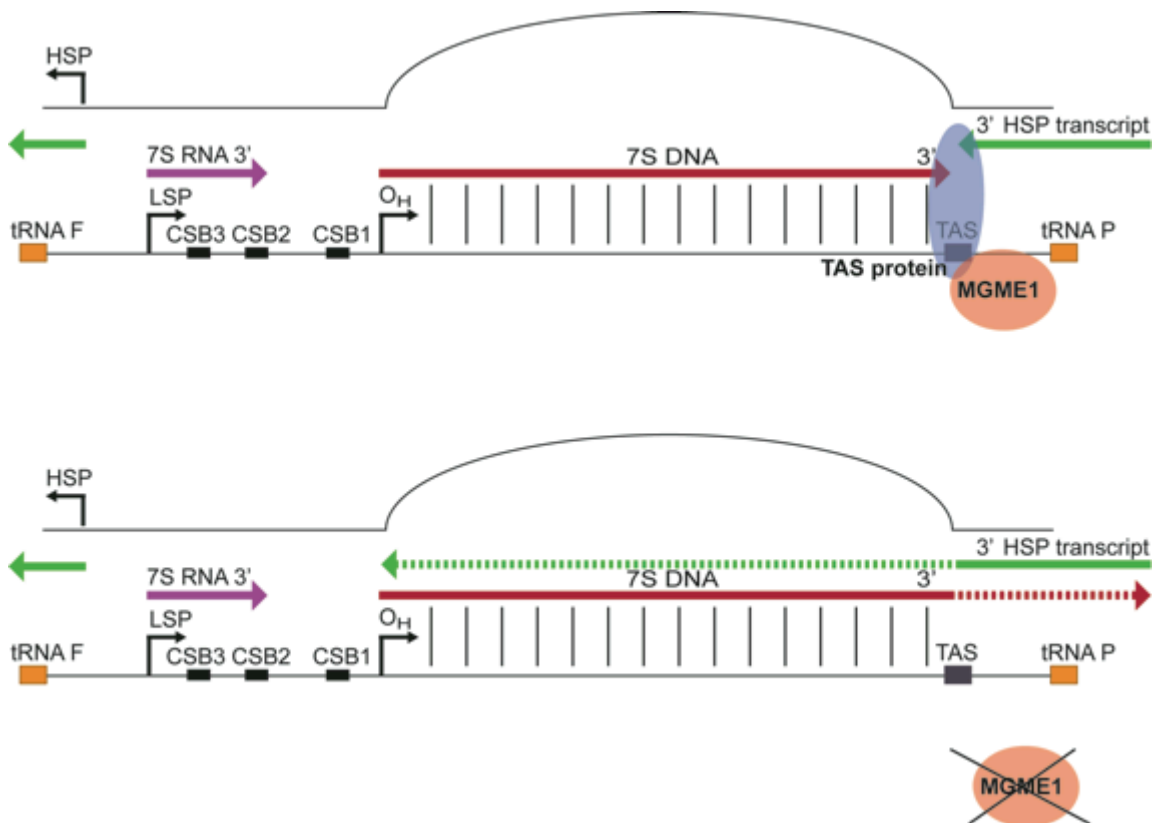


Figure 4.2: The termination complex at the end of D-loop region. Upper panel: replication is terminated in presence of MGME1 and TAS protein producing 7S DNA. The same complex terminates HSP transcription. Lower panel: Model to show full-length mtDNA production and HSP transcription over the D-loop region in absence of MGME1 protein due to termination complex destabilization or loosening.

We suggest that most LSP initiation events are used up for DNA synthesis and mtDNA transcription resulting in the absence of longer polyadenylated 7S RNA in *Mgme1* knockout mice. According to the most commonly accepted mechanism, 7S RNA is synthesized by transcription from LSP¹¹⁰ and our results would suggest that both - transcription at LSP and thereby replication at O_H - are increased. This replication

initiation boost at O_H is also evident from our sequence coverage reads in D-loop region. Additionally we detected upregulation of LSP proximal promoter transcripts in *Mgme1* knockout mice.

The observed tissue-specificity of our *Mgme1* knockout mouse model is in accord with the well-known tissue heterogeneity of mitochondrial disorders¹³⁰. This tissue-specificity may be linked to the observation that different tissues have different energy demands and biosynthetic capacities. For instance, brain mitochondria can oxidize ketones, whereas skeletal-muscle mitochondria are particularly efficient in oxidizing fatty acids. In the liver, a wide range of unique biochemical reactions take place that aim at the metabolism and synthesis of diverse molecules, and include xenobiotic detoxification, protein synthesis, transmethylation and transulfation reactions, and the processing of various other metabolites¹²⁹. Therefore it is possible that the mitochondrial function and energy homeostasis process in the liver is subject to unique cues, and this may contribute to the distinct molecular phenotype observed in the livers of our *Mgme1* knockout mice.

All the observed changes in mitochondrial protein and respiratory chain complexes levels in *Mgme1* homozygous knockout mice support the proposed regulatory role of MGME1 protein in mtDNA replication.

Therefore, we hypothesize that MGME1 could regulate processes at the end of the control region to arrest replication and H-strand synthesis (Figure 4.2 upper panel). In the absence of MGME1, the termination complex at the end of D-loop region will be disengaged and replication and transcription machineries will proceed past this site. (Figure 4.2 lower panel). In support of our model, both DNA replication and transcription termination events at this site are diminished when mtDNA synthesis needs to recover after depletion (block is released)¹¹¹.

In order to further investigate regulatory role of TWINKLE and MGME1 in mtDNA replication we aim to identify their interaction partners with a particular interest in discovering potential TAS interacting replication regulators. In a search for interaction proteins we will employ Co-IP, proximity-dependent biotin identification, (BioID)¹⁶⁵ and DNA Electrophoretic Mobility Shift Assay (EMSA) methods .

5. METHODS

Generation of MGME1 knockout mice

To generate conditional knockout *Mgme1* mice, exons III was flanked by loxP sites. The puromycin resistance cassette was introduced as a selection marker and removed by mating of *Mgme1*^{+/loxP-pur} mice with transgenic mice ubiquitously expressing Flp-recombinase. *Mgme1*^{+/loxP} mice were mated with mice ubiquitously expressing cre recombinase to generate heterozygous knockout *Mgme1*^{+/-} mice (Figure 4A)

Further to obtain tissue specific (heart and skeletal muscle) mice^{104,166-168}, *Mgme1* knockout mice we crossed *Mgme1*^{loxP/loxP} mice with transgenic mice expressing cre-recombinase under the control of the muscle creatinine kinase promoter (*Ckmm-cre*). Double heterozygous mice (*Mgme1*^{+/loxP, +/Ckmm-cre}) were mated to homozygous *Mgme1*^{loxP/loxP} mice to generate tissue-specific knockout (*Mgme1*^{loxP/loxP, +/Ckmm-cre}) and control (*Mgme1*^{loxP/loxP}) mice.

Generation of BAC and BAC FLAG TWINKLE transgenic mice

Clone Finder of the National Center for Biotechnology Information (NCBI) database was used to identify a BAC clone containing *Twinkle*. The clone was 218 kb long, with two flanking sequences upstream and downstream of *Twinkle* (95 and 67 kb respectively) and it was obtained from Children's Hospital Oakland-BAC-PAC Resources. The BAC was modified by ET recombination to allow discrimination between transcripts expressed from the endogenous *Twinkle* gene and the introduced BAC clone. Alteration of the coding sequence created a synonymous change to introduce a *XhoI* restriction enzyme site in exon 1, allowing the distinction between transcripts expressed from the endogenous *Twinkle* gene and the introduced BAC clones.

Southern blot analysis

Genomic DNA from tissues of *Mgme1* mice was isolated by Genra Puregene Tissue Kit and extraction was performed as instructed in the kit. A total of 2 µg from heart, brain, kidney and skeletal muscle tissue were digested with the restriction enzyme *SacI*, *XhoI* or *SphI*, and then separated DNA molecules by electrophoresis on a 0.8% Agarose gel. Wet transfer was completed in 20xSSC (150mM NaCl, 15mM Na₃CitrateX2H₂O) overnight on a nylon membrane (Amersham HybondTM-N+). Probes were labeled with ³²P-dCTP and hybridization was performed for detection of total mtDNA, D-loop (7S DNA) or nuclear DNA (18S rDNA). For the D-loop, Southern samples were heated for 3 min at 93°C prior loading.

***De novo* DNA synthesis**

Heart mitochondria (1 mg) was resuspended in 0.5 ml of incubation buffer (25 mM sucrose, 75 mM sorbitol, 100 mM KCl, 10 mM K₂HPO₄, 0.05 mM EDTA, 5 mM MgCl₂, 1 mM ADP, 10 mM glutamate, 2.5 mM malate, 10 mM Tris-HCl, pH 7.4) also containing 1 mg/ml fatty acid-free bovine serum albumin (BSA), 50 µM each dTTP, dCTP and dGTP and 20 µCi [α -³²P]dATP (3000 Ci/mmol). Incubation was carried out at 37°C for 2h on a rotating wheel. For pulse-chase experiments, mitochondria were incubated with [α -³²P]dATP (final concentration 5 µM) for 2h, followed by a chase with non-radiolabeled dATP (5 mM) and further incubation for 1h. After incubation, mitochondria were pelleted at 9000rpm for 4 min and washed twice with 10% glycerol, 10 mM Tris-HCl, pH 6.8, 0.15 mM MgCl₂.

The pellet was then resuspended in 300 µl of Lysis buffer and DNA was isolated by Genra Puregene Tissue Kit (QIAGEN) and extraction was performed as instructed in the kit. After precipitation and centrifugation, the pelleted nucleic acids were dissolved in 25mM EDTA. Pellet was dissolved on 55°C for 1h and treated with RNase A for 15 min, 37°C.

Before loading samples were heated at 93°C for 5 min to release 7S DNA and analyzed by 1% agarose gel electrophoresis. After the run, wet transfer was completed in 20xSSC (150mM NaCl, 15mM Na₃CitrateX2H₂O) overnight on a nylon membrane (Amersham HybondTM-N+).

Northern blot analysis

RNA isolation from mouse heart tissues was done using RNeasy Mini Kit and a fast prep machine with 2x30 sec pulses at speed 6. Following RNA isolation, procedures were performed as instructed in the kit (RNeasy Mini Kit, QIAGEN). RNA concentration was detected on a Spectrophotometer (NanoDrop 2000c, Peqlab) and 2µg of total RNA was separated on a 1.2% agarose gels containing formaldehyde and transferred to nylon membranes (Amersham HybondTM-N+).

***De novo* Transcription Assay**

Isolated mitochondria (2 mg) from heart were resuspended in 500 µl of transcription buffer containing 25 mM sucrose, 75 mM sorbitol, 100 mM KCl, 10 mM K₂HPO₄, 50 mM EDTA, 5 mM MgCl₂, 1 mM ADP, 10 mM glutamate, 2.5 mM malate, and 10 mM Tris-HCl (pH 7.4) with 1 mg of BSA/ml. The mitochondrial suspension containing 50 µCi of [α -³²P]UTP (Amersham Biosciences) was incubated by rotating the mixture for 40 h at 37 °C. After the incubation, the mitochondria were pelleted and washed twice with resuspension buffer containing 10% glycerol, 10 mM Tris-HCl (pH 6.8), and 0.15 mM MgCl₂. Mitochondrial RNA was isolated from the final pellet using the Trizol and chloroform, and resuspended in 10 µl of nuclease free water.

After adding Sigma RNA leading buffer samples were separated in 1.2% agarose gel containing formaldehyde at 120 V for 2 h.

Quantitative PCR

Total RNA from mouse heart was extracted using the RNeasy Mini Kit, QIAGEN kit. Reverse transcription and quantitative RT-PCR were performed using the High Capacity RNA-to-cDNA kit (Applied Biosystems) and TaqMan® 2× Universal PCR Master Mix, No AmpErase® UNG (Applied Biosystems). The following TaqMan probes

against mouse mitochondrial transcripts were obtained from Applied Biosystems: TFAM, POLRMT, PGC1 α , TWINKLE, COX1, POLG, DNA2, EXOG, MGME1, FEN1 and COXI. 18 S rRNA was used as a probe to detect this nuclear transcript.

Western Blot analysis

20 μ g of isolated mitochondria (obtained by differential centrifugation as previously described¹⁰⁴) from heart and liver tissue were resuspended in SDS 4X Lämmli-Buffer (4% SDS, 20% Glycerol, 120mM Tris, 0,02% Bromophenol Blue). Proteins were separated on in 4-12% NuPage gels (Invitrogen) and transferred on HyboundTM-P membrane (GE Helthcare).

Rabbit polyclonal antisera were used to detect POLRMT, EXOG, HSP60, COX II, TFAM and TWINKLE. MitoProfile total OXPHOS antibody cocktail (MitoSciences, 1:1000), was used for analysis of mitochondrial respiratory chain complexes.

Long-extension PCR

Using 2 ng of total DNA mtDNA was amplified from *Mgme1* knockout and control with the primers using P1 and P2 primers (P1:cctactagcaattatcccca, P2:catagtgggtatctaattccag) using LA Taq polymerase (TAKARA), Japan

Phenol chloroform extraction

A small piece of mouse tissue from heart, liver, brain, kidney, muscle or tail was incubated in 400 μ l lysis solution (0.5% SDS, 0.1 M NaCl, 50mM Tris-HCl, pH8.0, 2.4mM EDTA) supplied with 8 μ l proteinase K (10mg/ml) shaking at 55°C for 2-3 hrs, until the tissue was completely dissolved. Next, 75 μ l of 8M potassium acetate and 0.5ml chloroform were added and the samples were vortexed for 10 sec. followed by incubation at - 80 °C for at least 30min or o/n. Phase separation was achieved by centrifugation at maximum speed in a bench top centrifuge (Eppendorf). The upper (aqueous) phase was transferred to a new eppendorf tube and 1 ml 99% ethanol was added to each sample to precipitate the DNA. Tubes were inverted several times at room temperature and centrifuged at maximum speed in a benchtop centrifuge for 10min at RT. Pellets were rinsed with 0.5 ml 75% ethanol and spinned for another 5

min at max speed. All residual ethanol was removed and the pellet was dissolved in an appropriate amount of dH₂O. For long term storage samples were stored at - 20°C.

DNA extraction with Puregene® Core Kit A (Qiagen)

A small piece of frozen tissue from mouse brain, heart, liver, kidney or muscle was grinded with mortar and pestle in liquid nitrogen. The frozen tissue powder was transferred into a new eppendorf tube and mixed with 300µl Cell lysis solution (Qiagen). DNA was extracted as recommended by the manufacturer and kept at +4°C for short term and -20°C for long term storage.

RNA isolation with ToTALLY RNA™ kit (Ambion)

A small piece of fresh or frozen tissue from mouse brain, heart, liver, kidney or muscle was extracted with Lysing Matrix D tubes from MP Bio and ToTALLY RNATM kit from Ambion by following manufacturers instructions. The final RNA pellet was dissolved in an appropriate amount of DEPC treated water at 50°C for 15 min. RNA was stored at -80°C.

DNA/RNA quantification with Qubit® 1.0 fluorometer (Invitrogen)

DNA quantification with the Qubit® 1.0 fluorometer is based on intercalation of the reagent in double stranded DNA. For standard preparation 190µl working solution (Invitrogen) and 10µl Standard (Invitrogen) were vortexed and incubated at RT for 2 min. Sample preparation was performed by mixing 198µl working solution with 2µl DNA sample, vortexing and incubation at RT for 2 min. In the following, tubes were analysed in the Qubit® fluorometer (Invitrogen) according to the manufacturers instructions.

DNA agarose gelelectrophoresis

For separation of DNA fragments, DNA samples were run on a 0.8%-1.8 % agarose gel, depending on size and number of the DNA fragments. 0.8-1.8 g agarose were mixed with 100ml 0.5 x TBE buffer (90mM Tris-Base, 90mM H₃BO₃, 2.5 mM EDTA) and cooked in a microwave until the agarose got dissolved completely. Before the melted agarose was poured into a gel chamber, few microliter of ethidium bromide were added. After the gel was polymerized, DNA samples were loaded and run at 135 – 150 V. The gel was analysed in an UV imaging system (Syngene u:Genius).

Reverse transcription

1-2 μ g of DNase treated RNA (see section 2.4.7) was dissolved in DEPC-water with a final volume of 10 μ l. Another 10 μ l of a reverse transcription mastermix containing 10 x RT buffer,

25 x dNTP mix, 10x random primers, reverse transcriptase, RNase inhibitor and nuclease-free H₂O as recommended in the manufacturer's instructions of the High capacity cDNA Reverse Transcription Kit (Applied Biosystems) RT reaction was performed in a thermocycler (Applied Biosystems) as recommended in the manufacturer's instructions. cDNA was stored at -20°C.

Isolation of mitochondria from mouse tissue

Dissected heart, brain, muscle, liver or kidney from mouse was washed with mito isolation buffer, followed by homogenization on ice with a glass-teflon homogenizer (Sartorius, Potter S) in 10 ml (liver in 13 ml) mito isolation buffer 1X complete protease inhibitor cocktail (Roche) at 600rpm with 20 strokes. Next, the lysate was centrifuged for 10 min, at 1000xg, 4°C. The supernatant was transferred in a fresh, pre-cooled falcon tube and spun for 10 min at 12.000 x g, 4°C. Mitochondria were washed with mito isolation buffer three times for 5 min at 12.000 x g, 4°C, before the pellet was resuspended in an appropriate volume of mito isolation buffer. For storage, mitochondria were frozen in liquid nitrogen and put into -80°C.

Blue Native PAGE

To study the assembly of respiratory chain complexes Blue Native gel analyses was performed. Twenty μg of isolated mitochondria were pelleted and solubilized in cold 1 x NativePAGE Sample buffer (Invitrogen) containing 1% DDM. Proteins were incubated at 4°C for 15 min and pelleted at 20.000 x g for 30 min, 4°C. The supernatant was loaded on NativePAGETMNovex®Bis-Tris gel and run at 150V for 60 min using NativePAGETM Running buffer and NativePAGETM Cathode buffer as described in the manufacturer's instructions. Later voltage was increased to 250 V for the remainder of the run. For blotting procedure see western blot section.

Probe labelling with [α -32P] dCTP using Prime-It® II Random Primer Labeling Kit (Agilent)

50 – 80 ng template DNA (1 μl) were mixed with 10 μl Random Primer Mix (Agilent) and 23 μl dH₂O. reaction was heated for 5 min at 100°C, before addition of 10 μl of 5 x dCTP primer buffer, 1 μl Exo(-) Klenow enzyme (5 U/ μl) and 5 μl [α -32P]dCTP at 3000 Ci/mmol (Perkin Elmer). Next, the reaction was incubated at 37°C for 30 min, to allow radioactive labelling of the oligonucleotides. Purification of the radiolabeled probe was performed in an illustra MicroSpin G-50 column (GE Healthcare) at 3000rpm for 2min. In the final step the radioactive oligonucleotides were cooked at 100°C for 5min, to melt the double strands. If not used immediately, probes were stored at -20°C.

Oligonucleotide labelling with [γ -32P] ATP using T4-polynucleotide kinase

50 – 80 ng template DNA (1 μl) were mixed with 12 μl dH₂O, 2 μl of 10 x polynucleotide kinase buffer (NEB), 1 μl T4 polynucleotide kinase and 4 μl [γ -32P] ATP at 3000 Ci/mmo (Perkin Elmer). The reaction was heated at 37°C for 45 min, and subsequently purified in an illustra MicroSpin G-25 column (GE Healthcare) at 3000rpm for 2min. If not used immediately, probes were stored at -20°C.

ACR transcript labeling using Riboprobe System T7 Kit (Promega)

2,5µg pCR-II-TOPO- D-loop plasmid was digested with HindIII at 37°C, o/n. In the following, plasmid was purified using PCR purification kit (QIAGEN). Subsequently, the DNA was used as template for the Riboprobe in vitro transcription system (Promega). A transcription reaction containing of rNTPs, DTT, transcription buffer, RNasin ribonuclease inhibitor, linearized DNA template, [α -32P] rCTP (50µCi at 10µCi/µl) and T7 polymerase was pipetted following the manufacturers instructions and incubated at 37°C for 2hrs. After addition of DNase I and another incubation at 37°C for 15min, the probe was purified using a illustra MicroSpin G-50 column (GE Healthcare). If not used immediately, probes were stored at -20°C.

Preparation of purified mitochondria from different tissue and mitochondrial DNA

Mitochondria from the brain were isolate following protocol from Milenyi Biotec mitochondrial extraction tissue kit using TOM22 MicroBeads. Briefly, whole brains were treated with extraction buffer, homogenized using the gentleMACS Dissociator. Homogenate was filtrated and mitochondria were labeled with Anti-TOM22 mouse MicroBead. Magnetically labeled material was applied on a MACS Colum in a MACS Separator. Finally column is removed and intact mitochondria were eluted.

Mitochondria from liver and heart was isolated according to standard protocol where all liver and hearts were homogenized under ice-cold conditions and cell debris pelleted by low speed centrifugation (1000 g, 4uC for ten minutes). The supernatant was transferred and the mitochondria pelleted by centrifugation at 100000 g for 10 min. Resuspended mitochondria were isolated by centrifugation in a 1.0M/1.5M two-phase sucrose gradient.

mtDNA from all tissues was isolated by Genra Puregene Tissue Kit and extraction was performed as instructed in the kit. The DNA was treated with RNase prior to use.

Northern Blotting using biotinylated probes

RNA was isolated from hearts using the miRNeasy Mini kit (QIAGEN) incorporating an on-column RNase-free DNase digestion to remove all DNA. RNA (5 µg) was resolved on 1.2% agarose formaldehyde gels and then transferred to 0.45 µm Hybond-N⁺ nitrocellulose membrane (GE Healthcare Life Sciences) and hybridized with biotinylated oligonucleotide probes specific to mouse mitochondrial mRNAs, rRNAs, and tRNAs. Hybridizations were carried out overnight at 50°C in 5× saline sodium citrate (SSC), 20 mM Na₂HPO₄, 7% SDS, and 100 µg × ml⁻¹ heparin, followed by washing. The signal was detected using either streptavidin-linked horseradish peroxidase or streptavidin-linked infrared-labeled antibody (diluted 1:2,000 in 3× SSC, 5% SDS, 25 mM Na₂HPO₄ [pH 7.5]) by enhanced chemiluminescence (GE Healthcare Life Sciences) or using an Odyssey Infrared Imaging System (Li-COR Biosciences).

Sequencing library preparation and pair-end DNA sequencing

mtDNA Quality control was done using the Agilent TapeStation Genomic DNA ScreenTape and the Qubit BR kit. The library preparation protocol/kit was the NEBNext Ultra™ DNA Library Prep Kit for Illumina (NEB) after fragmentation of 150 ng gDNA with the Covaris to the requested insert size of > 500 bp. The sequencing run conditions were 2x250 bp on the Illumina HiSeq2500, using HiSeq Rapid v2 Kits from Illumina.

Each library was indexed individually with the provided barcodes and sequenced to 6 000 000 reads (tolerance range - 30 %) The reads were aligned to the C57Bl/6j mouse mtDNA reference sequence (NC_005089.1), using the corona lite mapping algorithm (Applied Biosystems) with default settings. The first 49 bases of the mtDNA sequence were appended to the end of the reference to avoid that reads fail to align due to the circularity of the mitochondrial genome. This alignment procedure attempts to map each read at full length to the reference sequence, allowing for at most 6 mismatches for each 50 bp read.

Two-Dimensional (2D) Agarose Gel Electrophoresis

For two-dimensional gels, mtDNA was isolated from fresh sucrose purified mitochondria from liver and heart tissue and then by sequential phenol-chloroform extraction according to established protocols³⁹. Resulting DNA (10–20 µg) was digested BclI and separated on agarose gels with according to the manufacturer's instructions (NEB) and to protocols described in detail. Gels were then blotted, hybridized with two different probes: OH-containing fragment and OL-containing fragment. Membranes were washed with 1× SSC three times for 20 min and then with 1× SSC with 0.1% SDS three times for 20 min. The primer sequences used to produce the probes are:

Cell culture and ddC treatment

Mouse embryonic fibroblast were grown at 37°C, 5% CO₂ and 95% humidity in 10cm dishes supplied with 10ml Dulbecco's Modified Eagle Medium (DMEM; Gibco) containing 10% Fetal Bovine Serum and penicilline (100µg/ml /streptomycine (100µg/ml). ddC (Sigma) 100mM stock solution was used at a final concentration of 20 µM. Cells were treated for 3 days and afterwards resuspended in fresh medium at a concentration of $1.5-2 \times 10^5$ cells/ml. A subsequent complete medium replacement without ddC allowed recovery of mtDNA. Total DNA was isolated by Gentra Puregene Tissue Kit and extraction was performed as instructed in the kit.

Material

Used chemicals were ordered from Ambion, Invitrogen, Qiagen, AppliChem, Fisher Scientific, Fluka, Roth, and Sigma Aldrich. Enzymes and their according buffers were delivered from New England Biolabs. Transfer of nucleic acids was done on Amersham Hybond-N+ nylon (GE Healthcare) membranes from. Protein transfer was performed on Hybond- C extra (GE Healthcare) nitrocellulose membranes or Hybond-P PVDF (GE Healthcare) membranes. Radioactivity (³²P) to label nucleic acids was used from Perkin Elmer. Autoradiography was performed by using Amersham Hyperfilm MP (GE Healthcare) and ECL solutions were bought from Biorad. Protein samples for

Western Blots were loaded on Invitrogen or Criterion gels from Biorad. For Blue Native PAGE experiments Invitrogen gels were used.

The following primary antibodies were used:

MitoProfile total oxidative phosphorylation mixture	Mitosciences
ExoG	Proteintech
HSP 60	Cell signaling
COX1	Invitrogen
MTERF1	Proteintech
TFAM	Abnova
POLRMT	produced in-house
TWINKLE	produced in-house
POL γ	produced in-house
COX2	produced in-house
LRPPRC	produced in-house

Secondary antibodies

The following secondary antibodies were all purchased at GE Healthcare: HRP-conjugated sheep anti mouse IgG HRP-conjugated donkey anti rabbit IgG HRP-conjugated goat anti rat IgG

Oligomers

All oligomers were customized and ordered at eurofins. Primers used for genotyping:

Primer	Sequence 5'-3'
TWINKLE BAC Forward	CGACTGAAATCCGCCAGTAT
TWINKLE BAC Reverse	AGAACACAATCCGACGGAAC
MGME1 Lox P Forward	GAGGTAGGAGAGGCATGAGG
MGME1 lox P Reverse	GGAAGAGAGTTGATGTTTCAGGG
MGME1KO Forward	GTGGCTGCTTGTCAAACCTT
MGME1KO Reverse	ATGTTTCAGGGCCAACAGATC

5' Biotinylated oligomers for probing northern blots

biotinGCTTTGAAGGCTCTTGGTCTGT	Trpprobe
biotinCACTCTGCATCAACTGAACGCA	Alaprobe
biotinGAATGATGGCTAGGGTGAATTC	ND1probe
biotinTGCTAGGTGTGGTTGGTTGATG	ND5probe
biotinGGAGAAGATGGTTAGGTCTACG	COXIprobe
biotinGACTTGGGTTAATCGTGTGACC	12Sprobe
biotinTGTCTGGTAGTAAGGTGGAGTG	16Sprobe

Oligomers for probing radioactive northern blots

7S RNA:

5'-GACATATAATATTA ACTATCAAACCCTATGTCCTGATCAATTCTA

Oligomers capture 7S ends

7S 5' ends:

GCTGATGGCGATGAATGAACACTGCGTTTGCTGGCTTTGATGAAA 5'DNA Adapter
GCTGATGGCGATGAATGAACACTG5'RACE Outer Primer
ATCTGGTTCTTACTTCAGGGCCATC 15813fwd (PCR/sequencing)

7S 3' ends:

ACCTATAGTGAGTCGTATTAATTCTGTGCTCGC 3'DNA Adapter (5' Phosphorylation,
3' C3 Spacer)
GCGAGCACAGAATTAATACGACTCACTATAGGTTTTTTTTTTTTTVN 3'oligo dT
Primer
GCGAGCACAGAATTAATACGACT 3'RACE Outer Primer
GTTTAGCTACCCCAAGTTTAATGG 15748rev (PCR/sequencing)

2.1.3 Plasmids

The following constructs were used for generation of radiolabeled probes and were made without exception in the department of Prof. Nils Göran Larsson:

pCR2.1-*cox1* pCR2.1-*cytb* pCR2.1-*12s* pCR2.1-*18s* pCR2.1-*nd1* pCR-Blunt-II-*nd5* pCR-Blunt-II-*nd6* pCR-Blunt-II-*16s*

6. REFERENCES

1. Timmis, J. N., Ayliffe, M. A., Huang, C. Y. & Martin, W. Endosymbiotic gene transfer: organelle genomes forge eukaryotic chromosomes. *Nat Rev Genet* **5**, 123–135 (2004).
2. Martin, W. F., Garg, S. & Zimorski, V. Endosymbiotic theories for eukaryote origin. *Phil. Trans. R. Soc. B* **370**, 20140330 (2015).
3. Rochette, N. C., Brochier-Armanet, C. & Gouy, M. Phylogenomic Test of the Hypotheses for the Evolutionary Origin of Eukaryotes. *Mol Biol Evol* **31**, 832–845 (2014).
4. Adams, K. Evolution of mitochondrial gene content: gene loss and transfer to the nucleus. *Molecular Phylogenetics and Evolution* **29**, 380–395 (2003).
5. Heijne, von, G. Why mitochondria need a genome. *FEBS Lett.* **198**, 1–4 (1986).
6. Jukes, T. H. & Osawa, S. in *Evolution of Life* 79–95 (Springer Japan, 1991). doi:10.1007/978-4-431-68302-5_6
7. Gray, M. W., Burger, G. & Lang, B. F. The origin and early evolution of mitochondria. *Genome Biology* **2**, 1018.1–1018.5 (2001).
8. Gray, M. W. Evolution of organellar genomes. *Current Opinion in Genetics & Development* **9**, 678–687 (1999).
9. Voet, D. & Voet, J. G. *Biochemistry*. (Wiley, 2009).
10. Gilkerson, R. W., Selker, J. M. L. & Capaldi, R. A. The cristal membrane of mitochondria is the principal site of oxidative phosphorylation. *FEBS Lett.* **546**, 355–358 (2003).
11. Hällberg, B. M. & Larsson, N.-G. Making Proteins in the Powerhouse. *Cell Metabolism* **20**, 226–240 (2014).
12. Falkenberg, M. & Larsson, N.-G. Structure casts light on mtDNA replication. *Cell* **139**, 231–233 (2009).
13. Saraste, M. Oxidative phosphorylation at the fin de siècle. *Science* **283**, 1488–1493 (1999).
14. Darrouzet, E., Moser, C. C., Dutton, P. L. & Daldal, F. Large scale domain movement in cytochrome bc(1): a new device for electron transfer in proteins. *Trends in Biochemical Sciences* **26**, 445–451 (2001).
15. Mills, D. A. & Ferguson-Miller, S. Influence of structure, pH and membrane potential on proton movement in cytochrome oxidase. *Biochimica et Biophysica Acta (BBA) - Bioenergetics* **1555**, 96–100 (2002).
16. Schultz, B. E. & Chan, S. I. Structures and proton-pumping strategies of mitochondrial respiratory enzymes. *Annu Rev Biophys Biomol Struct* **30**, 23–65 (2001).
17. Lancaster, C. R. & Kröger, A. Succinate: quinone oxidoreductases: new insights from X-ray crystal structures. *Biochim. Biophys. Acta* **1459**, 422–431 (2000).
18. Nunnari, J. & Suomalainen, A. Mitochondria: in sickness and in health. *Cell*

- 148**, 1145–1159 (2012).
19. Falkenberg, M., Larsson, N.-G. & Gustafsson, C. M. DNA replication and transcription in mammalian mitochondria. *Annu. Rev. Biochem.* **76**, 679–699 (2007).
 20. Freyer, C. *et al.* Variation in germline mtDNA heteroplasmy is determined prenatally but modified during subsequent transmission. *Nat. Genet.* **44**, 1282–1285 (2012).
 21. Kukat, C. *et al.* Super-resolution microscopy reveals that mammalian mitochondrial nucleoids have a uniform size and frequently contain a single copy of mtDNA. *PNAS* **vol. 10**, 13534–13539 (2011).
 22. Ngo, H. B., Lovely, G. A., Phillips, R. & Chan, D. C. Distinct structural features of TFAM drive mitochondrial DNA packaging versus transcriptional activation. *Nature Communications* **5**, 3077 (2014).
 23. Jans, D. C. *et al.* Super-resolution microscopy reveals that mammalian mitochondrial nucleoids have a uniform size and frequently contain a single copy of mtDNA. **108**, 13534–13539 (2011).
 24. Hällberg, B. M. & Larsson, N.-G. TFAM forces mtDNA to make a U-turn. *Nat. Struct. Mol. Biol.* **18**, 1179–1181 (2011).
 25. Wang, Y. & Bogenhagen, D. F. Human mitochondrial DNA nucleoids are linked to protein folding machinery and metabolic enzymes at the mitochondrial inner membrane. *J. Biol. Chem.* **281**, 25791–25802 (2006).
 26. Gilkerson, R. W. Mitochondrial DNA nucleoids determine mitochondrial genetics and dysfunction. *The International Journal of Biochemistry & Cell Biology* **41**, 1899–1906 (2009).
 27. Korhonen, J. A., Pham, X. H., Pellegrini, M. & Falkenberg, M. Reconstitution of a minimal mtDNA replisome in vitro. *EMBO J* **23**, 2423–2429 (2004).
 28. Fusté, J. M. *et al.* Mitochondrial RNA Polymerase Is Needed for Activation of the Origin of Light-Strand DNA Replication. *Molecular Cell* **37**, 67–78 (2010).
 29. Clayton, D. A. Replication of animal mitochondrial DNA. *Cell* **28**, 693–705 (1982).
 30. Holt, I. J. *et al.* Mammalian mitochondrial nucleoids: Organizing an independently minded genome. *Mitochondrion* **7**, 311–321 (2007).
 31. Yasukawa, T. *et al.* Replication of vertebrate mitochondrial DNA entails transient ribonucleotide incorporation throughout the lagging strand. *EMBO J* **25**, 5358–5371 (2006).
 32. Pohjoismäki, J. L. O. *et al.* Mammalian Mitochondrial DNA Replication Intermediates Are Essentially Duplex but Contain Extensive Tracts of RNA/DNA Hybrid. *Journal of Molecular Biology* **397**, 1144–1155 (2010).
 33. Fusté, J. M. *et al.* In Vivo Occupancy of Mitochondrial Single-Stranded DNA Binding Protein Supports the Strand Displacement Mode of DNA Replication. *PLoS Genet* **10**, e1004832 (2014).
 34. Wanrooij, S. *et al.* In vivo mutagenesis reveals that OriL is essential for mitochondrial DNA replication. *EMBO Rep.* **13**, 1130–1137 (2012).
 35. Jemt, E. *et al.* The mitochondrial DNA helicase TWINKLE can assemble on a closed circular template and support initiation of DNA synthesis. *Nucleic Acids Res.* **39**, 9238–9249 (2011).
 36. Wanrooij, S. & Falkenberg, M. The human mitochondrial replication fork in health and disease. *Biochim. Biophys. Acta* **1797**, 1378–1388 (2010).

37. Kühl, I. *et al.* POLRMT regulates the switch between replication primer formation and gene expression of mammalian mtDNA. *Science Advances* **2**, e1600963–e1600963 (2016).
38. Wanrooij, S. *et al.* Human mitochondrial RNA polymerase primes lagging-strand DNA synthesis in vitro. *Proceedings of the National Academy of Sciences* **105**, 11122–11127 (2008).
39. Reyes, A., Yasukawa, T., Cluett, T. J. & Holt, I. J. in *Mitochondrial DNA* **554**, 15–35 (Humana Press, 2009).
40. Holt, I. J., Lorimer, H. E. & Jacobs, H. T. Coupled Leading- and Lagging-Strand Synthesis of Mammalian Mitochondrial DNA. *Cell* **100**, 515–524 (2000).
41. Walberg, M. W. & Clayton, D. A. Sequence and properties of the human KB cell and mouse L cell D-loop regions of mitochondrial DNA.
42. Chang, D. D. & Clayton, D. A. Priming of human mitochondrial DNA replication occurs at the light-strand promoter.
43. Pham, X. H. *et al.* Conserved sequence box II directs transcription termination and primer formation in mitochondria. *J. Biol. Chem.* **281**, 24647–24652 (2006).
44. Kai, Y. *et al.* Mitochondrial DNA replication in human T lymphocytes is regulated primarily at the H-strand termination site. *Biochimica et Biophysica Acta (BBA) - Gene Structure and Expression* **1446**, 126–134 (1999).
45. Doda, J. N., Wright, C. T. & Clayton, D. A. Elongation of displacement-loop strands in human and mouse mitochondrial DNA is arrested near specific template sequences. *Proc. Natl. Acad. Sci. U.S.A.* **78**, 6116–6120 (1981).
46. Nicholls, T. J. & Minczuk, M. In D-loop: 40 years of mitochondrial 7S DNA. *Exp. Gerontol.* **56**, 175–181 (2014).
47. Madsen, C. S., Ghivizzani, S. C. & Hauswirth, W. W. Protein binding to a single termination-associated sequence in the mitochondrial DNA D-loop region.
48. Roberti, M. *et al.* Multiple protein-binding sites in the TAS-region of human and rat mitochondrial DNA. *Biochem. Biophys. Res. Commun.* **243**, 36–40 (1998).
49. Polosa, P. L., Deceglie, S., Roberti, M., Gadaleta, M. N. & Cantatore, P. Contrahelicase activity of the mitochondrial transcription termination factor mtDBP. *Nucleic Acids Res.* **33**, 3812–3820 (2005).
50. Mulugu, S. *et al.* Mechanism of termination of DNA replication of *Escherichia coli* involves helicase–contrahelicase interaction.
51. Hance, N., Ekstrand, M. I. & Trifunovic, A. Mitochondrial DNA polymerase gamma is essential for mammalian embryogenesis. *Human Molecular Genetics* **14**, 1775–1783 (2005).
52. Kaguni, L. S. DNA polymerase gamma, the mitochondrial replicase. *Annu. Rev. Biochem.* **73**, 293–320 (2004).
53. Maria A Graziewicz, Matthew J Longley, A. & Copeland, W. C. DNA Polymerase γ in Mitochondrial DNA Replication and Repair. *Chemical Reviews* **106**, 383–405 (2005).
54. Macao, B. *et al.* The exonuclease activity of DNA polymerase γ is required for ligation during mitochondrial DNA replication. *Nature Communications* **6**, 7303 (2015).
55. Uhler, J. P. *et al.* MGME1 processes flaps into ligatable nicks in concert with

- DNA polymerase γ during mtDNA replication. *Nucleic Acids Res.* gkw468 (2016). doi:10.1093/nar/gkw468
56. Trifunovic, A. *et al.* Premature ageing in mice expressing defective mitochondrial DNA polymerase. *Nature* **429**, 417–423 (2004).
 57. Humble, M. M. *et al.* Polg2 is essential for mammalian embryogenesis and is required for mtDNA maintenance. *Human Molecular Genetics* **22**, 1017–1025 (2013).
 58. Carrodeguas, J. A., Theis, K., Bogenhagen, D. F. & Kisker, C. Crystal structure and deletion analysis show that the accessory subunit of mammalian DNA polymerase gamma, Pol gamma B, functions as a homodimer. *Molecular Cell* **7**, 43–54 (2001).
 59. Farge, G., Pham, X. H., Holmlund, T., Khorostov, I. & Falkenberg, M. The accessory subunit B of DNA polymerase gamma is required for mitochondrial replisome function. *Nucleic Acids Res.* **35**, 902–911 (2007).
 60. Lohman, T. M. Helicase-catalyzed DNA unwinding. *J. Biol. Chem.* **268**, 2269–2272 (1993).
 61. Spelbrink, J. N. *et al.* Human mitochondrial DNA deletions associated with mutations in the gene encoding Twinkle, a phage T7 gene 4-like protein localized in mitochondria. *Nat. Genet.* **28**, 223–231 (2001).
 62. Suomalainen, A. & Kaukonen, J. Diseases caused by nuclear genes affecting mtDNA stability. *Am. J. Med. Genet.* **106**, 53–61 (2001).
 63. Sarzi, E. *et al.* Twinkle helicase (PEO1) gene mutation causes mitochondrial DNA depletion. *Ann Neurol.* **62**, 579–587 (2007).
 64. Goffart, S. *et al.* Twinkle mutations associated with autosomal dominant progressive external ophthalmoplegia lead to impaired helicase function and in vivo mtDNA replication stalling. *Human Molecular Genetics* **18**, 328–340 (2009).
 65. Sanchez-Martinez, A. *et al.* Modeling Pathogenic Mutations of Human Twinkle in *Drosophila* Suggests an Apoptosis Role in Response to Mitochondrial Defects. *PLoS ONE* **7**, e43954 (2012).
 66. Wanrooij, S., Goffart, S., Pohjoismaki, J. L. O., Yasukawa, T. & Spelbrink, J. N. Expression of catalytic mutants of the mtDNA helicase Twinkle and polymerase POLG causes distinct replication stalling phenotypes. *Nucleic Acids Res.* **35**, 3238–3251 (2007).
 67. Matsushima, Y., Farr, C. L., Fan, L. & Kaguni, L. S. Physiological and Biochemical Defects in Carboxyl-terminal Mutants of Mitochondrial DNA Helicase.
 68. Tyynismaa, H. *et al.* Mutant mitochondrial helicase Twinkle causes multiple mtDNA deletions and a late-onset mitochondrial disease in mice.
 69. Hakonen, A. H. *et al.* Infantile-onset spinocerebellar ataxia and mitochondrial recessive ataxia syndrome are associated with neuronal complex I defect and mtDNA depletion. *Human Molecular Genetics* **17**, 3822–3835 (2008).
 70. Nikkanen, J. *et al.* Mitochondrial DNA Replication Defects Disturb Cellular dNTP Pools and Remodel One-Carbon Metabolism. *Cell Metabolism* **23**, 635–648 (2016).
 71. Matsushima, Y. & Kaguni, L. S. Differential phenotypes of active site and human autosomal dominant progressive external ophthalmoplegia mutations in *Drosophila* mitochondrial DNA helicase expressed in

- Schneider cells. *J. Biol. Chem.* **282**, 9436–9444 (2007).
72. Milenkovic, D. *et al.* TWINKLE is an essential mitochondrial helicase required for synthesis of nascent D-loop strands and complete mtDNA replication. *Human Molecular Genetics* **22**, 1983–1993 (2013).
 73. Gaspari, M., Falkenberg, M., Larsson, N.-G. & Gustafsson, C. M. The mitochondrial RNA polymerase contributes critically to promoter specificity in mammalian cells. *EMBO J* **23**, 4606–4614 (2004).
 74. Falkenberg, M., Larsson, N.-G. & Gustafsson, C. M. DNA Replication and Transcription in Mammalian Mitochondria. *Annu. Rev. Biochem.* **76**, 679–699 (2007).
 75. Zhang, H. *et al.* Human mitochondrial topoisomerase I.
 76. Zhang, H. *et al.* Increased negative supercoiling of mtDNA in TOP1mt knockout mice and presence of topoisomerases II α and II β in vertebrate mitochondria. *Nucleic Acids Res.* **42**, 7259–7267 (2014).
 77. Dalla Rosa, I. *et al.* Mapping Topoisomerase Sites in Mitochondrial DNA with a Poisonous Top1mt. *J. Biol. Chem.* (2014).
doi:10.1074/jbc.M114.555367
 78. Reyes, A. *et al.* RNASEH1 Mutations Impair mtDNA Replication and Cause Adult-Onset Mitochondrial Encephalomyopathy. *The American Journal of Human Genetics* **97**, 186–193 (2015).
 79. Perez-Jannotti, R. M., Klein, S. M. & Bogenhagen, D. F. Two forms of mitochondrial DNA ligase III are produced in *Xenopus laevis* oocytes. *J. Biol. Chem.* **276**, 48978–48987 (2001).
 80. Lakshmiathy, U. & Campbell, C. Antisense-mediated decrease in DNA ligase III expression results in reduced mitochondrial DNA integrity. *Nucleic Acids Res.* **29**, 668–676 (2001).
 81. Szczesny, R. J. *et al.* Identification of a novel human mitochondrial endo-/exonuclease Ddk1/c20orf72 necessary for maintenance of proper 7S DNA levels. *Nucleic Acids Res.* **41**, 3144–3161 (2013).
 82. Kornblum, C. *et al.* Loss-of-function mutations in MGME1 impair mtDNA replication and cause multisystemic mitochondrial disease. *Nat. Genet.* **45**, 214–219 (2013).
 83. Nicholls, T. J. *et al.* Linear mtDNA fragments and unusual mtDNA rearrangements associated with pathological deficiency of MGME1 exonuclease. *Human Molecular Genetics* (2014). doi:10.1093/hmg/ddu336
 84. Uhler, J. P. & Falkenberg, M. Primer removal during mammalian mitochondrial DNA replication. *DNA Repair* **34**, 28–38 (2015).
 85. Liu, P. *et al.* Removal of Oxidative DNA Damage via FEN1-Dependent Long-Patch Base Excision Repair in Human Cell Mitochondria. *Mol. Cell. Biol.* **28**, 4975–4987 (2008).
 86. Zheng, L. *et al.* Human DNA2 Is a Mitochondrial Nuclease/Helicase for Efficient Processing of DNA Replication and Repair Intermediates. *Molecular Cell* **32**, 325–336 (2008).
 87. Gustafsson, C. M., Falkenberg, M. & Larsson, N.-G. Maintenance and Expression of Mammalian Mitochondrial DNA.
<http://dx.doi.org/10.1146/annurev-biochem-060815-014402> (2015).
doi:10.1146/annurev-biochem-060815-014402
 88. Shadel, G. S. & Clayton, D. A. MITOCHONDRIAL DNA MAINTENANCE IN VERTEBRATES. <http://dx.doi.org/10.1146/annurev.biochem.66.1.409> **66**,

- 409–435 (1997).
89. Ojala, D., Montoya, J. & Attardi, G. tRNA punctuation model of RNA processing in human mitochondria. *Nature* **290**, 470–474 (1981).
 90. Falkenberg, M. *et al.* Mitochondrial transcription factors B1 and B2 activate transcription of human mtDNA. *Nat. Genet.* **31**, 289–294 (2002).
 91. ALONI, Y. & Attardi, G. Symmetrical In Vivo Transcription of Mitochondrial DNA in HeLa Cells. *Proc. Nat. Acad. Sci* **Vol. 68**, 1757–1761 (1971).
 92. Bonawitz, N. D., Clayton, D. A. & Shadel, G. S. Initiation and Beyond: Multiple Functions of the Human Mitochondrial Transcription Machinery. *Molecular Cell* **24**, 813–825 (2006).
 93. Posse, V., Shahzad, S., Falkenberg, M., Hällberg, B. M. & Gustafsson, C. M. TEFM is a potent stimulator of mitochondrial transcription elongation in vitro.
 94. Minczuk, M. *et al.* TEFM (c17orf42) is necessary for transcription of human mtDNA.
 95. Fisher, R. P. & Clayton, D. A. Purification and characterization of human mitochondrial transcription factor 1.
 96. Larsson, N. G. *et al.* Mitochondrial transcription factor A is necessary for mtDNA maintenance and embryogenesis in mice. *Nat. Genet.* **18**, 231–236 (1998).
 97. Parisi, M. A. & Clayton, D. A. Similarity of human mitochondrial transcription factor 1 to high mobility group proteins. *Science* **252**, 965–969 (1991).
 98. Ngo, H. B., Kaiser, J. T. & Chan, D. C. The mitochondrial transcription and packaging factor Tfam imposes a U-turn on mitochondrial DNA. *Nat. Struct. Mol. Biol.* **18**, 1290–1296 (2011).
 99. Ohgaki, K. *et al.* The C-terminal Tail of Mitochondrial Transcription Factor A Markedly Strengthens its General Binding to DNA.
 100. Rubio-Cosials, A. *et al.* Human mitochondrial transcription factor A induces a U-turn structure in the light strand promoter. *Nat. Struct. Mol. Biol.* **18**, 1281–1289 (2011).
 101. Sologub, M., Litonin, D., Anikin, M., Mustaev, A. & Temiakov, D. TFB2 is a transient component of the catalytic site of the human mitochondrial RNA polymerase. *Cell* **139**, 934–944 (2009).
 102. Cotney, J., Wang, Z. & Shadel, G. S. Relative abundance of the human mitochondrial transcription system and distinct roles for h-mtTFB1 and h-mtTFB2 in mitochondrial biogenesis and gene expression. *Nucleic Acids Res.* **35**, 4042–4054 (2007).
 103. Seidel-Rogol, B. L., McCulloch, V. & Shadel, G. S. Human mitochondrial transcription factor B1 methylates ribosomal RNA at a conserved stem-loop. *Nat. Genet.* **33**, 23–24 (2003).
 104. Metodiev, M. D. *et al.* Methylation of 12S rRNA Is Necessary for In Vivo Stability of the Small Subunit of the Mammalian Mitochondrial Ribosome. *Cell Metabolism* **9**, 386–397 (2009).
 105. Agaronyan, K., Morozov, Y. I., Anikin, M. & Temiakov, D. Mitochondrial biology. Replication-transcription switch in human mitochondria. *Science* **347**, 548–551 (2015).
 106. Montoya, J., Christianson, T., Levens, D., Rabinowitz, M. & Attardi, G. Identification of initiation sites for heavy-strand and light-strand

- transcription in human mitochondrial DNA. *Proc. Natl. Acad. Sci. U.S.A.* **79**, 7195–7199 (1982).
107. Martin, M., Cho, J., Cesare, A. J., Griffith, J. D. & Attardi, G. Termination factor-mediated DNA loop between termination and initiation sites drives mitochondrial rRNA synthesis. *Cell* **123**, 1227–1240 (2005).
108. Terzioglu, M. *et al.* MTERF1 Binds mtDNA to Prevent Transcriptional Interference at the Light-Strand Promoter but Is Dispensable for rRNA Gene Transcription Regulation. *Cell Metabolism* **17**, 618–626 (2013).
109. Shi, Y. *et al.* Mitochondrial transcription termination factor 1 directs polar replication fork pausing. *Nucleic Acids Res.* **44**, 5732–5742 (2016).
110. Wanrooij, P. H. *et al.* A hybrid G-quadruplex structure formed between RNA and DNA explains the extraordinary stability of the mitochondrial R-loop. *Nucleic Acids Res.* **40**, 10334–10344 (2012).
111. Jemt, E. *et al.* Regulation of DNA replication at the end of the mitochondrial D-loop involves the helicase TWINKLE and a conserved sequence element. *Nucleic Acids Res.* **43**, 9262–9275 (2015).
112. Lagouge, M. & Larsson, N. G. The role of mitochondrial DNA mutations and free radicals in disease and ageing. *J. Intern. Med.* **273**, 529–543 (2013).
113. Balaban, R. S., Nemoto, S. & Finkel, T. Mitochondria, Oxidants, and Aging. *Cell* **120**, 483–495 (2005).
114. Bratic, A. & Larsson, N.-G. The role of mitochondria in aging. *J Clin Invest* **123**, 951–957 (2013).
115. Turrens, J. F. Mitochondrial formation of reactive oxygen species. *J. Physiol. (Lond.)* **552**, 335–344 (2003).
116. HARMAN, D. Aging: a theory based on free radical and radiation chemistry. *J Gerontol* **11**, 298–300 (1956).
117. Kauppila, J. H. K. & Stewart, J. B. Mitochondrial DNA: Radically free of free-radical driven mutations. *Biochim. Biophys. Acta* **1847**, 1354–1361 (2015).
118. Sawyer, D. E. & Van Houten, B. Repair of DNA damage in mitochondria. *Mutat. Res.* **434**, 161–176 (1999).
119. Driggers, W. J., LeDoux, S. P. & Wilson, G. L. Repair of oxidative damage within the mitochondrial DNA of RINr 38 cells. *J. Biol. Chem.* **268**, 22042–22045 (1993).
120. Roginskaya, M., Mohseni, R., Moore, T. J., Bernhard, W. A. & Razskazovskiy, Y. Identification of the C4'-oxidized abasic site as the most abundant 2-deoxyribose lesion in radiation-damaged DNA using a novel HPLC-based approach. *Radiat. Res.* **181**, 131–137 (2014).
121. Chi, N. W. & Kolodner, R. D. The effect of DNA mismatches on the ATPase activity of MSH1, a protein in yeast mitochondria that recognizes DNA mismatches. *J. Biol. Chem.* **269**, 29993–29997 (1994).
122. Mason, P. A., Matheson, E. C., Hall, A. G. & Lightowlers, R. N. Mismatch repair activity in mammalian mitochondria. *Nucleic Acids Res.* **31**, 1052–1058 (2003).
123. Sakamoto, K. *et al.* MUTYH-null mice are susceptible to spontaneous and oxidative stress induced intestinal tumorigenesis. *Cancer Res* **67**, 6599–6604 (2007).
124. Sampath, H. *et al.* 8-Oxoguanine DNA Glycosylase (OGG1) Deficiency Increases Susceptibility to Obesity and Metabolic Dysfunction. *PLoS ONE* **7**, e51697 (2012).

125. Vartanian, V. *et al.* The metabolic syndrome resulting from a knockout of the NEIL1 DNA glycosylase. *Proc. Natl. Acad. Sci. U.S.A.* **103**, 1864–1869 (2006).
126. Halsne, R. *et al.* Lack of the DNA glycosylases MYH and OGG1 in the cancer prone double mutant mouse does not increase mitochondrial DNA mutagenesis. *DNA Repair* **11**, 278–285 (2012).
127. Suomalainen, A. Mitochondrial roles in disease: a box full of surprises. *EMBO Mol Med* **7**, 1245–1247 (2015).
128. Larsson, N.-G. Somatic mitochondrial DNA mutations in mammalian aging. *Annu. Rev. Biochem.* **79**, 683–706 (2010).
129. Vafai, S. B. & Mootha, V. K. Mitochondrial disorders as windows into an ancient organelle. *Nature* **491**, 374–383 (2012).
130. Chinnery, P. F. & Hudson, G. Mitochondrial genetics. *Br Med Bull* **106**, 135–159 (2013).
131. Larsson, N.-G. & Clayton, D. A. Molecular Genetic Aspects of Human Mitochondrial Disorders. <http://dx.doi.org/10.1146/annurev.ge.29.120195.001055> **29**, 151–178 (2003).
132. Stewart, J. B. & Chinnery, P. F. The dynamics of mitochondrial DNA heteroplasmy: implications for human health and disease. *Nat Rev Genet* **16**, 530–542 (2015).
133. Thorburn, D. R. & Dahl, H. H. Mitochondrial disorders: genetics, counseling, prenatal diagnosis and reproductive options. *Am. J. Med. Genet.* **106**, 102–114 (2001).
134. Rotig, A. Genetic Features of Mitochondrial Respiratory Chain Disorders. *Journal of the American Society of Nephrology* **14**, 2995–3007 (2003).
135. Copeland, W. C. Defects of mitochondrial DNA replication. *J. Child Neurol.* **29**, 1216–1224 (2014).
136. Ronchi, D. *et al.* Mutations in DNA2 Link Progressive Myopathy to Mitochondrial DNA Instability. *The American Journal of Human Genetics* **92**, 293–300 (2013).
137. Cerritelli, S. M. *et al.* Failure to Produce Mitochondrial DNA Results in Embryonic Lethality in Rnaseh1 Null Mice. *Molecular Cell* **11**, 807–815 (2003).
138. Copeland, W. C. Inherited Mitochondrial Diseases of DNA Replication*. *Annu. Rev. Med.* **59**, 131–146 (2008).
139. Gorman, G. S. *et al.* Mitochondrial diseases. *Nat Rev Dis Primers* **2**, 16080 (2016).
140. Bonod-Bidaud, C. *et al.* Induction of ANT2 gene expression in liver of patients with mitochondrial DNA depletion. *Mitochondrion* **1**, 217–224 (2001).
141. Spinazzola, A. *et al.* MPV17 encodes an inner mitochondrial membrane protein and is mutated in infantile hepatic mitochondrial DNA depletion. *Nat. Genet.* **38**, 570–575 (2006).
142. Van Keuren, M. L., Gavrilina, G. B., Filipiak, W. E., Zeidler, M. G. & Saunders, T. L. Generating transgenic mice from bacterial artificial chromosomes: transgenesis efficiency, integration and expression outcomes. *Transgenic Res* 769–785 (2009).
143. Ekstrand, M. I. *et al.* Mitochondrial transcription factor A regulates mtDNA

- copy number in mammals. *Human Molecular Genetics* **13**, 935–944 (2004).
144. Tyynismaa, H. Twinkle helicase is essential for mtDNA maintenance and regulates mtDNA copy number. *Human Molecular Genetics* **13**, 3219–3227 (2004).
145. Gensler, S. *et al.* Mechanism of mammalian mitochondrial DNA replication: import of mitochondrial transcription factor A into isolated mitochondria stimulates 7S DNA synthesis. *Nucleic Acids Res.* **29**, 3657–3663 (2001).
146. Kai, Y. *et al.* Mitochondrial DNA replication in human T lymphocytes is regulated primarily at the H-strand termination site. *Biochim. Biophys. Acta* **1446**, 126–134 (1999).
147. Brown, T. A. Release of replication termination controls mitochondrial DNA copy number after depletion with 2',3'-dideoxycytidine. *Nucleic Acids Res.* **30**, 2004–2010 (2002).
148. Freyer, C. *et al.* Maintenance of respiratory chain function in mouse hearts with severely impaired mtDNA transcription. *Nucleic Acids Res.* **38**, 6577–6588 (2010).
149. Williams, S. L. *et al.* The mtDNA mutation spectrum of the progeroid Polg mutator mouse includes abundant control region multimers. *Cell Metabolism* **12**, 675–682 (2010).
150. Putter, V. & Grummt, F. Transcription termination factor TTF-I exhibits contrahelicase activity during DNA replication. *EMBO Rep.* **3**, 147–152 (2002).
151. Ylikallio, E., Tyynismaa, H., Tsutsui, H., Ide, T. & Suomalainen, A. High mitochondrial DNA copy number has detrimental effects in mice. *Human Molecular Genetics* **19**, 2695–2705 (2010).
152. Hayashi, J. *et al.* Introduction of disease-related mitochondrial DNA deletions into HeLa cells lacking mitochondrial DNA results in mitochondrial dysfunction. *Proc. Natl. Acad. Sci. U.S.A.* **88**, 10614–10618 (1991).
153. Cortopassi, G. A. & Arnheim, N. Detection of a specific mitochondrial DNA deletion in tissues of older humans. *Nucleic Acids Res.* **18**, 6927–6933 (1990).
154. Fayet, G. *et al.* Ageing muscle: clonal expansions of mitochondrial DNA point mutations and deletions cause focal impairment of mitochondrial function. *Neuromuscul. Disord.* **12**, 484–493 (2002).
155. Bender, A. *et al.* High levels of mitochondrial DNA deletions in substantia nigra neurons in aging and Parkinson disease. *Nat. Genet.* **38**, 515–517 (2006).
156. Taylor, R. W. *et al.* Mitochondrial DNA mutations in human colonic crypt stem cells. *J Clin Invest* **112**, 1351–1360 (2003).
157. Baris, O. R. *et al.* Mosaic Deficiency in Mitochondrial Oxidative Metabolism Promotes Cardiac Arrhythmia during Aging. *Cell Metabolism* **21**, 667–677 (2015).
158. Bailey, L. J. *et al.* Mice expressing an error-prone DNA polymerase in mitochondria display elevated replication pausing and chromosomal breakage at fragile sites of mitochondrial DNA. *Nucleic Acids Res.* **37**, 2327–2335 (2009).
159. Vermulst, M. *et al.* DNA deletions and clonal mutations drive premature aging in mitochondrial mutator mice. *Nat. Genet.* **40**, 392–394 (2008).

160. Uhler, J. P. *et al.* MGME1 processes flaps into ligatable nicks in concert with DNA polymerase γ during mtDNA replication. *Nucleic Acids Res.* gkw468 (2016). doi:10.1093/nar/gkw468
161. Sbisà, E., Tanzariello, F., Reyes, A., Pesole, G. & Saccone, C. Mammalian mitochondrial D-loop region structural analysis: identification of new conserved sequences and their functional and evolutionary implications. *Gene* **205**, 125–140 (1997).
162. Selwood, S. P., McGregor, A., Lightowlers, R. N. & Chrzanowska-Lightowlers, Z. M. Inhibition of mitochondrial protein synthesis promotes autonomous regulation of mtDNA expression and generation of a new mitochondrial RNA species. *FEBS Lett.* **494**, 186–191 (2001).
163. Clayton, D. A. Transcription and replication of mitochondrial DNA *Human Reproduction, Vol. 15, (Suppl. 2), pp. 11-17, 2000* 1–7 (2008).
164. Ameer, A. *et al.* Ultra-Deep Sequencing of Mouse Mitochondrial DNA: Mutational Patterns and Their Origins. *PLoS Genet* **7**, e1002028 (2011).
165. Roux, K. J., Kim, D. I., Raida, M. & Burke, B. A promiscuous biotin ligase fusion protein identifies proximal and interacting proteins in mammalian cells. *The Journal of Cell Biology* **196**, 801–810 (2012).
166. Park, C. B. *et al.* MTERF3 is a negative regulator of mammalian mtDNA transcription. *Cell* **130**, 273–285 (2007).
167. Ruzzenente, B. *et al.* LRPPRC is necessary for polyadenylation and coordination of translation of mitochondrial mRNAs - Ruzzenente - 2011 - The EMBO Journal - Wiley Online Library. *EMBO J* **31**, (2011).
168. Camara, Y. *et al.* MTERF4 Regulates Translation by Targeting the Methyltransferase NSUN4 to the Mammalian Mitochondrial Ribosome. *CMET* **13**, 527–539 (2011).

Erklärung

Ich versichere, dass ich die von mir vorgelegte Dissertation selbständig, die benutzen Quellen und Hilfsmittel vollständig angegeben und die Stellen der Arbeit – einschließlich Tabellen, Karten und Abbildungen –, die anderen Werken im Wortlaut oder dem Sinn nach entnommen sind, in jedem Einzelfall als Entlehnung kenntlich gemacht habe; dass diese Dissertation noch keine andere Fakultät oder Universität zur Prüfung vorgelegen hat; dass die – abgesehen von unten angegebenen Teilpublikationen – noch nicht veröffentlicht worden ist sowie, dass ich eine solche Veröffentlichung vor Abschluss des Promotionsverfahrens nicht vornehmen werde. Die Bestimmungen dieser Promotionsordnung sind mir bekannt. Die von mir vorgelegte Dissertation ist von Prof. Nils-Göran Larsson betreut worden.

Köln, November 2016

Stanka Matic

Acknowledgments

I wish to thank the people without whom this work would not have been possible.

Firstly, my gratefulness goes to Professor Nils Göran-Larsson for giving me the opportunity to work in his group and for his belief on me and on the project. He has continuously offered his expert knowledge and provided much of the intellectual background to this project; without his help and guidance in this project this work would not have been possible. The group he has established is of the highest caliber, and the resources and academic interactions with other scientists have provided a strong basis for much of this work. I'm especially very thankful for the pleasant atmosphere in his lab, for the stimulating environment, and for the very positive interpersonal bonds in the lab, and for the chance to carry out an internship in Australia, and for being very supportive regarding my future career development.

I wish to thank Dr. Dusanka Milenkovic for being my close supervisor, a great mentor, a supportive friend throughout the all this years. She has guided me through the entire PhD, has taught me with patience from the basic skills that allowed me to perform this research, and for giving me the opportunity to pursue my scientific career and for changing my life by opening the door to this experience. Overall, I want to thank her for being a great friend and giving me continuous support on a personal level. For all this, I am deeply and eternally grateful. Dusice, hvala na zivotnoj sansi, zastiti, znanju, podrsci i prijateljstvu koje si mi pruzila sve ove godine. Sa tobom sam sazrela kao licnost i kao istrazivac. Hvala ti na beskonacnom strpljenju i razumevanju za sve. Bilo mi je zadovoljstvo biti tvoj student i blizak prijatelj.

I want to thank Prof. Aleksandra Filipovska for coming into my PhD work at a crucial point, and for providing a boost and new skills and tools to address the various challenges of my projects. She gave me great support with successfully applying for the EMBO short-term fellowship and for the chance to do an internship in her lab in Perth. I wish to thank her especially for being a great friend and for all her personal support. Hvala profesorka za svu podrsku, razumevanje, druzenje i divne baklave.

Prof. Aleksandra Trifunovic has offered her valuable support through her position as my PhD thesis committee member since 2012, for which I'm indebted to

her. I am also very appreciative for her scientific help and her personal support. Hvala profesorka za divna druzenja, zivotne i naucne savete.

I wish to thank Professoressa Paola Loguercio Polosa for being a great collaborator and for teaching me great biochemistry techniques, including heparin-sepharose purification and gel shift assays. Furthermore, I want to thank her for her great very pleasant demeanor, and for making my work easier and sharing many science and life stories with me. Thank you Paolina for your being there.

Dr. Ana Grönke/Bratic, for being my office, science, and personal support, for teaching me and sharing her knowledge, and for understanding the PhD troubles and young female worries. Anči moja, hvala ti za divno drugarstvo, za svu podršku i pomoć kao studentu i kao osobi. Bilo je divno deliti sve ove godine sa tobom.

Dr. Jim Stewart for his scientific support and always interesting and stimulating discussions about science, politics, or sequencing data. It's been a pleasure to meet you and your family, especially kids, and to be your colleague.

Prof. Oliver Rackham for great support, understanding and contribution to my PhD work.

I also want to thank our master student Caren Dirksen for my first experiences in mentoring and teaching, and for her being a great student, and sharing a great common time and diverse discussions in the office.

Finally I want to thank all of my current and former lab colleagues for their great support and atmosphere in the lab:

Maria del Pilar Miranda (Maria Bella), Johanna Kauppila, Timo Kauppila, Jakob Busch, Eduardo Silva Ramos, Vyara Todorova, Henrik Spahr, Nina Bonekamp, Inge Kühl, Francesca Baggio, Min Jiang, Elisa Motori, Sara Ruth, Marita Isokallio, Marie Lagouge, Arnaud Mourier, Benedetta Ruzzenente and Julia Harmel.

To Corinna Schwierzy-Krämer and Miriam Krähling for their great and constant assistance regarding everything administrative and scientific during these years. You have been amazing support and always ready to answer all my requests and questions.

To great technicians in the lab: Nadine Hochhard, Marie-Lune Simard, Avan Taha, Lysann Schmitz and especially to Petra Kirschner and Regina Dirksen for amazing help during last year of my PhD.

At more personal level I want to thank George Soultoukis for being my half and supporting me through entire PhD personally and scientifically. Thank you for all your love and inspiration for biology, astronomy, physics, cosmos, music and politics.

I wish to thank my “Mitbewohnerin” and great friend Huri Köse. Thank you for your love, warm home, understanding, support and care that you gave me since 1st of April 2012. I also appreciate yours and Volker’s acceptance and friendship.

Zelim puno da se zahvalim Isidori Jeremic, mojoj najboljoj drugarici i kumi. Hvala ckezo sto si uvek verovala u mene, sto si mi prva ukazala na vaznost moje profesije, sto si uvek bila uz mene i pomagala mi u svemu. Hvala ti puno sto si prosirila moj um i naucila me prve korake za landaranje po svetu.

Jeleni Milovanovic mojoj dragoj drugarici sa osnovnih studija. Jeco, hvala puno za divno prijateljstvo i podrsku tokom svih ovih godina.

Aleksandru Milutinovicu za svu ljubav, razumevanje, motivaciju i podrsku tokom celog skolovanja.

Tihomiru Karlovicu za podrsku i divno prijateljstvo tokom mojih studija u Kelnu.

Mojoj porodici majci Vesni, ocu Radivoju, bratu Milovanu, dedi Milosu, tetkama Radi i Andji i teci Stevi za svu ljubav i podrsku tokom celog skolovanja. Narocito zelim da se zahvalim majci za bezgranicnu ljubav, zrtvovanje, oslonac i inspiraciju koji mi je pruzila. Dedi Milosu koji je uvek cenio nauku i obrazovanje i njegovu ogromnu podrsku tokom mojih studija.

Curriculum Vitae

PERSONAL INFORMATION

Date of birth: June 9th 1985

Place of birth: Ljubovija, Serbia

Citizenship: Serbian

Current residence: Germany

Address: Einhardstrasse 11, 50937 Köln

E-mail: smatic@yahoo.com

EDUCATION/RESEARCH EXPERIENCE

March 2012 – January 2017

- PhD student at the Max Planck institute for Biology of Ageing (Cologne, Germany), Department for Mitochondrial Genetics. Supervisor: Prof. Dr. Nils-Göran Larsson
- Project: Replications mechanisms of mitochondrial DNA

May 2011 – March 2012

- Research Assistant at the Vinča Institute for Nuclear Sciences (Belgrade, Serbia), Department of Molecular Radiobiology and Endocrinology, Supervisor: Dr. Aleksandra Ristic-Fira
- Project: Proton irradiation effect on human melanoma

October 2004 - March 2011

- Bachelor & Master of Science, University of Belgrade (Serbia), Faculty of Biology, department for Ecology and Environmental Protection.

FUNDING & AWARDS

Funded by Max Planck fellowship during doctoral studies

Awarded by EMBO short-term fellowship for an internship

PUBLICATIONS

1. Milenkovic D, **Matic S**, Kühl I, Ruzzenente B, Freyer C, Jemt E, Park CB, Falkenberg M, Larsson NG. TWINKLE is an essential mitochondrial helicase required for synthesis of nascent D-loop strands and complete mtDNA replication', Human Molecular Genetics, 2013, 1-11.
2. Mourier, A., **Matic, S.**, Ruzzenente, B., Larsson, N.-G. & Milenkovic, D. The Respiratory Chain Supercomplex Organization Is Independent of COX7a2l Isoforms. CMET 20, 2014, 1069–1075.
3. Uhler, J.P., Thörn, C., Nicholls, T., **Matic, S.**, Milenkovic, D., Gustafsson, C.M., Falkenberg M. MGME1 processes flaps into ligatable nicks in concert with DNA polymerase γ during mtDNA replication. Nucleic Acids Research, 2016.
4. Rackham,O., Busch, J.D., **Matic, S.**, Siira, S., Kuznetsova, I., Atanassov, I., Ermer, J.A., Shearwood, AM.J., Richman, T.R., Stewart, J., Mourier, A., Milenkovic, D., Larsson, NG., Filipovska, A. Hierarchical RNA processing is rate limiting for mitochondrial ribosome assembly, Cell Reports, submitted.
5. **Matic, S.**, Milenkovic, D., Stewart, J., Nicholls, T.J., Uhler, J.P., Rackham,O., Falkenberg M., Larsson, NG., The in vivo role of the mitochondrial DNA nuclease MGME1, in preparation.

STUDENT SUPERVISED

2014 - 2015 – Caren Dirksen (26/03- 30/08/2015 – Master Program Modules)

RELEVANT QUALIFICATIONS & TRAINING

- Felasa B Course (Theoretical and practical mouse training course with qualification awarded) - 11/2012 (5 days) - Berlin, Germany
- National and European research funding for young researchers (MPI Age – CECAD Information Event) – 10/2013 (1 day) - MPI Age, Robert Koch Strasse, Cologne Germany
- Scientific presentation course 04/2014 – University of Cologne, Germany
- Data visualization workshop (Science Craft training seminar of data visualization) - 11/2015 (3 days) - University of Cologne, Germany
- Effective scientific writing workshop – 03/2015 (2 days) – University of Cologne, Germany
- Gene Expression Application Training – 04/2015 (1 day) – MPI Age, Joseph-Stelzmann-Str. 9b, Cologne Germany